NASA CR 72466
SERT 069-074

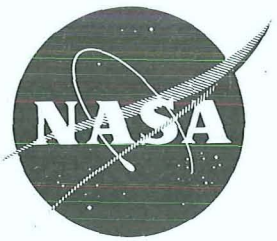

SUMMARY REPORT ON THE DEVELOPMENT OF THE SERT II SPACECRAFT SUPPORT UNIT

PREPARED BY

FAIRCHILD HILLER CORPORATION
GERMANTOWN, MARYLAND

FOR

NATIONAL AERONAUTICS AND SPACE ADMINISTRATION

NASA LEWIS RESEARCH CENTER
CONTRACT NAS3-9716
WILLIAM HAWERSAAT, SSU PROJECT MANAGER

NOTICE

This report was prepared as an account of Government-sponsored work. Neither the Unites States, nor the National Aeronautics and Space Administration (NASA), nor any person acting on behalf of NASA:

A.) Makes any warranty or representation, expressed or implied, with respect to the accuracy, completeness, or usefulness of the information contained in this report, or that the use of any information, apparatus, method, or process disclosed in this report may not infringe privately-owned rights; or

B.) Assumes any liabilities with respect to the use of, or for damages resulting from the use of, any information, apparatus, method or process disclosed in this report.

As used above, "person acting on behalf of NASA" includes any employee or contractor of NASA, or employee of such contractor, to the extent that such employee or contractor of NASA or employee of such contractor prepares, disseminates, or provides access to any information pursuant to his employment or contract with NASA, or his employment with such contractor.

Requests for copies of this report should be referred to

National Aeronautics and Space Administration
Scientific and Technical Information Facility
P.O. Box 33
College Park, Md. 20740

NASA CR-72466
SERT 069-074

SUMMARY REPORT

on the

DEVELOPMENT OF THE SERT II SPACECRAFT SUPPORT UNIT

prepared by

FAIRCHILD HILLER CORPORATION
Germantown, Maryland

for

NATIONAL AERONAUTICS AND SPACE ADMINISTRATION

April 30, 1970

CONTRACT NAS 3-9716

NASA Lewis Research Center
Cleveland, Ohio
William Hawersaat, Project Manager

ABSTRACT

This report describes the efforts of the Space and Electronics Systems Division of Fairchild Hiller Corporation in the design and development of the Spacecraft Support Unit (SSU) for the SERT II, a spacecraft used to test electron - bombardment ion engines. The SSU contained two telemetry transmitters, two command systems and two tape recorders for data storage along with the power distribution system, a battery for reacquisition control and four control moment gyros to help stabilize the spacecraft.

Three units, experimental, prototype and flight were delivered to NASA Lewis Research Center along with two complete sets of Ground Support Equipment.

FOREWORD

The development work described herein was performed by the Space and Electronics Systems Division of Fairchild Hiller Corporation under Contract NAS 3-9716. The work was done under the Technical direction of NASA Project Manager, William Hawersaat.

TABLE OF CONTENTS

TABLE OF CONTENTS (con't)

TABLE OF CONTENTS (con't)

LIST OF TABLES

LIST OF TABLES (con't)

LIST OF TABLES (con't)

LIST OF ILLUSTRATIONS

LIST OF ILLUSTRATIONS (con't)

LIST OF ILLUSTRATIONS (con't)

SECTION I

INTRODUCTION

This report is submitted by Fairchild Hiller Corporation Space and Electronics Systems Division in compliance with the schedule constituting NASA Contract NAS 3-9716 issued by the Lewis Research Center. This contract was for the development of a Spacecraft Support Unit for the SERT II. This is the Final Report which covers the design, development and integration effort accomplished by Fairchild Hiller during the period starting July 1, 1967 and ending with the delivery of the Flight Model SSU on August 23, 1968. The report is complete in itself, however, where additional historical data are desired reference can be made to the Monthly Reports submitted to NASA - LeRC during the course of the contract.

The effort on the SERT II SSU Program at Fairchild Hiller progressed through three major phases. During the early months of the program the primary effort was devoted to evaluation and selection of vendors for the major components of the system, preparation of specifications for these components and negotiation and placement of purchase orders with the selected vendors. One of the contractual requirements was that, where ever possible, space proven components be used in the SSU. Fairchild Hiller adhered strictly to this basic philosophy.

The second phase of the program, which of course overlapped the first phase, included the design and development of the three components and the system interconnecting cable to be built by Fairchild Hiller. These three units, the Command Relay Junction Box, the Signal Conditioner and the Power Control Electronics Unit and the harnesses provided the means for integrating the various subsystems into a working system. During this same period, effort was devoted to design of the mechanical subsystem. This included both structural and thermal analysis. The structural analysis resulted in the choice of RIGIDAMP material for the shelves. The thermal analysis resulted in recommendations for venting provisions as well as for paint patterns to achieve passive thermal control. The Spacecraft Support Unit structure was designed to be a simple rigid structure with a bay arrangement. The outer skin can be removed from any of the bays thus affording easy access to the equipment in any of the subsystems.

The final phase of the program covered the manufacturing, testing and integration of the Spacecraft Support Units. This phase included the performance of the acceptance tests on and the delivery of the Experimental, Prototype and Flight Model SSU's along with spares for designated critical components.

In addition to the work on the Spacecraft Support Unit, there was a parallel effort on the design and integration of the Ground Support Equipment. Two sets of GSE were delivered, one with the Experimental Unit, mounted in a van, the other, with the Flight Unit mounted in a mobile rack configuration. The ground equipment performs the function of encoding and transmitting the commands for the SERT II as well as receiving the data sent from the SERT II.

SECTION II

PROGRAM CONTROL

2.1 SCHEDULE AND PERT

In order to meet the schedule imposed by the contract, it was necessary to establish rigid controls within the Fairchild Hiller Organization. The systems used provided supervision and management with timely information so that any problem areas or incipient program delays would become immediately evident and action could be taken to alleviate any problems.

One of the internal documents that served to provide a means of communication among the various departments was the "Schedule of Events" published weekly. This document, which listed the events that were scheduled to occur each day of the current week and for the next three weeks served as the agenda for weekly program meetings. The "Schedule of Events" was excerpted from the Program PERT charts, augmented with intermediate events as required.

Each of the participating departments in the program (Engineering R&QA and Manufacturing) was required to submit an estimate to complete for the remainder of the program at the first of each month. This information along with the weekly tabulation of the actual man hours expended on the program served as a basis for the data submitted on the 533 Financial Report submitted to NASA. The weekly tab runs provide the name, section and department of each individual who charged to the program that week. From this information the project continually monitored the manpower expenditure to ensure that the tasks were properly assigned.

In addition to the tab runs monitored above, SERT II Program Management was supplied with a weekly Cost Control Sheet by the Finance Department. This sheet gave the total cost of the program for the preceding week, including both labor and materials, and the accumulated cost of the program. It also predicted the final status of the program based on the estimates-to-complete.

The reports and technique described above along with the NASA PERT system not only provided the means for achieving an effective cost control system but also was instrumental in allowing us to meet every major milestone established by NASA during the SERT II SSU Program. The Experimental Unit along with the first set of GSE was delivered in February 1968, two months after the originally scheduled date. This delay, however, was necessitated by a complete redesign of the power subsystem. The redesign, recommended by Fairchild Hiller after a thorough analysis of the

original approach, resulted in a substantial improvement in the probability of success of the SERT II mission.

The Prototype Unit was delivered on schedule in June 1968 and the Flight Model along with the second set of Ground Support Equipment in August 1968.

Budget:

As of the close of the accounting period for August 1968 the man-hour expenditures on the SERT II Program were as follows:

Engineering	57,604
R&QA	26,530
Mfg.	41,514
Total Hours	125,648

The total amount for materials and subcontracts and unliquidated commitments at this date is $1,115,055.

2.2 DOCUMENTATION

During the course of the program, copies of all drawings, specifications and test procedures were forwarded to the Program Manager at NASA - LeRC. A total of twenty-seven (27) non-standard parts data sheets along with the accompanying specifications were generated.

Table 2.2-1 is a list of all the specifications released on the SERT II SSU program.

TABLE 2.2-1

SPECIFICATIONS RELEASED ON SERT II SSU PROGRAM

Spec No	Rev	Title	Date of Release
833-PP-1000	Rev A	Quality Control Plan	9/15/67
833-10000	Rev A	R&QA Provisions	7/21/67
833-12300-P001		Connectors, Miniature Slide Mounting	10/18/67
833-14292-P001		Connector, High Performance Crimp Contract	3/13/68
833-14293-P001		Integrated Circuit, High Gain Amplifier	3/11/68
833-14294-P001		Low Power Diod - Transistor Micrologic	2/12/68
833-14295-P001		Connectors, Bayonet-Lock, Snap - In Contacts	3/15/68
833-14296-P001		Connector, Miniature Electrical	2/7/68
833-14297-P001		Connectors, Sub-miniature	4/10/68
833-14298-P001		Connectors, Precision RF Coaxial	1/22/68
833-14299-P001	Amend 1B	Connectors, Sub-miniature Rectangular	4/4/68
833-15100-P001	Amend 3	Telemetry Subsystem	5/3/68
833-15201-P001	Amend 4	Current Sensor	4/14/68
833-15202-P001	Amend 2A	Constant Current Regulator	12/18/67
833-15204-P001	Amend 1	Relay, Special Purpose	11/1/68
833-15293-P001	Amend 2	Current Sensor	2/14/68
833-15294-P001		Connectors, Bayonet-coupling	4/10/68
833-15295-P001	Amend 1	Fuses, Sub-miniature	12/12/67
833-15296-P001	Amend 1A	Relay, Micro-miniature	1/18/68
833-15297-P001		Printed Circuit Connector	10/16/67

TABLE 2.2-1 (con't)

833-15298-P001	Amend 1B	Relay Miniature, Magnetic Latching	1/8/68
833-15299-P001	Amend 1	Silicon Zener Diodes	8/23/68
833-15401-P001	Amend 2A	Command Receiver	12/13/67
833-15402-P001	Amend 1	Phase Demodulator	9/11/67
833-15403-P001	Amend 4	DC to AC Inventor	1/17/68
833-15404-P001	Amend 1	Tape Recorder	5/6/68
833-15405-P001	Amend 2A	Transmitter	4/10/68
833-15409-P001	Rev A	Command Decoder	9/21/67
833-15410-P001		Diplexer Assembly	7/26/67
833-15411-P001		Hybrid Power Divider	7/24/67
833-15415-P001	Amend 1	DC to DC Converter	9/11/67
833-15416-P001	Amend 4	Silver Oxide - Zinc Battery	4/4/68
833-15417-P001	Amend 2	Battery Charge	10/30/67
833-15418-P001	Amend 1	Zener Voltage Limiter Assembly	8/14/67
833-15420-P001	Rev A	Terminal Junction	1/6/68
833-15424-P001	Amend 2	Switching Mode Regulator	6/12/68
833-15631-P001	Amend 2B	Relay, Micro-Miniature	1/19/68
833-15697-P001		Therma-Link Retainer/Dissipators	12/7/67
833-15698-P001		Standoff Terminal	11/14/67
833-15699-P001	Rev B	Connectors, #20 Contacts	1/6/68
833-15701-P001		Amplifiers, Three (3) for Signal Conditioner	8/14/67
833-15799-P001	Amend	Power Supply, Miniature	12/6/67
833-15996-P001	Rev B	50 W. Silicon Zener Diode	2/19/67
833-15996-P001		Probe (Isotherm) Thermistor	11/21/67
833-20101-P001	Rev A	Terminal Board	2/23/68
833-20101-P001	Amend 2A	Command Encoder	3/13/68

SECTION III

MECHANICAL/STRUCTURAL

The basic structural design of the SERT II Spacecraft Support Unit, consistent with the design of the SERT II Spacecraft, was obtained from the Lewis Research Center. The SERT II SSU is required to mate between the Agena and spacecraft, as well as providing necessary mounting provisions for the SSU electrical components. A simple rigid structure, consisting of eight (8) circumferential bays and a center bay, utilizing removable trays for equipment installation was considered.

The structural design efforts of Fairchild Hiller Corporation included the following tasks:

1. Control of the Spacecraft Support Unit weight and center of gravity.
2. Trays which support the electronic components.
3. Installation of four Control Moment Gyros.
4. Structural integrity of electronic packages.
5. Installation of Silver-zinc Battery.
6. Modifications to Lewis Research Center design structure necessitated by installation of FHC components.

The first five of these design efforts are discussed in further detail in following paragraphs. The modifications to the Lewis Research Center (LeRC) designed structure were made using an "equal strength" criteria, (i.e., any modification left the structural member with equal or greater load carrying capacity than the original design).

The component designs were based on the inertial loadings induced by a combined vibratory and quasi-steady environment. Although a mathematical simulation of the complete SSU structure was not performed, the elasticity of the individual components was considered. During design, emphasis was placed on elimination of coincidental resonance between components and the SSU structure. Limited data on the structural properties of the SSU were available from tests performed at LeRC.

3.1 WEIGHT

An initial weight design goal of four hundred eighty (480) pounds and a target goal of four hundred fifty-five (455) pounds was established for the Spacecraft Support Unit. During the development of the SSU structural design several modifications resulted in weight increases, among them the CMG mounting structure redesign and addition of gussets for increased strength of the structure. The weight increases were more than offset by weight reduction factors. Magnesium was utilized for structural components including posts, doublers, skins, and some gussets. The use of magnesium resulted in a weight savings of approximately twenty-three (23) pounds. Redesign of the Power Control Electronics Unit resulted in saving approximately six (6) pounds. Table 3.1-1 lists a summary of weights including the first estimated weight.

The Flight Model SSU was weighed by placing the unit on three (3) calibrated load cells which were located in relation to the interface hole pattern. The instrumentation consisted of the load cells, harness, spider box, and SR-4 strain indicator. The system was calibrated to read within one-half (1/2) pound per load cell. The Flight Model SSU weighed 444.44 pounds without skins or their attaching hardware. The unpainted skins weighed 10.0 pounds and the attaching hardware weighed 2.5 pounds. The total weight of the Flight Model SSU is therefore 456.9 ± 1.5 pounds.

3.2 CENTER OF GRAVITY LOCATION

The design goal for location of the c.g. was for it to be located within 1/2 inch of the longitudinal axis of the Spacecraft Support Unit. Table 3.2-1 lists the final Summary Weight and Balance Estimation of the SSU. Table 3.2-2 The Equipment Weight and Balance estimate.

Center of gravity was measured on the Flight Model Spacecraft Support Unit. The Flight Model c.g. was found to be at:

$$z = +.08 \text{ in}$$

$$y = -.45 \text{ in}$$

The measured location compares favorably with the estimated location of $z = +.245$ in and $y = -.404$ in. It should be noted that the addition of skins and hardware to the Flight Model SSU would tend to move the c.g. closer to the theoretical center. The c.g. location in the x direction was not measured.

TABLE 3.1-1

SUMMARY WEIGHT ESTIMATION OF SSU

	First Estimated WT (lb)	Flight Unit Estimated WT (lb)	Flight Unit Measured WT (lbs)
1. Structure	131.46	108.5	-
2. Bay #9 - CMG Structure	15.2	26.5	-
3. Shelf structure	45.78	36.00	-
4. Electronic Equipment	254.36	240.1	-
5. Harness Assemblies	35.0	49.5	-
6. Point	3.0	3.0	-
Totals	484.78	463.6	456.9

TABLE 3.2-1

SUMMARY WEIGHT & BALANCE ESTIMATION OF SSU

		Wt. (lb)	Y mom (in-lb)	Z mom (in-lb)	X mom (in-lb)
1.	Structure	108.5*	0	0	1033.9
2.	Bay #9 - CMG Structure	26.5*	0	0	1001.3
3.	Shelf Structure	36.00	0	+104.2	+ 209.7
4.	Electronic Equipment	240.1*	- 28.31	+ 22.82	+ 1418.0
5.	Harness Assemblies	49.5*	-159.4	+ 32.1	+ 646.5
6.	Paint	3.0	0	0	0
	Totals	463.6	-187.71	+113.48	+ 4309.4

C. G. Location $\bar{y} = \frac{-187.71}{463.6} = -.404$ in $\quad \bar{x} = \frac{4309.4}{463.6} = +\ 9.40$ in

$\bar{z} = \frac{+113.48}{463.6} = -.245$ in

Note: It is assumed that the basic structure, the CMG installation, the antenna installation and paint are all summetrically placed about the center line in the Y and Z directions.

*Note: Actual Weight of Prototype System

TABLE 3.2-2

EQUIPMENT WEIGHT AND BALANCE

Bay #2 Upper	Wt. (lb)	Y arm (in)	Y mom (in-lb)	Z arm (in)	Z mom (in-lb)	X arm (in)	X mom (in - lb)
A17 Time Code Gen	2.0	+ 13.88	+ 27.76	+ 8.25	+ 16.50	13.15	26.3
A36 Terminal Blocks	1.0	+ 16.00	+ 16.00	- 11.00	- 11.00	18.75	18.5
A16 2 Pt Calb Gen	.24*	+ 19.16	+ 4.00	+ 10.00	+ 2.40	12.68	3.0
A31 PCM Subcom	2.3 *	+ 23.94	+ 55.06	+ 6.64	+ 15.27	13.06	30.0
A30 " "	2.3 *	+ 23.94	+ 55.06	- 0.00	0.00	13.06	30.0
A29 " "	2.3 *	+ 23.94	+ 55.06	- 6.64	- 15.27	13.06	30.0
A28 " "	2.3 *	+ 14.61	+ 33.60	+ 8.28	+ 19.04	13.06	30.0
A27 PCM Multicoder	4.8 *	+ 14.40	+ 69.12	- 2.95	- 14.16	13.97	67.1
A35 " "	4.8 *	+ 14.40	+ 69.12	- 2.95	+ 14.16	13.97	67.1
	22.04 *		+ 385.53		+ 26.94		302.3
Bay #2 Lower							
A12 Tape Recorder	9.3 *	+ 15.60	+ 145.00	+ 6.82	+ 63.40	3.66	34.0
A13 " "	9.3 *	+ 15.60	+ 145.00	- 6.82	+ 63.40	3.66	34.0
A26 VCO Mixer	1.8	+ 25.30	+ 45.54	- 1.85	- 3.33	2.06	3.7
A18 Filter	1.8	+ 25.70	+ 27.70	+ 7.00	+ 7.00	2.06	2.1
	22.4		+ 361.24		+ 3.67		73.8

* Actual Weight

TABLE 3.2-2 (continued)

EQUIPMENT WEIGHT AND BALANCE

Bay #4 Upper	Wt. (lb)	Y arm (in)	Y mom (in-lb)	Z arm (in)	Z mom (in-lb)	X arm (in)	X mom (in-lb)
A33 SMR (Main)	4.8 *	- 8.70	- 34.80	+ 15.70	+ 62.8	13.56	54.2
A34 SMR (Standby)	4.8 *	+ 8.70	+ 34.80	+ 15.70	+ 62.8	13.56	54.2
A32 Signal Conditioner	4.62 *	0	0	+ 24.00	+111.00	14.31	66.1
A39 Battery Charger	2.8 *	0	0	+ 15.70	+ 59.60	13.56	51.5
	17.02		0		+296.2		226.0
Bay #4 Lower							
A9 Inverter	11.5 *	+ 5.60	+ 64.40	- 14.88	+171.12	3.15	36.2
A 10 "	11.5 *	- 5.60	- 64.40	- 14.88	+171.12	3.15	36.2
	23.0		0		+342.24		72.4
Bay #6 Upper							
A37 Comm'd Relay Junc Box	8.6 *	- 18.31	- 157.50	+ 6.09	+ 59.30	15.06	129.5
A 24 & A25 Comm'd Receiver	2.2 *	- 14.9	- 32.78	- 0.60	- 1.32	13.19	29.0
A 19 Comm'd Decoder	5.9 *	- 21.88	- 129.09	- 7.65	-45.14	13.31	78.5
	16.7		- 319.37		12.84		237.0

TABLE 3.2-2 (continued)

EQUIPMENT WEIGHT AND BALANCE

Bay #6 Lower	Wt. (lb)	Y arm (in)	Y mom (in-lb)	Z arm (in)	Z mom (in-lb)	X arm (in)	X mom (in-lb)
A 5 & A6 Phase Sens Demon	1. *	-17.15	- 17.15	+ 8.20	+ 11.40	1.76	1.8
A7 & A8 " "	1. *	-17.15	- 17.15	- 8.20	- 11.48	1.76	1.8
All Power Control	26.0 *	-17.15	-445.9	0.00	0.00	4.56	118.6
	28.0		-480.2		0		122.2
Bay 8							
A20 Diplexer	3.4 *	+ 7.38	+ 25.09	-21.13	- 71.84	2.86	9.7
A44 Diplexer	3.4 *	+ .33	- 1.12	-23.63	- 80.34	2.86	9.7
A45 Hybrid	3.7 *	- 7.90	- 29.23	-22.59	- 83.58	1.50	5.6
A14 Xmtr	1.04 *	+ 1.06	+ 1.06	-14.50	- 14.50	1.86	1.9
A15 Xmtr	1.04 *	- 7.31	- 7.31	-14.5	- 14.50	1.86	1.9
A38 Battery	34.3 *	0.00	0.00	-12.71	-435.95	10.25	351.6
	46.83		- 11.51		-704.71		380.4
Miscellaneous					(See CMG Structure)		
CMG (4)	62.8	0	0	0	0		
Antennas (4)	1.3 *	0	0	0	0	3.00	3.9
	64.1		0		0		3.9
	240.09		- 28.31		- 22.82		+1418.0

* Actual Weight of Experimental SSU Components

3.3 TRAY DESIGN

The SSU tray design was founded upon the following considerations:

A. Thermal Sink - The tray must provide a sufficient conduction path for the heat being dissipated from tray mounted packages.

B. Frequency - An octave separation between the tray frequency and the overall SSU fundamental frequency was desired.

C. Resonant Amplification - The proximity of the electronic package qualification vibration level to the SSU prototype structural input limits the allowable amplification.

D. Strength - Trays were designed to withstand the inertial load of the electronic packages due to the combined vibratory and sustained "g" boost environment.

E. Weight - The normal procedure of reducing the weight without adversely affecting the four previous considerations was established.

The following paragraphs present the design philosophy, and a brief history of the evolution of the final tray design.

Figure 3.3-1 presents the electronic package qualification vibration level, and the SSU prototype vibration level. From these two curves and the predicted resonance of the overall structure, the desired tray frequendy was established. A 60 to 100 Hz region was selected for the tray frequencies. Maximum allowable amplification and weight consideration were the reasons for the selection of the low frequency tray.

Attempting to reduce the amplification below that of conventional structure, a structural damping technique known as RIGIDAMP sheet was utilized. RIGIDAMP sheet obtains a high degree of damping by laminating conventional structural materials with thin layers, .005 inch, of viscoelastic damping material. A tray analysis was performed using amplification factors from test data. From this analysis the final tray design was established as two .071 inch 2024-T3 aluminum laminates bonded together to form a RIGIDAMP sheet. Based on this design the lowest tray frequency was found to be 43 Hz. This Frequency is somewhat lower than originally desired but still is separated from "POGO" and CMG frequencies. The original 60-100 Hz region for tray resonances was relaxed for two reasons; the CMG system frequency was lower than predicted which allowed a lower tray frequency without coincident amplification, and the weight penalty associated with the thicker laminate necessary for the 60-100 Hz tray frequencies was undesirable, Table 3.3-1 shows

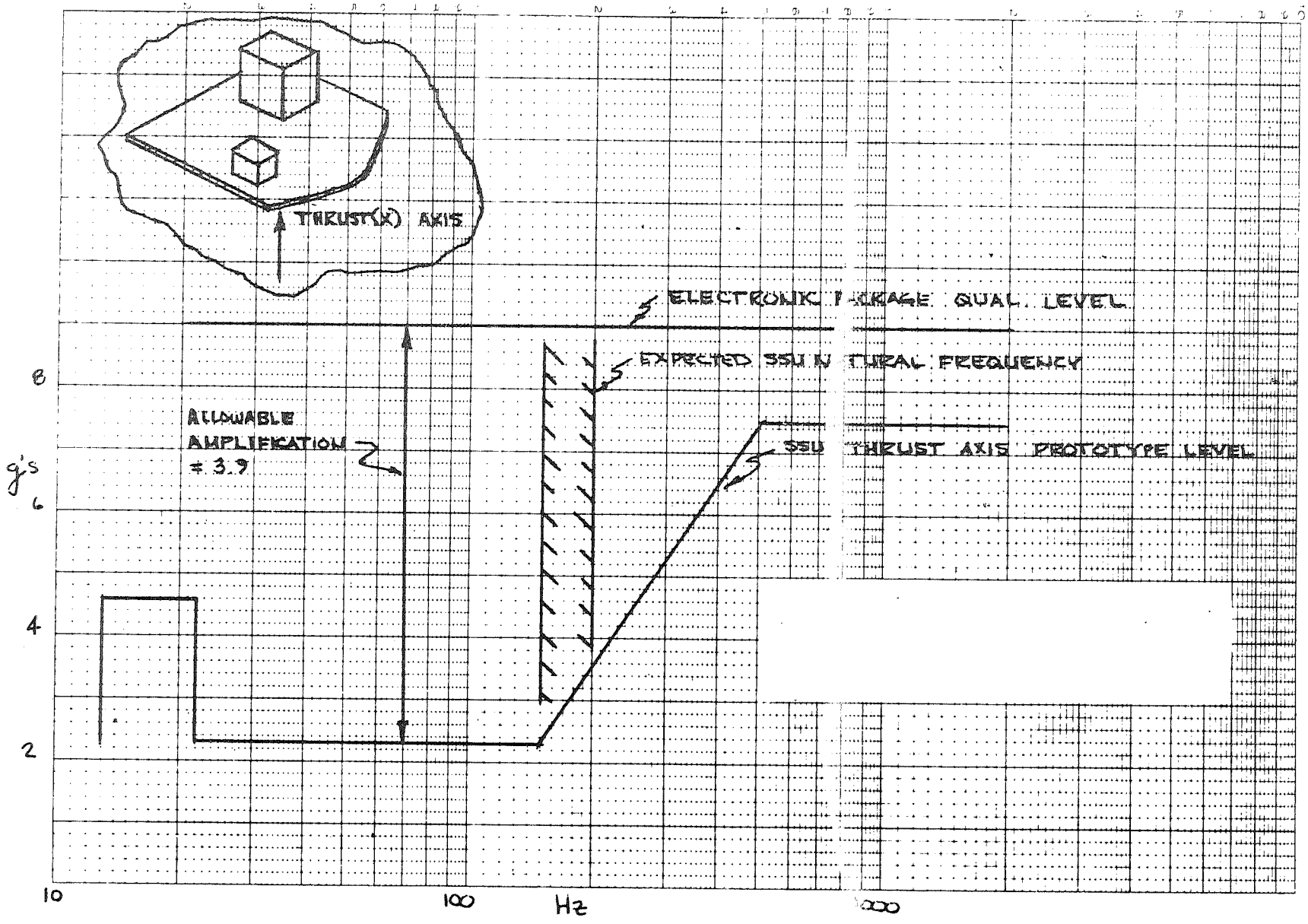

Figure 3.3-1. Comparison of Qualification Vibration Levels

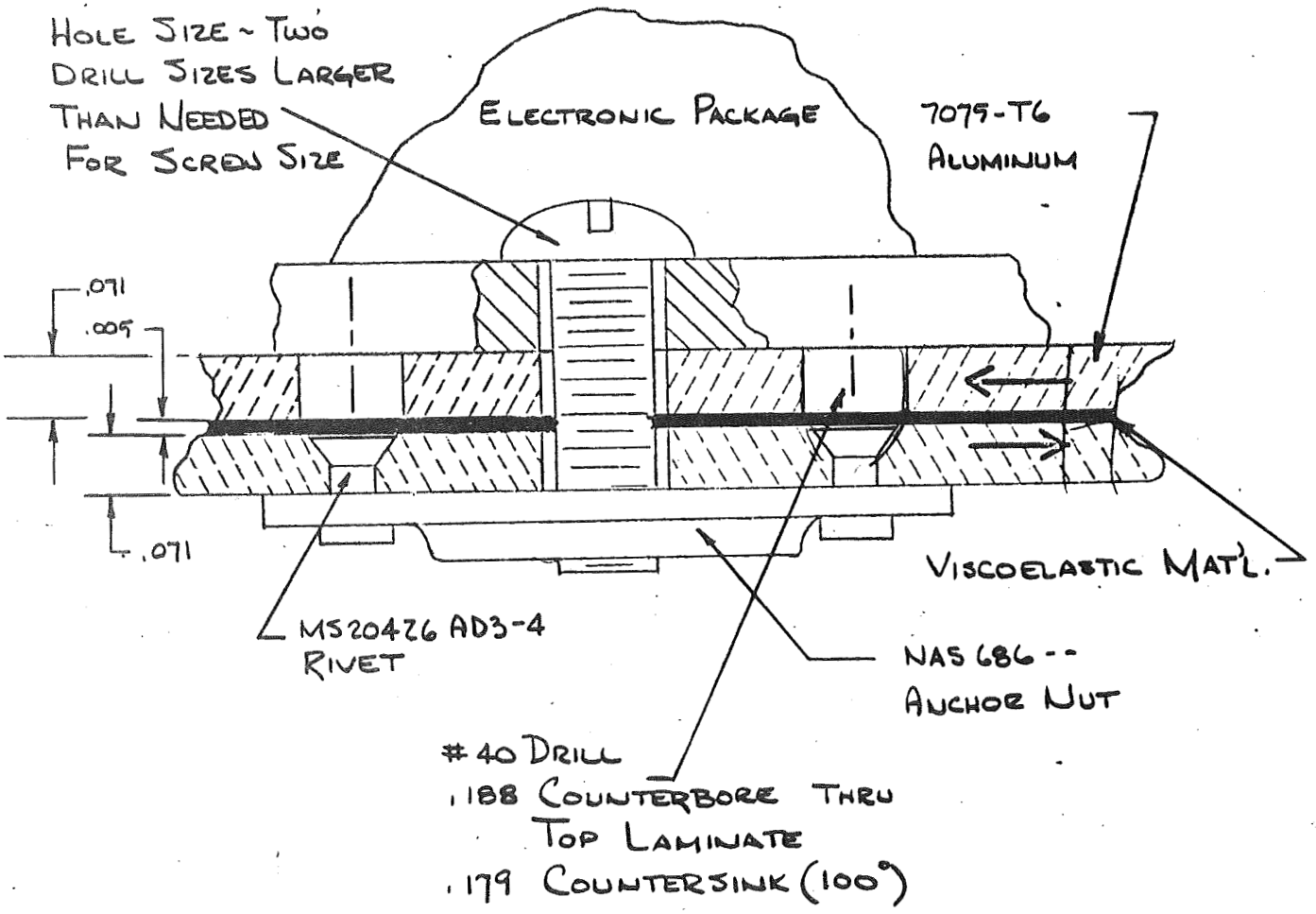

Figure 3.3-2. Attachment of Electronic Packages to RIGIDAMP Tray

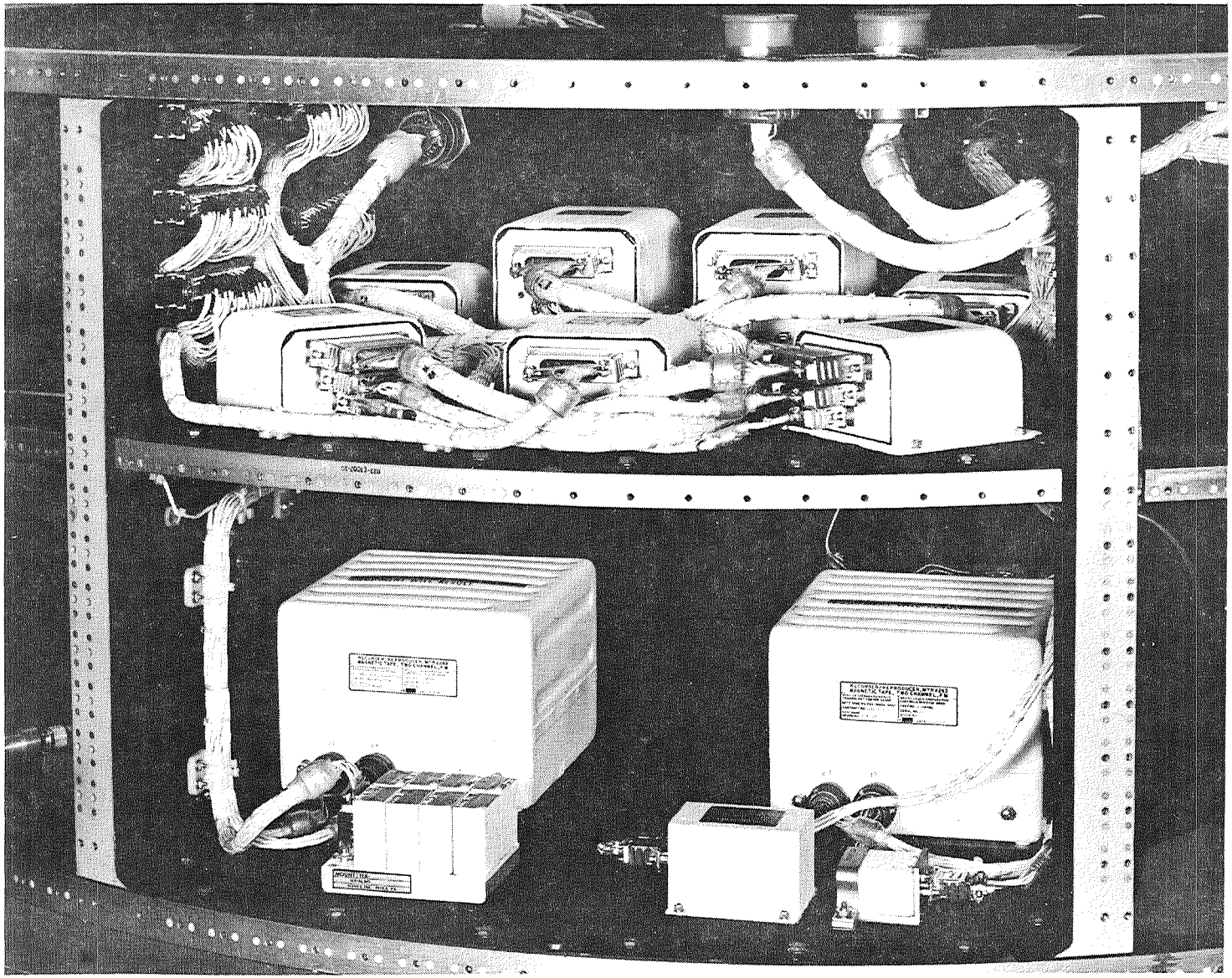

Figure 3.3-3. Equipment Configuration - Bay 2

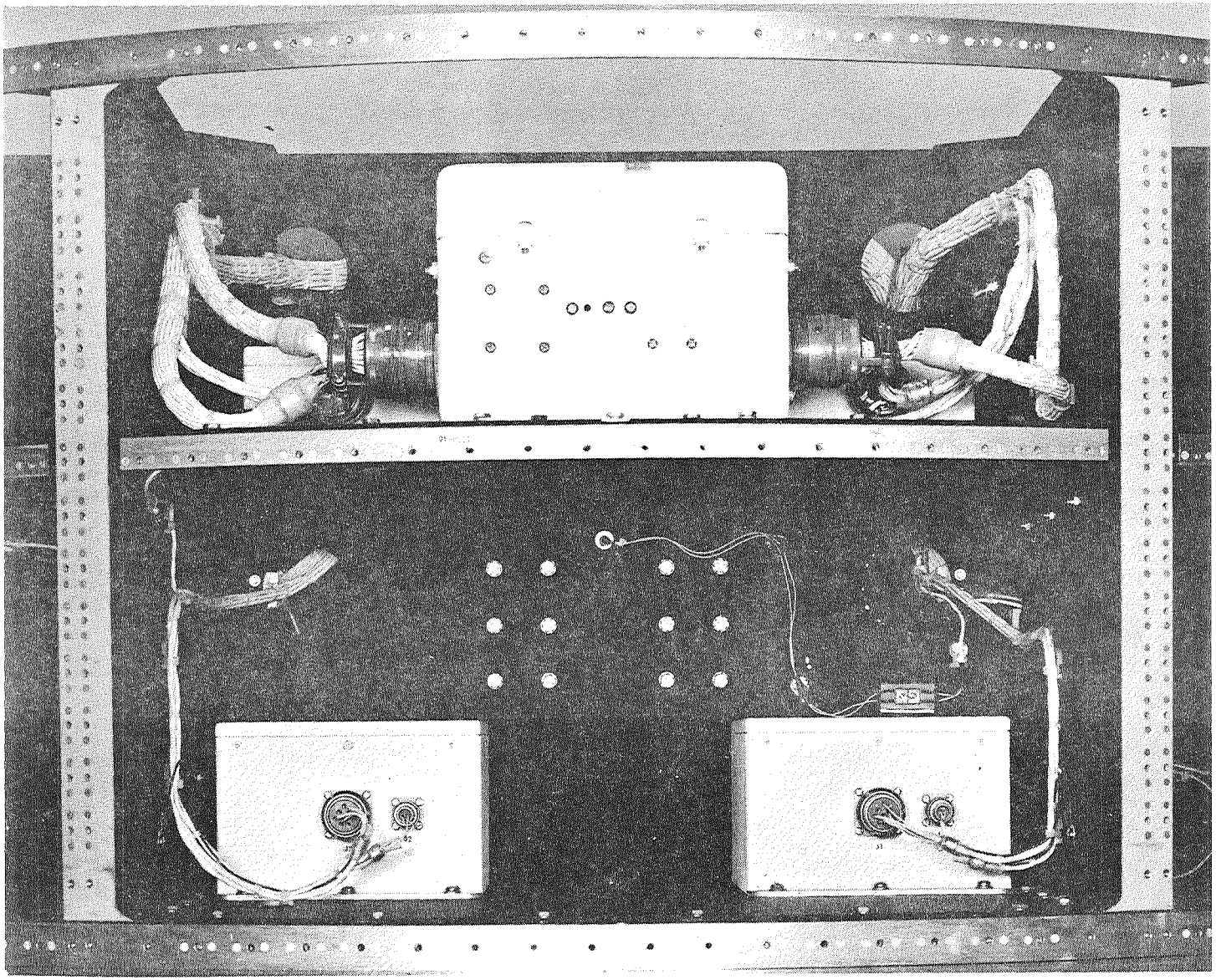

Figure 3.3-4. Equipment Configuration - Bay 4

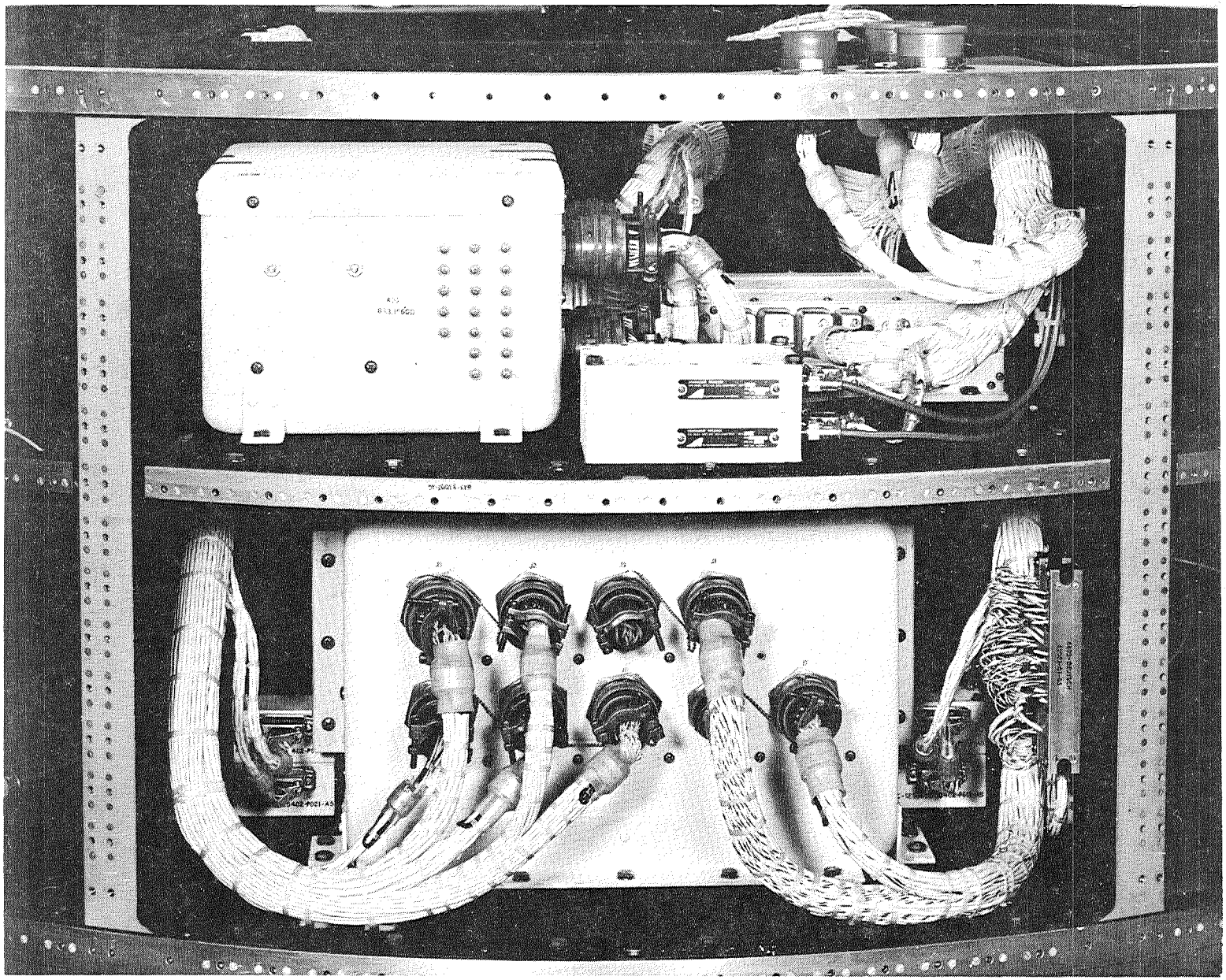

Figure 3.3-5. Equipment Configuration - Bay 6

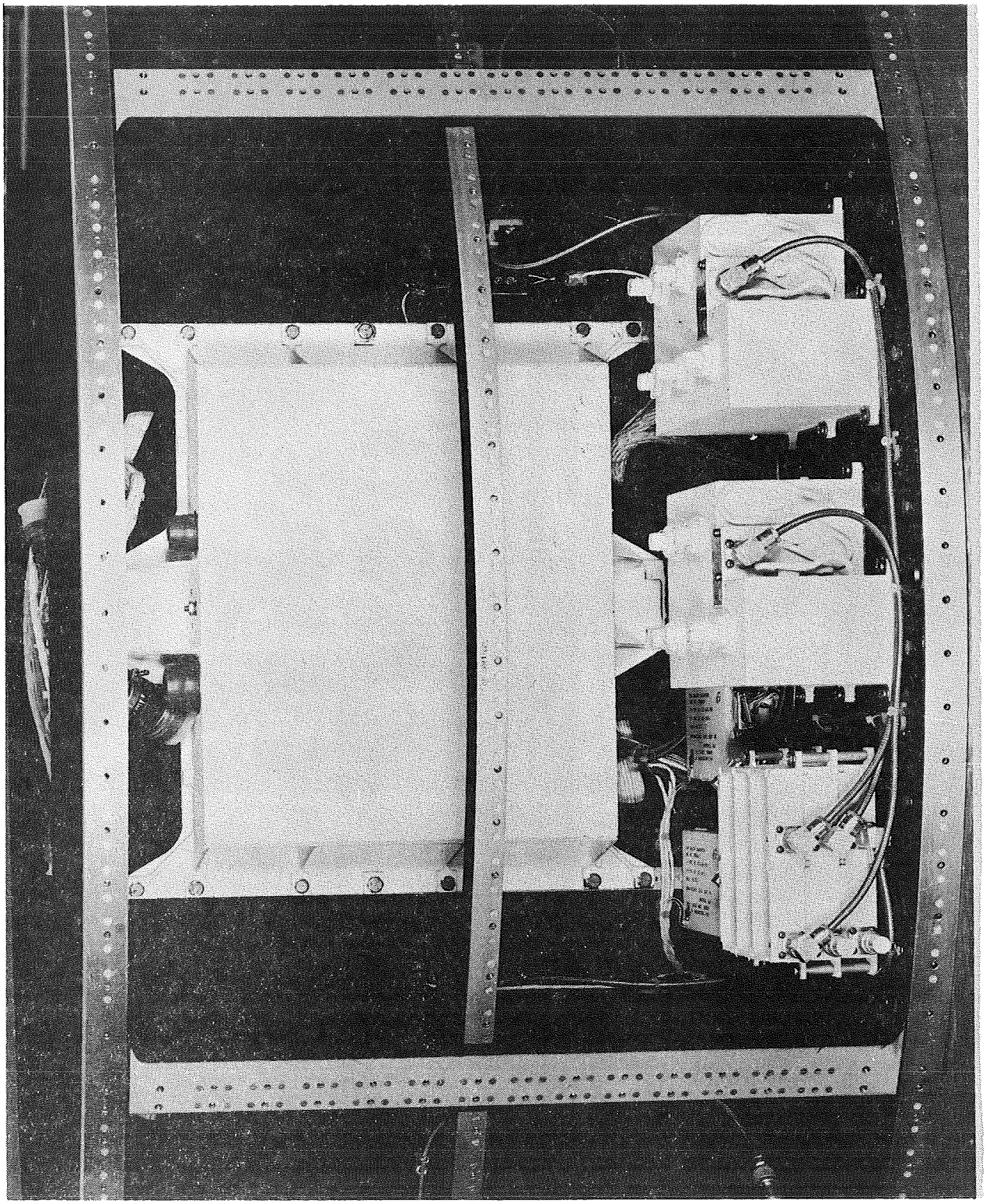

a comparison of the .125 inch RIGIDAMP tray. Table 3.3-2 shows the reduction in frequency of a .125 inch RIGIDAMP tray mounted to the shaker vs. being mounted to the SSU.

Bay 6 Lower (FHC Test Data)	fn	Resonant Amplification
.125 in. Solid Aluminum Tray	62 Hz	14.6
.125 in. RIGIDAMP Tray	45	8.0

Table 3.3-1 Comparison of .125 in Solid and RIGIDAMP Tray Characteristics (Shaker Mounted)

Bay 6 Lower RIGIDAMP	fn	Resonant Amplification
FHC (Shaker Mounted)	45 Hz	8.0
LeRC (SSU Mounted)	40	5.0

Table 3.3-2. RIGIDAMP Tray Data - Rigid and Elastic, SSU Structure Support

To allow the viscoelastic material to function properly, the mounting of the electronic packages were as shown in Figure 3.3-2. This technique allows the necessary relative motion between the two laminates. The harness tie downs were also designed to allow for the energy dissipating slip plane. Over size holes were drilled such that the connector through the tray did not prohibit relative motion.

Figures 3.3-3 through 3.3-6 are pictures that display the final configuration of equipments in Bays 2, 4, 6, and 8 respectively.

3.4 CONTROL MOMENT GYRO INSTALLATION

3.4.1 DESIGN PHILOSOPHY

Two requirements dictated the design philosophy for mounting the four Control Moment Gyros, (CMG), in the central bay of the SSU. These requirements were the low allowable vibration input to the CMG's, and the severe alignment tolerances.

A comparison of the SSU prototype vibration input and the CMG qualification vibration levels is presented in Figure 3.4-1. In the thrust axis the structural input exceeded the qualification level of the gyros from 150 to 2000 Hz. Since the SSU structure did not possess dynamic characteristics which would attenuate vibration throughout this frequency range, isolation of the CMG's was necessary.

Due to the alignment tolerances, later to be discussed in detail, the four CMG's were rigidly mounted to a platform which was supported on four multi-directional vibration isolators. This technique prevented untolerable relative displacement between the gyros, which could occur if each gyro were to be isolated individually. The CMG platform, consist of four major fittings mounted on a 4 x 6 inch built-up box beam 20 inches long and is illustrated in Figure 3.4-2.

The design of the beam and fittings was determined not by strength requirements but by stiffness which greatly exceeded the needed strength. The required beam stiffness, and thus the natural frequency were dictated by the dynamic characteristics of the isolators, critical frequencies of the gyros, and the overall structural characteristics of the SSU. The natural freauency of the beam was to be such that the isolators would sufficiently attenuate the vibration when the beam assembly went into resonance. Although the isolators would be isolating the CMG beam from the SSU structure when the overall structure resonated, there would be a higher vibration level experienced by the gyros at this time. Therefore, separation of beam and overall SSU resonances was deemed necessary. Certain critical bandwidths of the gyros had been established during previous Lewis Research Center tests, and it was also desirable to separate beam resonances from these regions. The design approach minimizes the coupling between the structure, gyros, isolators, and beam, and the accompanying high vibratory amplifications.

3.4.2 PRELIMINARY BEAM ANALYSIS

During the design of the CMG beam the exact characteristics of the isolators were still unknown as final selection of the isolator model was to be based on future FHC testing. Estimating the highest natural frequency expected from the isolators and noting the minimum isolator frequency ratio, f/f_n, at which maximum attenuation occurs, a minimum beam frequency of 500 Hz was established. A built up box beam 4.5 inches high and approximately 6 inches wide was designed to give this required frequency.

At this time, a calculation which treated the beam as a simply supported lumped mass beam was performed. Treating the beam as simply supported yielded the lowest possible frequency, as the isolator flexibility will allow the beam to act somewhere between the simply supported and the higher frequency free-free system. The calculation produced a simply supported beam frequency of 337 cps. A frequency much greater than 500 cps was expected when the isolator flexibility was considered.

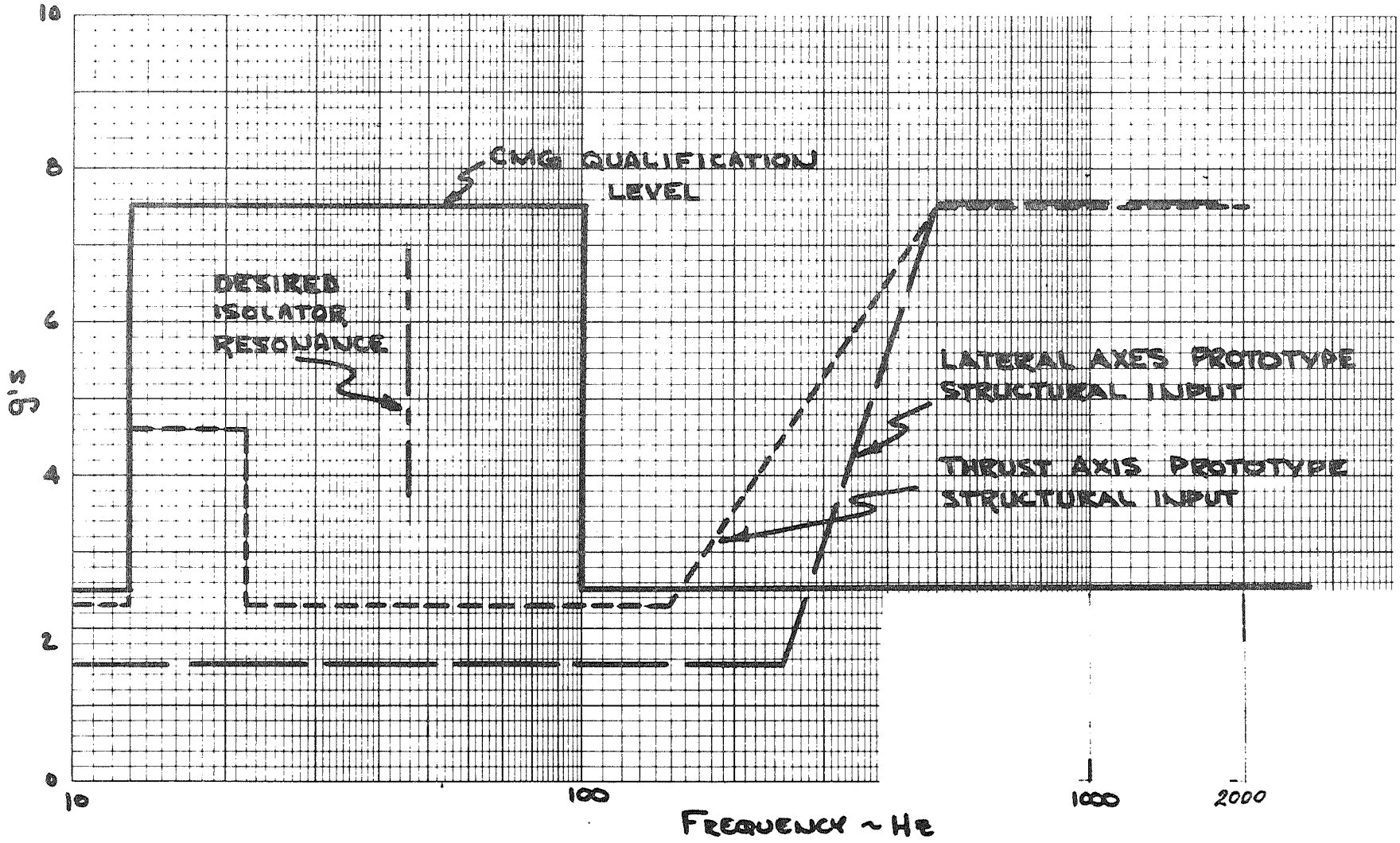

Figure 3.4-1. Comparison of CMG Qualification and Structural Input Levels

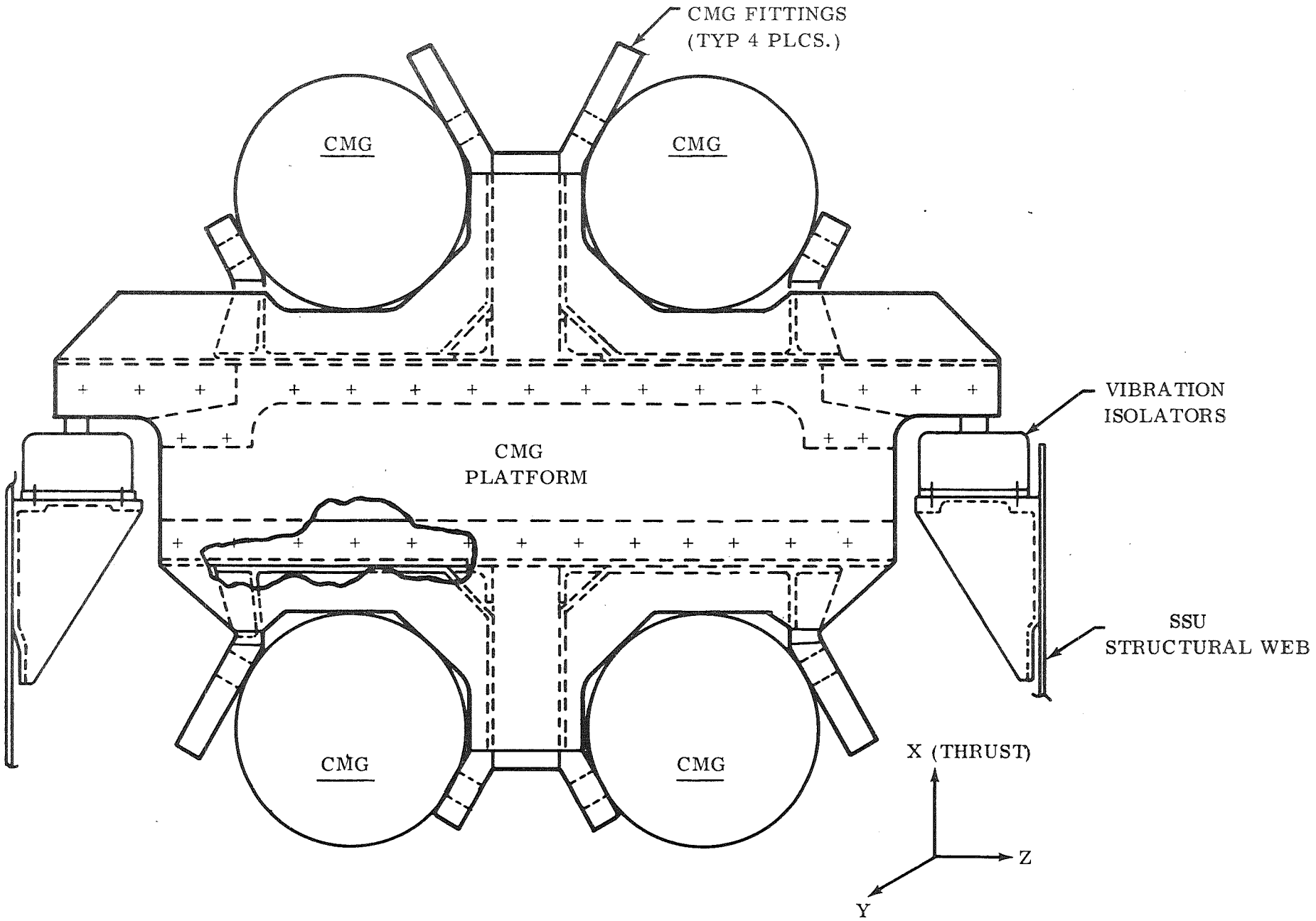

Figure 3.4-2. CMG Platform

3.4.3 SELECTION AND TESTING OF ISOLATORS

Lord Manufacturing Company Broad Temperature Range HT2- series elastomeric mountings were selected as the CMG vibration isolators. The particular mountings were selected based on their estimated natural frequency when supporting the CMG's and platform. It was desired to locate the natural frequency midway in the 22-100 Hz region of the vibration spectrum, Figure 3.4-1, where the unavoidable isolator resonant amplification could be tolerated. Two models of this series, HT2-35 and HT2-50, were selected to undergo a series of tests at FHC. This test series was to investigate both the vibration characteristics, and the ability of the isolators to maintain the critical angularity tolerances imposed on the CMG's.

The first of these tests was to establish the natural frequency, resonant amplification, attenuation, and the dependency of these vibration characteristics on sustained acceleration. The isolators, being heavily damped non-linear springs, have dynamic characteristics which are a function of the deflection of the isolators. Sustained acceleration such as the booster environment will cause increased deflection and an associated change in isolation properties. The isolator dynamic characteristics were to be obtained for 1g, 5g, and 10g simulated sustained accelerations which are the extremes and mid point of the sustained boost acceleration.

A dummy mass equivalent to that which the isolator will support in the SSU was attached to a vibration isolator, as shown in Figure 3.4-3, and the isolator mounted to the head of a shaker. An input accelerometer was mounted on the shaker head, and a response accelerometer on the mass. These were monitored and recorded by the system shown in Figure 3.4-4.

For the sustained 1g condition the SSU structural qualification vibration level was simply input to the shaker and both the input and response monitored, and plotted as g level verses frequency. The sustained 5 and 10g conditions were simulated by applying a load to the isolator causing a deflection equivalent to that which the desired sustained g level would produce. The load is applied through elastic chord as shown in Figure 3.4-3. A 28 inch free length of two-strand 3/8 inch diameter chord was attached to the mass through the eye bolt and to a dial indicator scale on a chain fall which was supported on a portable gantry. The tension in the elastic chord was increased to the desired value by means of the chain fall with a maximum stretched length for the sustained 10g condition of 60 inches. Once the desired load was attained the vibration level was input, and both input and response monitored as in the 1g sustained condition. Analytical justification of this simulation is presented on pages one and two of Appendix C. The dial indicator, monitoring chord tension, was also monitored during the test to assure any resonant oscillations of the chord occurred at a low frequency which did not interfere with the isolator response.

Two of each isolator model were tested to insure repeatibility of data. The four isolators were tested where SSU prototype level vibration was input to the isolator and the response of the dummy mass was compared to the CMG qualification level. Although both the HT2-35 and HT2-50 mounts exceeded the qualification level

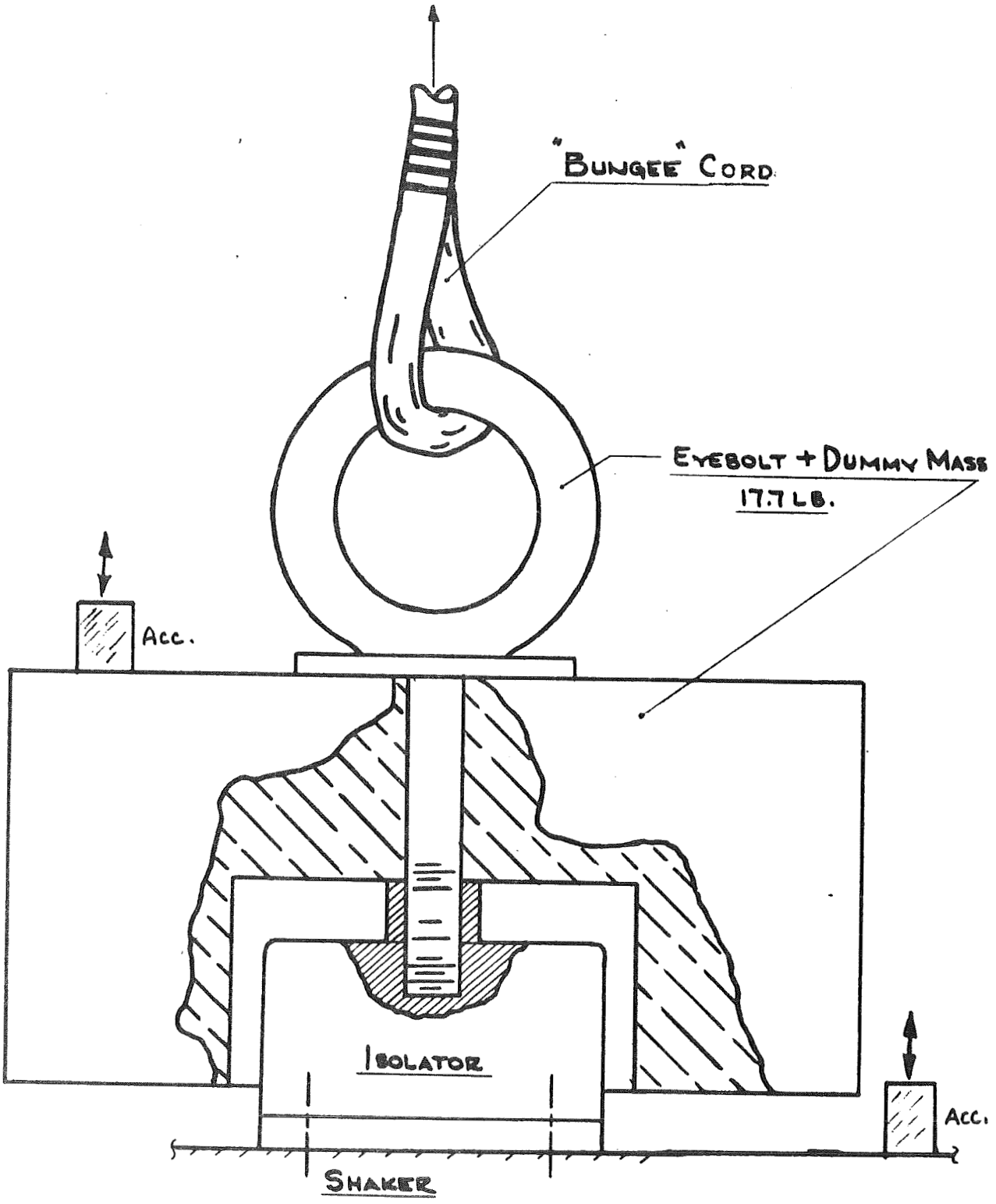

Figure 3.4-3. Test Configuration

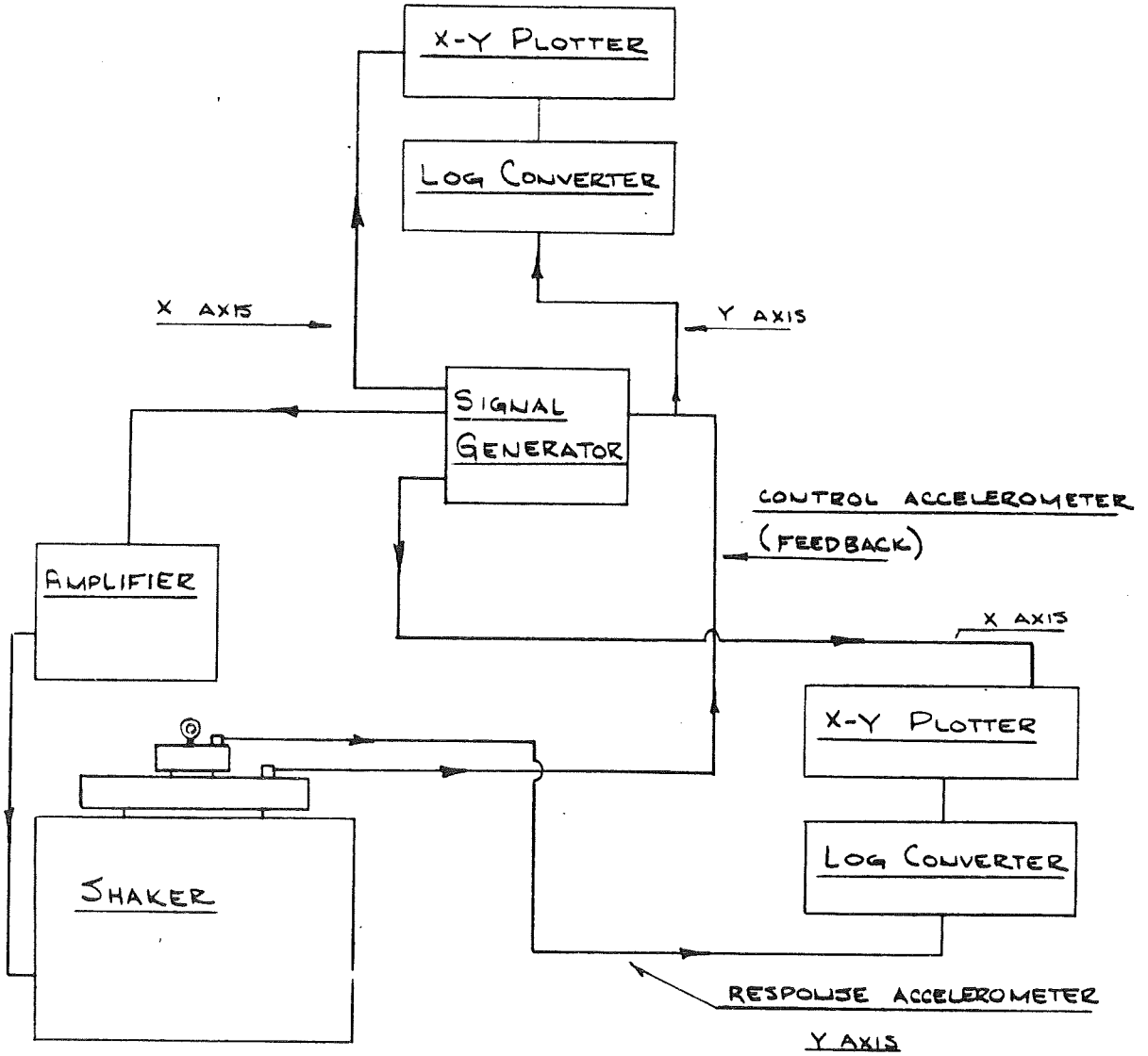

Figure 3.4-4. Schematic Diagram of Isolator Response Test

during narrow frequency bands only during the higher sustained g cases did the HT2-35 mounts exceed this level. The lower frequency of the HT2-35 mounts was also more desirable since it afforded greater separation from the expected 150 to 200 Hz overall SSU fundamental frequency. The HT2-35 mounts were initially selected as the isolators for the CMG installation, and later changed to HT2-50 due to a 10 pound increase in the weight of the CMG assembly.

Due to the lesser distance between the isolators, the angularity tolerance about the Z axis is the most critical in terms of equivalent isolator deflection. Difference in residual deflections of only .008 in. are allowable in this plane. It was assumed that all manufacturing tolerances would be eliminated by shimming and that the total angular tolerance could be attributed to non-uniform returnability of the four isolators after vibration and sustained acceleration. The inability of the isolators to return to their initial position after vibration is due to the hysteresis of the elastomeric material. During sustained acceleration the elastomeric material is compressed and possibly shifted within the isolator housing.

A test which would simultaneously simulate the combined sustained and vibration accelerations, and also allow the isolator deflection to be measured precisely under a "0" g environment was considered rather complex and in fact unnecessary. The effect of the sustained and vibratory accelerations were considered independently and then linearly combined. This in fact is a more severe test than the simultaneous occurence of the two phenomena, as the vibration would help reduce the residual deflection from a sustained acceleration. A segment of the residual deflection from the sustained acceleration is due to binding between the compressed elastomeric material and the isolator housing, a simultaneous vibration environment would reduce this binding effect.

The deflection attributed to a sustained acceleration was simulated by compressing the isolator in a compression machine and approximating the load time history the isolator would experience during the boost phase. The applied loading consisted of an initial 20 lb. load which was steadily increased to 200 lbs. in a 5 minute interval. Three HT2-35 mounts were tested in this manner. The mounts were measured immediately prior to applying the load and after releasing load at intervals sufficient to yield a time history of the retained deflection of the mount.

Two of the three mounts were tested a second time which yielded much improved results. The difference between the first and second runs was attributed to manufacturing tolerances within the mount which were absorbed during the first run.

At 200 lbs. sustained load 10g environment, the isolators deflect approximately .2 in.

Test results indicate the steady boost acceleration alone would not cause the angularity tolerances of the CMG Assembly to be exceeded. The two mounts which were retested after being preloaded crept back to their initial position along curves which were always within .003 in. of one another.

The maximum isolator deflection due to prototype vibration was calculated to be less than .32 in. as compared to the .20 in. deflection from the sustained loading. The isolator manufacturer suggests that the maximum retained deflection, due to hysteresis, measured immediately after vibration would be less than .015 in. Given sufficient time this retained deflection will decreaseas in the sustained loading.

Once the spacecraft is out of atmospheric turbulence the thrust is assumed the only source of vibration. Therefore, the time for the vibration induced deflection to settle out would be the period from the Agena second burn cut-off until the activation of the CMG's, a period of 2.7 hours. Assuming the vibration induced deflection return rate to be similar to that of the sustained deflection, this time interval is sufficient to allow return of the isolators. Again it should be noted, however, that the difference in retained deflections of the four isolators is critical and not the retained deflections themselves. If the four isolators experience the similar vibration levels, as expected, the variation in their retained deflections will be similar to the variations when the isolators experienced similar sustained loadings.

As it was not conclusively demonstrated that the 0.1° tolerance could be achieved it was recommended that the angular attitude of the CMG beam be monitored prior to and after the SC/SSU system vibration, and that LeRC investigate the possibility of relaxing the angular tolerances. The Z-axis angularity tolerance was increased from 1/10° to 1/6°.

Prior to shipment of the flight unit the top surface of the CMG beam was surveyed and it was found that the maximum difference between any two measurements was .003 inch. Assuming this .003 to be across the beam top the angularity about the Z-axis is 1/30° well within the 1/6° required.

3.5 STRUCTURAL DESIGN OF ELECTRONIC BOXES

The structural design of the three FHC electronic boxes was based on a qualification level vibration environment. The 9g box qualification level was assumed to be amplified, at resonance, through the internal box structure by a factor of 20. Using a safety factor of 1.5 an ultimate load factor of 270 g's (9 x 20 x 1.5) was applied to the electronic components non concurrently in all directions. A static analysis was then performed utilizing the dynamically obtained load factor.

This design philosophy inherently produced an internal support structure with a stiffness which separated it from the fundamental tray frequencies, thus precluding coincidental amplification between the tray and its electronic components.

3.6 BATTERY INSTALLATION

The location of the Silver-Zinc battery within the SSU was dictated by thermal requirements. The Battery was rigidly mounted to the stiffened .063 in. shear web in Bay 8 as shown in Figure 3.3-6.

The installation technique is analytically justified in Appendix E of this report. The battery was structurally analyzed statically using a combined quasi-steady and magnified vibratory load factor.

The battery has been subjected to a previous qualification test during Mariner Program. A comparison of the SSU structural qualification level and the battery qualified level shows an allowable resonant amplification of the structure of 5.5 between 40 and 250 Hz. Although an amplification of 10 was the minimum to be normally expected it was decided not to vibration isolate the battery immediately since the Mariner test levels were based on the environment and did not demonstrate fully the capability of the battery to withstand vibration. An attempt was made to ascertain this capability from the vendor, but was unsuccessful.

During the SSU Mechanical Model vibration tests a wooden battery mass simulation was installed. The only purpose of this simulation was to observe the influence of the 34 lbs. on the overall structural characteristics, and not to monitor the vibratory levels on the wooden simulation. A magnesium battery case filled with dummy weight furnished by LeRC was therefore installed in the SSU and vibrated at prototype levels. This was felt to be as nearly indicative of the vibratory levels to be expected on the actual battery without testing actual components. The results of these tests exceeded the Mariner vibratory levels.

SECTION IV

THERMAL CONTROL

4.1 REQUIREMENTS

A passive thermal design for the SSU was required using space proven thermal coatings and design techniques. The design goal was to maintain the SSU and spacecraft component temperatures within the determined operating temperatures when subjected to the following conditions:

1. Preliminary operation of the SSU enclosed in the launch vehicle shroud with systems operative and external cooling

2. Launch to injection with all SSU systems inoperative

3. From injection until the spacecraft is positioned in orbit but prior to turning on the ion thrusters

4. During six months' mission in uneclipsed sunlight with either thruster operating under the following conditions:

   a) Normal thruster operation

   b) Flux input variations due to fluctuations in the orbit-sun line angle and the SSU attitude

   c) Changes in the optical properties of the coatings (α / ϵ ratio) due to the space environment and the angle of incidence

   d) Variation in the internal heat dissipation due to different modes of operation

5. As the satellite goes into and out of the shadow with thruster off

6. Random tumbling of the satellite with rate up to 1 rpm.

The computer model of the SSU was required to consider the following environmental and internal thermal conditions:

1. All external energy inputs including solar, albedo, and earth fluxes.

2. Conduction through the structure

3. Internal heat dissipation

4. The variation of the thermal control coatings due to space environment

5. Thermal interface with the spacecraft

It was further required that there be thermal conduction between the spacecraft and SSU and that the SSU be thermally isolated from the Agena.

4.2 THERMAL DESIGN

4.2.1 DESIGN APPROACH & PHILOSOPHY

A passive thermal control is only practical when the orbital temperature extremes are within the allowable temperature range of the electronic components. The orbital temperature extremes are determined from the internal power dissipations, the solar, albedo, and earth heat fluxes, and the optical properties of the vehicle coatings.

Heat fluxes influence the vehicle temperature variation in much the s same manner as internal power dissipation does, that is, by its value and range, and by the way it is distributed around the surface of the vehicle. The heat fluxes will vary due to solar activity and seasonal variations. In addition, the reflected solar flux may vary as a result of cloud cover and terrain. These variations are in addition to the basic variation of the fluxes due to the orbit altitude changes. The amount of vehicle heating is dependent upon the optical properties of the coatings. By proper choice of these coatings the vehicle temperatures may be varied to suit the needs of the components, but the temperature variations can only be reduced, not eliminated, by coatings.

The temperature capabilities of the electronic components must be greater than the vehicle temperature extremes.

4.2.2 ANALYSIS

4.2.2.1 Thermal Model

A thermal model was developed to obtain information based on the initial design parameters of the SSU-Spacecraft configuration. The model was designed to yield sufficient data from a minimum number of nodes and to ensure that parameters could be varied easily and quickly. To achieve this goal, forty-four nodal points were chosen as shown in Figure 4.2-1.

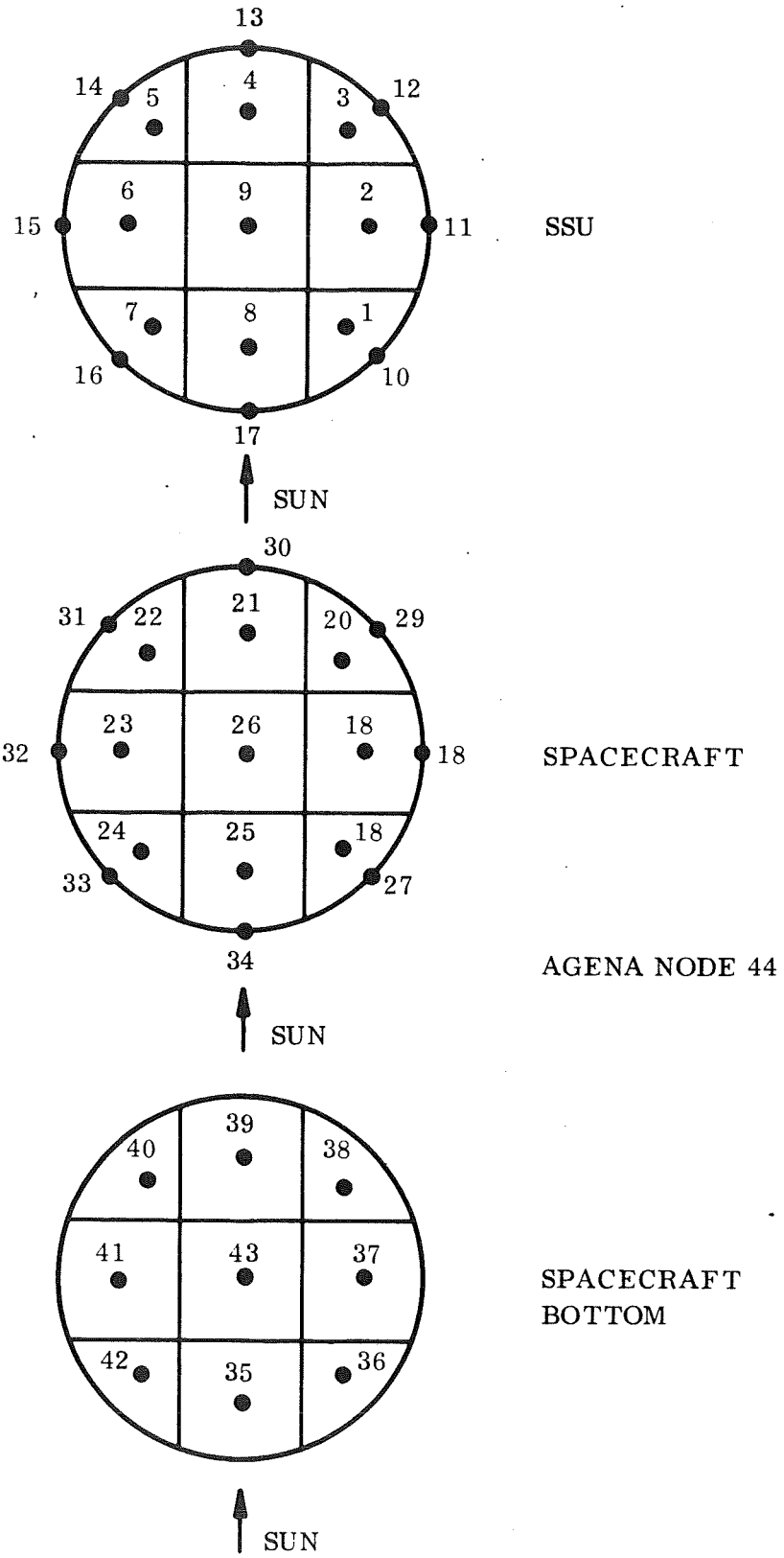

Figure 4.2-1. Thermal Model Nodes

The model was used to calculate temperatures with and without internal thermal radiation. Radiation was found to be significant and was used in all further analysis.

The model considered radiation between bays and units. A constant temperature node was used to represent the Agena vehicle; this was assumed reasonable since the SSU and Agena are thermally isolated by a gasket and radiation shield at the interface. Radiation was also considered between the earth facing side of the spacecraft and the interior of the spacecraft.

This forty-four node model was used to generate the data presented in this report.

In order to meet the requirements of the contract and to enable a more detailed temperature analysis to be performed, a larger thermal model of the SSU was developed in conjunction with NASA LeRC. This thermal model contained 312 nodes and included both radiation and conduction heat transfer. It was designed to be coupled to the Spacecraft thermal model prepared by NASA LeRC so that the complete vehicle could be simulated by computer. This large thermal model of the SSU was delivered to NASA LeRC on September 29, 1967 where it was planned to be used by them for a more comprehensive analysis of the SSU and Spacecraft as a unit.

Due to changes in the structure, the addition of magnesium skin, and changes in design of the CMG mounts, the large SSU CINDA Model required modification to incorporate these new items. This new program was sent to NASA LeRC on January 1968.

4.2.2.2 Orbital Environment

One of the primary design parameters is the variation in solar, reflected solar (commonly designated as albedo), and earth fluxes. It was decided that for the purposes of this analysis a $\pm 2\sigma$ variation would be sufficiently conservative. The nominal values for these fluxes and $\pm 2\sigma$ variation are shown below:

Solar	=	440.0	±	8.8	Btu/Ft^2 -Hr
Albedo	=	0.38	±	0.12	
Earth	=	68.2	±	13.33	Btu/Ft^2 -Hr

In addition to the incident flux variations, a ± 3.4% seasonal variation was also applied to the solar flux.

A combination of the orbital environment parameters, the incident flux 2 variation, and the solar flux seasonal variations yields three design orbits for the SSU vehicle. These three orbits are designated as Hot, Cold, and Nominal Cases.

The hot case orbit consists of + 2 σ variation on fluxes, + 3.4% seasonal variation on solar flux, orbit altitude of 478 nautical miles, and orbit norm normal to sun. The cold case consists of -2 σ variation on fluxes, -3.4% variation on solar flux, orbit altitude of 603 nautical miles, and orbit inclined 16° from normal to sun. The nominal case is based on a 540 nautical mile orbit with no variation in fluxes and an orbit normal to the sun. The three design cases are presented in Table 4.2-1.

Table 4.2-1. GENERAL FLUXES (BTU/HR-FT^2)

	Hot Case	Cold Case	Nominal Case
Altitude	478 NM	603 NM	540 NM
2 Variation	+2	-2	None
Seasonal Variation	+3.4%	-3.4%	None
Solar (S)	463.80	400.08	440.0
Earth (E)	81.54	54.86	68.2
Albedo (a)	.50	.26	.38

The power dissipations listed in Table 4.2-2 are the total dissipations per bay. They correspond to the three power modes of the vehicle during its life time.

Table 4.2-2. POWER DISSIPATIONS

Node	Normal (watts)	Normal Spacecraft Off (watts)	Battery Power Only (watts)
SSU 1	0.0	0.0	0.0
SSU 2	25.5	25.5	3.5
SSU 4	26.0	26.0	19.2
SSU 6	10.5	10.5	10.4
SSU 8	1.2	1.2	1.05
SSU 9	14.0	14.0	14.0
S/C 18	5.0	0.0	0.0
S/C 20	0.4	0.0	0.0
S/C 21	150.0	0.0	0.0
S/C 24	14.0	0.0	0.0
S/C 25	38.6	0.0	0.0
S/C 41	105.0	0.0	0.0

The power dissipation in all other internal Bay Nodes is 0.0.

The thermal coatings used for the SSU and Spacecraft are a critical factor in the overall thermal design. Variations in the absorptance and emittance may occur due to solar degradation and/or application methods. To account for this fact, a 0.03 variation was assumed for absorptance and emittance, and a combination of these values was chosen to give a maximum and minimum flux. (See Table 4-3 for the optical properties used). All interior nodes have an epsilon of 0.9 with the exception of the radiation shield between the SSU and the Agena which has an epsilon of 0.05.

4.2.2.3 Results of Analysis

The results of the initial analysis using the coatings suggested by LeRC for the hot and cold cases described above are summarized in Table 4.2-4. From these results it may be seen that temperatures on the battery, tape recorders and CMG's are the most critical ones. The battery has an allowable temperature range of 30°F to 90°F, while the analysis shows that a range of 31°F to 112°F may be experienced. It is possible to lower the 112°F temperature to 90°F, but this would result in a cold temperature lower than 31°F. However, this cold temperature extreme may be mitigated by the use of heaters on the battery. The tape recorders have an allowable operating range of 0°F to 130°F, however, the analysis indicated

a range of -10°F to 95°F. Since the -10°F temperature only occurs during the battery mode and the tape recorders do not operate during that time, it is possible to allow them to go below 0°F in a non-operating mode. Accuracy of the CMG's can only be maintained between 125°F and 25°F, but no damage will occur to the CMG if the temperature goes below 25°F during the cold environmental conditions. If these inaccuracies are not acceptable, a heater may be required to bring the CMG temperature up to an acceptable level.

These results lead to the decision to employ a coating selection computer program developed for NASA by General Electric. Through the use of the coating selected by this program, it was hoped that more acceptable temperatures could be achieved in the SSU. The program and results are described in the following section.

Table 4.2-3. COATINGS AT EXTERIOR NODES

NODES - (exterior)	Hot Coatings		Nominal Coatings		Cold Coatings	
	α	ϵ	α	ϵ	α	ϵ
17, 34	0.43	0.87	0.4	0.9	0.37	.93
10, 16, 27, 33	0.19	0.57	0.16	0.6	0.13	.63
11, 12, 14, 15, 28, 29, 31, 32	0.23	0.12	0.2	0.15	0.17	.18
13	0.13	0.07	0.1	0.1	0.07	.13
30	0.23	0.47	0.2	0.5	0.17	0.17
35, 36, 37, 38, 39, 40, 41, 42, 43	0.53	0.47	0.5	0.5	0.47	.53
44	0.45	0.90	0.45	0.9	0.45	.90

TABLE 4.2-4

COATINGS ANALYSIS RESULTS

Run #	1	2	3	4	5	6	7
α & ε	HOT	NOMINAL	NOMINAL	NOMINAL	COLD	COLD	NOMINAL
Fluxes	HOT	HOT	NOMINAL	COLD	COLD	COLD	COLD
Power S/C	NORMAL	NORMAL	NORMAL	NONE	NONE	BATTERY	BATTERY
SSU				NORMAL	NORMAL		
		TEMPERATURE (°F)					
NODE							
1	87	68	60	27	9	3	21
2	95	78	70	25	10	-10	6
3	80	63	56	- 4	-18	-30	-15
4	106	90	84	10	- 3	-14	- 1
5	85	68	61	- 7	-22	-28	-13
6	100	83	76	15	0	- 5	10
7	90	72	63	24	7	4	22
8	112	96	87	50	34	31	46
9	107	91	84	28	13	5	19
10	87	68	60	27	9	3	21
11	90	72	64	20	4	-12	4
12	80	63	56	- 4	-18	-30	-15
13	100	84	77	4	-10	-21	- 7
14	85	68	61	- 7	-22	-28	-13
15	96	78	70	12	- 4	- 8	7
16	90	72	63	24	7	4	22
17	120	104	94	7	46	43	58
18	92	76	67	-11	8	4	20
19	85	61	60	-15	- 8	-17	- 2
20	84	61	61	-13	-25	-34	-19
21	118	104	98	4	-29	-36	-22

TABLE 4.2-4 (con't)

Run #	1	2	3	4	5	6	7
α & ϵ	HOT	NOMINAL	NOMINAL	NOMINAL	COLD	COLD	NOMINAL
Fluxes	HOT	HOT	NOMINAL	COLD	COLD	COLD	COLD
Power S/C	NORMAL	NORMAL	NORMAL	NONE	NONE	BATTERY	BATTERY
Power SSU				NORMAL	NORMAL		
		TEMPERATURE (°F)					
NODE							
22	95	80	72	-13	-27	-33	-18
23	113	98	90	4	-11	-16	- 1
24	102	86	77	23	7	4	21
25	112	97	88	36	21	18	34
26	107	92	84	14	- 1	- 7	8
27	88	70	61	23	5	2	19
28	81	63	54	4	-12	-20	- 4
29	82	65	58	-14	-28	-36	-22
30	118	104	98	-15	-29	-36	-22
31	91	75	68	-15	-30	-35	-21
32	106	88	80	1	-15	-19	- 3
33	96	79	70	22	4	2	20
34	120	105	95	53	37	35	51
35	87	74	63	20	6	4	18
36	75	60	49	11	- 4	- 7	7
37	66	51	41	- 5	-18	-25	-12
38	69	55	46	-16	-29	-36	-24
39	84	70	61	-18	-31	-35	-23
40	141	129	121	- 8	-21	-24	-11
41	87	73	63	10	- 4	- 7	8

4.2.3 OPTIMUM COATINGS SELECTION

For any spacecraft whose temperature is passively controlled through selection of thermal properties of external surfaces, there exists at least one pattern of α's and ϵ's such that a minimum departure of selected component temperatures from the midpoint of their desired ranges is achieved. Consideration must, of course, be given to the variation in thermal environment (including internal dissipation) during the spacecraft lifetime.

These optimum surface properties can be rationally determined (without resorting to a long series of trial patterns based on, at best, educated guesses) with the aid of the "Coatings Selection Program," described in The General Electric Company's Document No. 65SD526, April 1965 (Final Report on NASA Contract NASw-960). The SSU S/C combination was analyzed accordingly to determine these optimum α's and ϵ's and the resultant improvement in temperatures, if any, over those associated with the coatings considered to date.

4.2.3.1 Thermal Model Description and Inputs

Figures 4.2-2 through 4.2-5 show the nodal breakdown of the analytical thermal model employed. Due to the limitation on the number of nodes (50 maximum), the assumption was made that enough structural, radiative-input, and thermal-dissipation symmetry exists to develop a half-model of the SSU S/C, with the dividing plane through the spacecraft center, containing the sun-line and the spacecraft-Earth line. This dividing plane thus creates an adiabatic surface; i.e., it is assumed that temperature gradients at the center of the spacecraft, normal to the dividing plane, are negligibly small. This assumption can be verified with temperature results from the more complete and extensive thermal model. This assumption appears to be not quite true in the area of the S/C engines, where a large internal dissipation difference occurs across the dividing plane with only one engine on. It is believed, however, that any such heat flow through this dividing plane not accounted for in the model would relieve the temperature modulating duty placed on the selected coatings, and in this sense, conservatism is implied.

Two extreme equilibrium cases (or "orbits" in the program nomenclature) are considered: "Hot" and "cold." Internal dissipation for the hot orbit includes full, nominal dissipation in the SSU and S/C, with 105 watts from the engine; for the cold case, the SSU is on battery power and there is no dissipation in the S/C. The "side" bay in the SSU half model has been taken as Bay 2 (rather than Bay 6) since the total power dissipation in this bay is higher for the hot case and lower for the cold. The hot solar flux is taken as 465 BTU/hr ft^2, the cold as 415, with corresponding Earth I.R. incident flux to lateral surfaces at 17 and 11 BTU/hr ft^2. Maximum albedo lateral surface flux is 5 and 2 BTU/hr ft^2 for the hot and cold cases, respectively. The incident fluxes on the Earth-facing S/C surfaces are 75., 40., and 3. BTU/hr ft^2 for Earth I.R. hot and cold and albedo hot and cold, respectively. A summary of thermal inputs in tabulated in Tables 4.2-5 and 4.2-6.

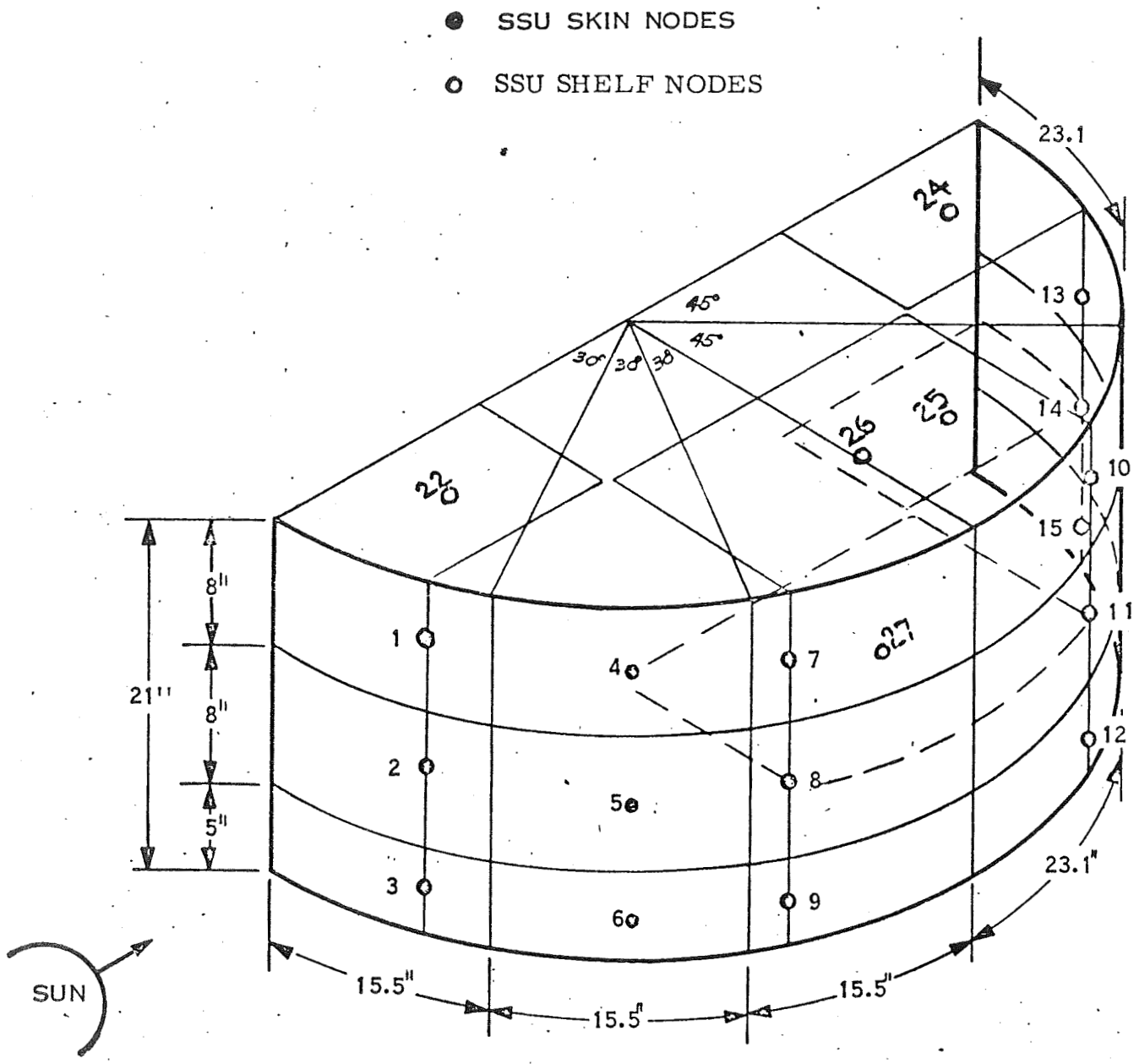

Note: Node 23 is a "spare" node.

Figure 4.2-2. SSU Skin and Shelf Nodes

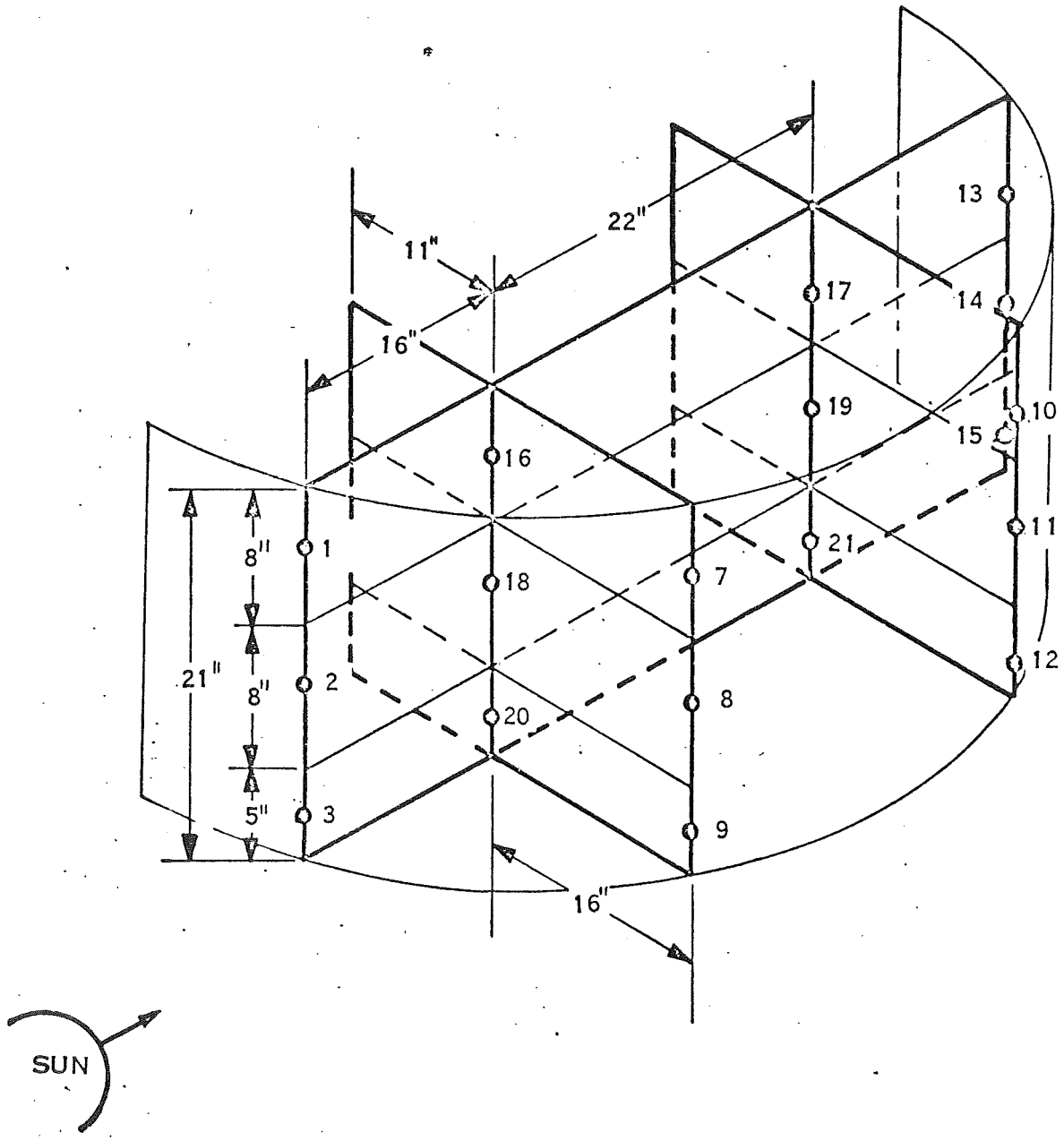

Figure 4.2-3. SSU Structural Nodes

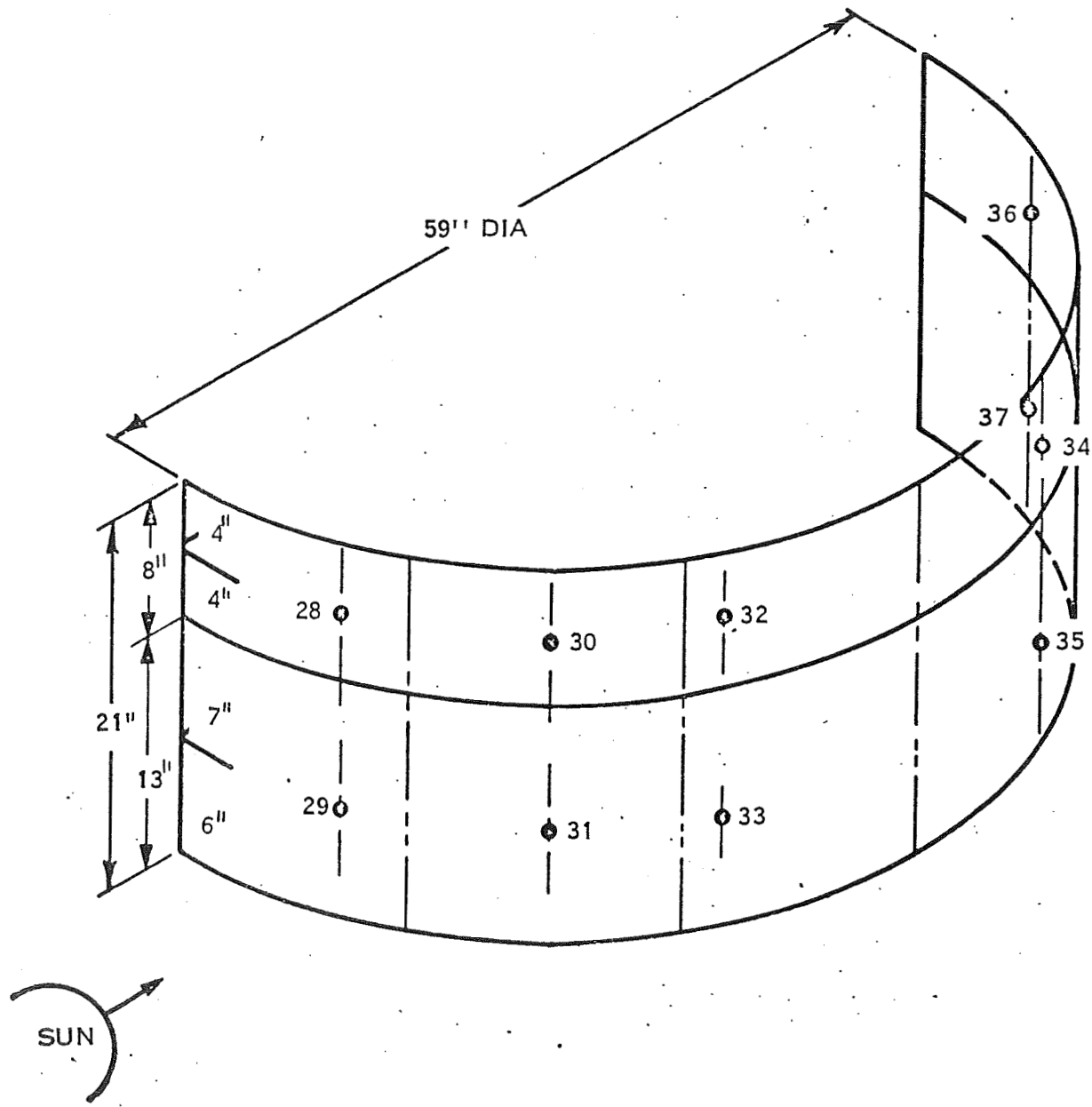

Figure 4.2-4. Spacecraft Skin Nodes

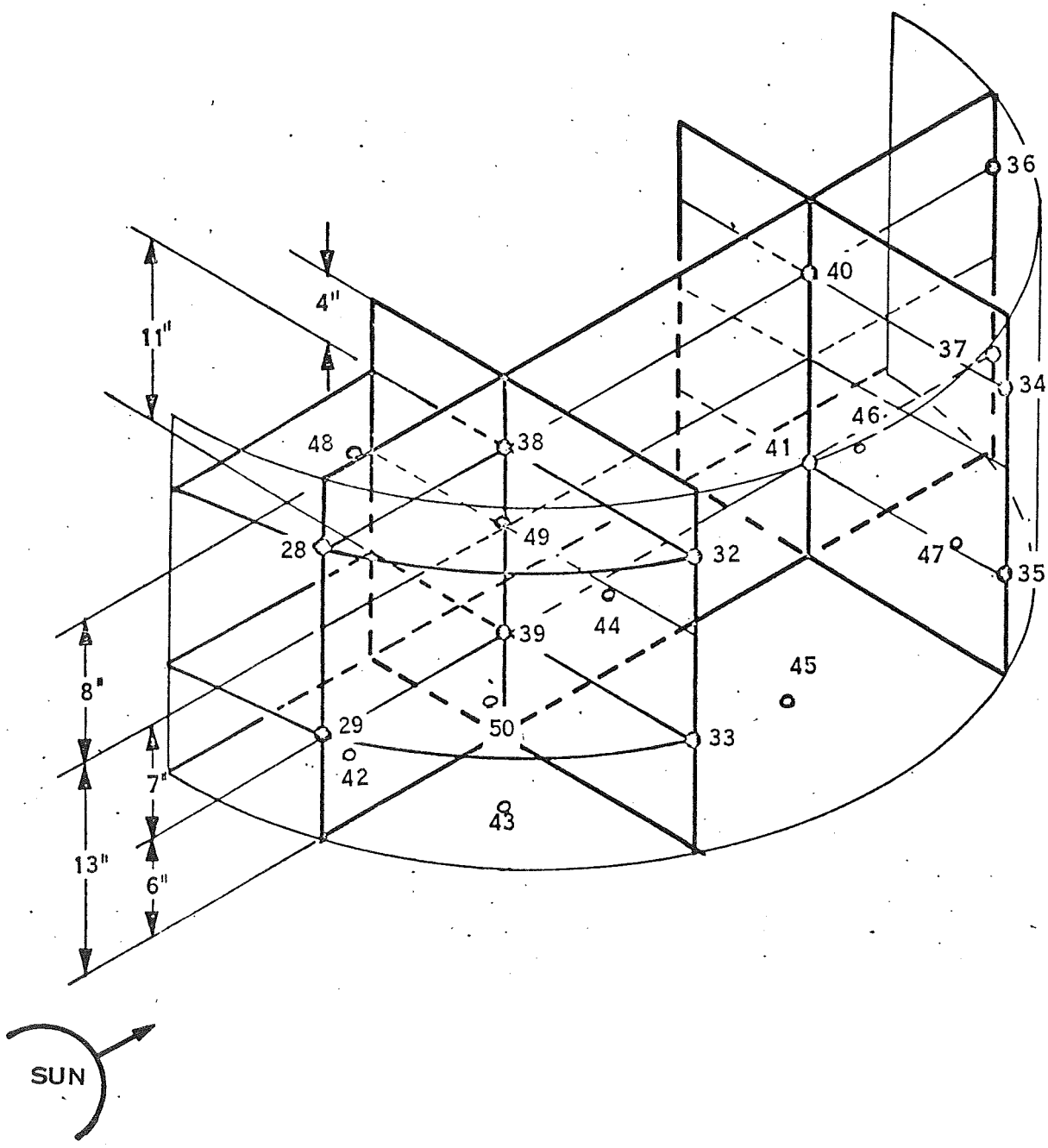

Figure 4.2-5. Spacecraft Structure Nodes

TABLE 4.2-5

THERMAL MODEL NODAL INCIDENT FLUX

External Surface Area, $Ft.^2$	HOT INCIDENT FLUX, BTU/HR			COLD INCIDENT FLUX, BTU/HR		
	Solar	Earth I.R.	Albedo	Solar	Earth I.R.	Albedo
.86	382.	14.7	4.3	340.	9.5	1.7
.538	238.	9.2	2.7	213.	5.9	1.1
.86	278.	14.7	3.9	248.	9.5	1.4
.538	173.	9.2	2.5	155.	5.9	.9
.86	103.	14.7	2.6	92.	9.5	.8
.538	64.5	9.2	1.7	57.6	5.9	.5
1.285	0	22.	2.0	0	14.1	0
.803	0	13.7	1.2	0	8.8	0
1.285	0	22.	0	0	14.1	0
.803	0	13.7	0	0	8.8	0
.86	382.	14.7	4.3	340.	9.5	1.7
1.4	620.	23.9	7.0	553.	15.4	2.8
.86	278.	14.7	3.9	248.	9.5	1.4
1.4	451.	23.9	6.4	403.	15.4	2.3
.86	103.	14.7	2.6	92.	9.5	0.8
1.4	167.5	23.9	4.3	150.	15.4	1.3
1.285	0	22	2	0	14.1	0
2.088	0	35.7	3.2	0	22.9	0
1.285	0	22	0	0	14.1	0
2.088	0	35.7	0	0	22.9	0
1.65	0	107.	13.2	0	65.	4.9
1.1	0	72.	8.8	0	44.	3.3
2.	0	130.	16.	0	80.	6.
3.	0	195.	24.	0	120.	9.
1.65	0	107.	13.2	0	65.	4.9
1.1	0	72.	8.8	0	44.	3.3

TABLE 4.2-6

THERMAL MODEL NODAL POWER DISSIPATIONS

		INTERNAL POWER DISSIPATION (WATTS)	
NODE	DESCRIPTION	HOT	CODE
18	CMG	3.5*	3.5*
19	CMG	3.5*	3.5*
22	Bay 8 Lower	1.0*	1.0*
24	Bay 4 Lower	9.0*	5.5*
25	Bay 4 Upper	4.1*	4.1*
26	Bay 2 Lower	18.7	3.0
27	Bay 2 Upper	6.9	0.5
36	Power Conditioner	29.0*	0
37	Power Conditioner	46.0*	0
39	Engine	52.5	0
41	Engine	52.5	0
48		15.0*	0
49		14.0	0
50		4.4*	0

* 1/2 of full component power in bay due to 1/2 model.

Throughout the many computer runs using this model, several levels of conductance values were used to observe the sensitivity of coatings selection to this parameter. These different values were based on: (a) zero resistance at all metal-to-metal connections, (b) one-half of all conductances thus calculated, (c) "perfect" conduction, and (d) one-fourth of the conductance through the SSU skin.

Internal radiative paths were calculated assuming an all black interior, except for the skins which do not receive direct solar input, i.e., nodes 10 through 15 on the SSU and 34 and 35 on the S/C. These interior surfaces were assumed perfect specular reflectors. It is believed that this concept will result in somewhat lower temperature gradients throughout the spacecraft interior.

Program input requires the selection of four coatings with a maximum "spread" of thermal properties so that the computer-performed coatings selection may have minimum restriction in the search for optimum values. The selected properties should be as close as possible to the ideal limits of (1) α/ϵ = 0/0, (2) α/ϵ = 1.0/0, (3) α/ϵ = 1.0/1.0, and (4) α/ϵ = 0/1.0. Although point (1) could be approached very closely with a "superinsulated" surface, other considerations have precluded the use of such a concept. Two other candidate surfaces were therefore considered. Initially, α/ϵ = .1/.03 was taken as point (1), implying an evaporatively-coated metal such as aluminum. However, the results of the first series of runs showed that the surfaces "chosen" for this particular coating were those receiving relatively small amounts of albedo and no direct solar energy; the α value was therefore assumed of secondary effect. In the interest of simplicity and reduced cost, brightly buffed aluminum (assuming aluminum skins) was assigned as coating (1), with α/ϵ = .18/.03. (Run E considered an α/ϵ = .01/.01 for this point, implying the possible use of super-insulation.) Somewhat the same philosophy was applied to coating (4); i.e., initially, α/ϵ = .2/.8 was used, to be obtained with either a very stable, low white paint or an "Alzac" treatment to the aluminum skins. After the first series of runs, however, a more practical and realistic approach introduced a surface of α/ϵ - .3/.85, representing a state-of-the-art, available white paint. The of this coating appears to be of primary concern however, since results seem to indicate the desirability of minimum α. Surface (2), α/ϵ = .55/.25, represents either a sandblasted aluminum or an evaporated metal deposit such as chromium or titanium. Black paint of α/ϵ .95/.9 was taken as surface (4).

The controlling "critical" temperature ranges assigned were 40°F to 100°F for nodes 22, 24, 25, 26, 27 in the SSU and -10°F to 110°F for nodes 36 and 37 and 10°F to 110°F for nodes 48, 49, and 50 in the S/C.

Results

Coatings selections from eight representative runs are presented in the α-ϵ tabulation of Table 4.2-7. The corresponding maximum and minimum temperatures of critical nodes are shown in Table 4.2-8. It should be noted that each computer run is composed of a set of approximately 30 "solutions" (the result of the iterative process of selectively changing α's and ϵ's in the search for an optimum combination);

Table 4.2-7. (Selected Coatings)

Run	A		B		C		D		E		F		G		H	
Node	α	ε	α	ε	α	ε	α	ε	α	ε	α	ε	α	ε	α	ε
1	.27	.79	.26	.79	.29(.29)	.78(.78)	.30	.82	.27	.77	.30	.83	.30	.83	.30	.84
2	.24	.79	.25	.79	.29(.29)	.78(.78)	.30	.83	.27	.77	.30	.83	.30	.83	.30	.84
3	.22	.79	.22	.80	.24(.24)	.79(.79)	.30	.82	.27	.77	.30	.83	.30	.83	.30	.85
4	.27	.80	.25	.79	.27(.27)	.78(.78)	.30	.82	.27	.78	.30	.83	.30	.83	.31	.85
5	.23	.79	.25	.79	.27(.27)	.78(.78)	.30	.83	.27	.78	.30	.83	.30	.83	.31	.84
6	.23	.80	.23	.80	.24(.24)	.79(.79)	.30	.82	.27	.78	.30	.82	.30	.82	.30	.85
7	.63	.67	.55	.56	.55(.55)	.55(.55)	.48	.60	.52	.54	.44	.66	.41	.69	.54	.73
8	.61	.67	.56	.55	.56(.56)	.54(.54)	.48	.60	.52	.54	.45	.64	.44	.66	.52	.74
9	.59	.58	.56	.52	.56(.56)	.52(.52)	.51	.56	.53	.52	.50	.57	.50	.58	.53	.63
10	.13	.20	.12	.16	.12(.12)	.15(.15)	.20	.18	.10	.12	.21	.23	.22	.27	.21	.26
11	.12	.17	.11	.13	.12(.12)	.12(.12)	.20	.17	.10	.12	.21	.19	.21	.22	.21	.24
12	.11	.10	.11	.08	.11(.11)	.07(.07)	.19	.09	.10	.08	.19	.09	.19	.09	.20	.13
13	.15	.12	.14	.28	.13(.13)	.19(.19)	.22	.27	.10	.19	.23	.31	.23	.36	.23	.20
14	.10	.03	.13	.19	.13(.13)	.12(.12)	.21	.21	.10	.17	.22	.22	.22	.24	.21	.05
15	.11	.03	.11	.10	.11(.11)	.06(.06)	.19	.10	.10	.12	.20	.07	.19	.07	.20	.04
28	.22	.79	.20	.79	.22(.22)	.78(.78)	.30	.82	.29	.81	.29	.81	.30	.82	.30	.84
29	.31	.81	.20	.79	.24(.23)	.79(.78)	.30	.83	.29	.83	.30	.84	.30	.84	.30	.84
30	.30	.81	.21	.81	.22(.22)	.80(.79)	.30	.84	.30	.85	.30	.85	.30	.85	.30	.85
31	.38	.81	.22	.80	.25(.23)	.79(.80)	.30	.84	.31	.85	.31	.85	.30	.85	.30	.58
32	.63	.54	.57	.58	.60(.60)	.60(.61)	.49	.67	.59	.67	.53	.72	.54	.69	.55	.59
33	.68	.51	.61	.59	.66(.66)	.61(.63)	.51	.72	.66	.70	.59	.75	.60	.71	.57	.60
34	.11	.09	.10	.05	.10(.10)	.03(.04)	.18	.06	.06	.05	.18	.04	.18	.06	.19	.06
35	.11	.08	.11	.05	.11(.11)	.04(.05)	.19	.08	.05	.05	.18	.05	.19	.07	.19	.05
36	.80	.66	.70	.47	.67(.67)	.40(.45)	.65	.51	.51	.31	.53	.33	.44	.32	.76	.61
37	.75	.61	.56	.26	.55(.55)	.24(.36)	.37	.30	.34	.30	.25	.29	.32	.35	.64	.44
42	.20	.26	.19	.36	.19(.19)	.41(.42)	.24	.46	.18	.50	.25	.48	.24	.44	.22	.33
43	.20	.21	.20	.24	.19(.19)	.25(.25)	.22	.33	.19	.35	.22	.34	.22	.32	.21	.26
44	.20	.28	.19	.34	.19(.19)	.39(.40)	.24	.43	.19	.47	.25	.52	.25	.49	.22	.31
45	.19	.31	.19	.42	.19(.19)	.50(.51)	.25	.51	.20	.56	.27	.63	.26	.60	.23	.36
46	.20	.27	.21	.29	.21(.21)	.34(.36)	.22	.32	.22	.37	.24	.42	.24	.39	.22	.26
47	.20	.25	.20	.26	.21(.21)	.29(.30)	.22	.28	.21	.32	.23	.35	.23	.33	.21	.24

Run - Brief Description

A - Perfect Conductance Between SSU and S/C

B - Same, Except 1/5 x Perfect Conductance

C - Same, Except 1/10 x Perfect Conductance

D - Same as B, Except Conductance Added Between S/C Structure & End "Skins" and Pt. 1 = $\frac{.18}{.03}$ and Pt. 4 = $\frac{.3}{.85}$

E - Same, Except Conductance Broken Between SSU & S/C and Pt. 1 Now = $\frac{.01}{.01}$

F - Same as D, Except all Conductances Reduced by 1/2

G - Same, Except all SSU Skin Conductances Reduced to 1/4 of Nominal

H - Same as D, Except SSU Allowed to Conduct to Undesirable Agena Temp.

Table 4.2-8. Temperature Extrems of Critical Nodes (°F)

Run	A		B		C		D		E		F		G		H	
Nodes	Hot	Cold	Hot	Cold	Hot	Cold	Hot	Cold	Hot	Cold	Hot	Cold	Hot	Cold	Hot	Cold
18	98	39	94	43	102(106)	56(57)	95	46	100	60	95	50	91	46	100	37
19	104	31	96	36	105(109)	50(52)	93	36	100	55	96	41	90	35	104	27
22	97	47	95	51	104(108)	64(65)	99	58	101	67	100	63	97	59	104	48
24	115	34	102	37	113(117)	53(55)	95	57	106	57	105	43	97	36	115	30
25	107	29	95	33	105(110)	49(51)	92	33	98	54	96	39	99	32	107	27
26	108	33	105	38	113(116)	51(53)	102	38	109	56	105	40	99	34	109	27
27	102	31	98	37	106(110)	50(52)	95	37	102	55	97	39	91	33	101	27
36	95	-31	121	-35	128(118)	-34(-39)	109	-37	129	-36	123	-43	121	-45	105	-37
37	96	-36	128	-35	134(120)	-34(-40)	115	-37	128	-36	125	-44	120	-47	108	-37
39	134	-8	126	0	129(129)	3(0)	120	5	125	5	129	3	129	3	128	11
41	125	-11	134	-21	137(117)	-21(-21)	123	-21	132	-21	132	-26	132	-27	127	-18
48	134	35	126	12	132(134)	18(15)	130	26	135	25	140	27	140	28	136	30
49	130	33	121	9	126(128)	14(11)	123	20	128	19	132	20	133	21	129	24
50	127	35	113	6	117(119)	11(8)	112	14	116	16	118	15	118	16	--	--

the ones presented in Table 4.2-7 are "optimum," or the ones resulting in minimum temperature deviation of all nodes from the midpoints of their desired temperature ranges. Usually there is little significant difference between this optimum and many other solutions with respect to temperature range; the difference is primarily shifting temperature levels up or down. As an example, two different solutions are shown for the same Run C. For one, an upper temperature limit was exceeded; for the other (numbers in parenthesis) a lower limit. The difference in α's and ϵ's is for all practical purposes, negligible, except for the critical node in this case, node 37.

It can be seen that the α and ϵ selections from run to run do not differ appreciably - they at least stay in the same $\alpha - \epsilon$ neighborhood. This is a desirable characteristic, since it indicates that a selected optimum pattern of thermal properties based on a particular thermal model will still be close to optimum should the thermal model be not exactly representative of actual thermal conditions.

Run-to-run comparisons may perhaps be more easily made with the aid of $\alpha - \epsilon$ plots as in Figure 4.2-9, shown with Runs A and B as an example. This is also a convenient way to determine what percentage of each of the four candidate coatings any particular coating is composed. Also by observing where coatings fall on the limiting boundaries, it can be determined whether it is worthwhile to extend these boundaries with coatings of less restrictive α's and/or ϵ's.

It should be remembered that nodal boundaries as fixed by the thermal model are not necessarily the best boundaries for the various coatings, and one should be judicious in transposing coating patterns from model to actual spacecraft. For example, a "white" coating is called for on the sunlit (SSU) nodes 1 through 6; the adjacent nodes 7, 8, and 9, receiving progressively less solar energy, call for coatings of approximately double the white α as well as a lower ϵ. This sharp change in coatings certainly need not come at the nodal boundaries. Rather, it seems that what is implied is a constant "white" coating, over nodes 1, 2, and 3 then a gradual increase in the α and decrease in ϵ as the non-sunlit skins are approached, until at the junction of nodes 7, 8, 9, and 10, 11, 12 there is a coating with a higher α and lower ϵ than the program picked for nodes 7, 8, and 9. The α and ϵ combinations for these surfaces should follow a straight line on that $\alpha - \epsilon$ plot passing through the white of nodes 1 through 6 and the white, black, and "sandblasted aluminum" of nodes 7, 8, and 9. Nodes 10 through 15 do not differ drastically, all being a combination of white, and primarily, buffed aluminum. There is, of course, the big change in coatings between those surfaces receiving direct solar energy and those that do not.

Comparing runs A, B, and C, which differ only in the degree of thermal connection between the SSU and S/C, it is seen that as the SSU becomes more and more isolated from the S/C, the difference between "hot" and "cold" SSU temperatures becomes progressively less, i.e., temperature control becomes more effective. Contrary to this trend, S/C temperature spread from hot to cold becomes progressively greater (except in the isolated instance of node 39). This indicates that the greatest temperature control burden lies within the S/C, due apparently to the large difference between hot and cold internal power dissipations. It should be noted that the temperature control effectiveness criterion here is not whether a particular

upper or lower temperature limit was exceeded, but rather the numerical difference between the calculated upper and lower temperatures for all nodes.

Continuing with this reasoning, it is seen that the best SSU temperature control of those runs tabulated is achieved in Run E, where there is no thermal interchange between SSU and S/C. The coatings selection program in this run was allowed a greater freedom of choice, as point 1 was changed from an aluminum surface to a hypothetical "superinsulated" surface with $\alpha / \epsilon = .01/.01$. However, not much of the temperature improvment noted can be attributed to this cince only two S/C nodes (34 and 35), and no SSU nodes, took even partial advantage of it. This implies that external superinsulation blanketing is not required.

Comparison of Runs F and D, which differ only due to conductances being arbitrarily halved for Run F, indicates that conduction changes of this magnitude are not at all critical with respect to SSU coatings selection and resultant temperatures, SSU temperature differences being negligible (except in the case of node 24). This case demonstrates that the use of magnesium for the SSU skins and posts has a negligible effect since the conductivity of magnesium is about half that of aluminum. Temperatures suffered somewhat greater in the S/C, as might be expected due to the higher internal heat flows and the resultant greater dependence upon conduction.

It is reassuring to find that reducing SSU skin conductance further by 1/2 (to 1/4 of nominal) as in Run G does little to change internal temperatures (compare Runs F and G).

Run H is included to show that undesirable Agena temperatures (at the SSU junction) do have an adverse effect on SSU temperatures. A constant Agena temperature of 140°F was used for the hot case, -30°F for the cold.

It was FHC's intent to have the results of this analysis used as a basis for a coatings pattern selection. The results from the computer were not to be used as the final pattern, but as a beginning point from which the results could be extended to a more comprehensive final coating pattern by the use of a detailed SSU-S/C CINDA model. The intent was to use the S/C CINDA model of LeRC together with the FHC SSU CINDA model in this final selection. With this in mind, the above data was presented to NASA-LeRC for use by them with the recommendation that run D would be the best starting point for further refinement.

SECTION V

HARNESS

5.1 REQUIREMENTS

Development of the SERT II Spacecraft Support Unit required design of an interconnecting cable network which would meet electrical and interference requirements, provide adequate failure protection, integrate mechanically with the SSU structure and connect the SSU electronic components into a functional system.

5.2 DESIGN

5.2.1 FABRICATION

The original Fairchild Hiller Corporation philosophy was conceived in compliance with the NASA - Lewis Research Center SERT II Design Manual (specifically, specifications 3-51, 3-51A, 3-52, 3-53, 3-55, 3-56). The description of material for construction and of design restriction was carefully considered. Selection of low voltage connectors, wire, and terminal junctions was in accordance with the aforementioned specifications. In addition, electrical design principles of grounding, shielding, and requirements for twisted pair conductors followed the design manual. Despite original efforts to stay completely within the specifications, several deviations were necessary. These deviations are listed below:

1. Several power return leads were installed in the harness between the power control electronics unit and the power return terminal junction blocks as unshielded wire (deviation from paragraph 4.4.1 of specification 3-51A).
2. Shields were carried across bulkhead interfaces (deviation from paragraph 4.4.3 of specification 3-51A).
3. Shields were grounded at both ends of the wire (deviation from paragraph 4.4.3 of specification 3-51A).
4. The SSU ground point (SSUGP) was not located as designated in paragraph 4.1.8 b of specification 3-51 because power ground was tied to the case within the transmitter.
5. The connectors utilized in the harness were not NAS-1599 as designated in specification 3-56. By Lewis Research Center direction, equivalent connectors were utilized.

6. Generally the telemetry signal wiring within the harness was a two wire system from the data source to the telemetry terminal blocks and a single wire between the terminal blocks and the telemetry system (reference paragraph 4.2 of specification 3-51A).

Lightweight coaxial cable was considered for use on the SSU harness. Because a suitable connector was not manufactured for use with this cable, RG 142 B/U coaxial cable was substituted. RG 142 B/U has identical electrical properties to the lightweight coaxial cable, but adds approximately one pound to the harness weight. The increased weight was accepted to ensure that qualified, proven connectors would be utilized.

The termination of shields to chassis ground is accomplished by using HY-RINGS. Generally, all conductors are shielded and each shield is tied at both ends. One exception is at the telemetry terminal blocks, where one end of the shield is unterminated.

5.2.2 LAYOUT

The SERT II SSU harness layout design was determined by the electrical interface requirements of the system and the desire to provide maximum accessability to each of the SSU system components.

The original layout configuration conceived a harness system that utilized only the outer bays leaving the center bay unused. This method resulted in the utilization of an excessive number of bulkhead connectors and was therefore abandoned. The original design was replaced with one which utilized the center bay for the bulk of the interconnecting wire, but maintained a dynamic envelope around the control moment gyros. This design incorporates two harnesses. The larger harness extends from the center bay into all bays except the telemetry subsystem bay (bay two upper). The smaller harness is contained mainly within the telemetry bay. The telemetry cabling was separated from the main harness because the number of connections within the subsystem resulted in a complicated harness with many connectors and large cables.

High density terminal blocks were used in both harnesses to facilitate design of the grounding system, interconnection of the redundant telemetry components, and interconnection with the housekeeping array. System grounding philosophy required isolation of chassis and power grounds except at a single point ground. It was originally planned to position the single point ground in the Bay #1 area. However, the transmitter design tied power return to chassis and this point (located in Bay #8) had to be used as the single point ground. This ground point is readily picked up by connecting to the solar array terminal block.

Interface connections between the SSU - Spacecraft and the SSU - Agena were implemented in accordance with the SSU Electrical Interface Design Guide provided by the Lewis Research Center. The SSU Spacecraft interface connectors are

located on bulkheads in the proximity of Upper Bay #2 and Upper Bay #6. Power, telemetry, timing, and command signals required for the integrated systems operation are provided on six connectors. The two SSU - Agena interface connectors are on cables located in the vicinity of Bay #8. Power, telemetry, and command signals are provided thru this interface. The solar array connects to a terminal block located in Bay #1.

5.3 DEVELOPMENT

During the fabrication and test of the Experimental Model SSU, it became apparent that the SSU harness could be improved by modifying its design and fabrication processes. Therefore, several changes were incorporated into the Prototype and Flight Model Spacecraft Support Unit harnesses. These changes are described below:

1. The method of terminating #16 wires at the solar array terminal block was modified from soldering the #16 conductor into a ferrule and inserting the ferrule into the terminal block to utilizing a #16 to #8 adapter crimped to the #16 conductor, inserting the adapter into a special #8 ferrule, and inserting the assembly into the terminal block.

2. The method of terminating shields at connectors was modified. Quality Directive 13-001-QD-02 was issued giving direction for selection of HY-RINGS based on cable dimension. The Quality Directive also provided detail instruction for correct HY-RING shield termination.

3. Prototype and Flight Model SSU harnesses were laced rather than ty-wrapped.

4. The telemetry bay (Upper Bay #2) equipment layout was changed to provide better harness routing and to relieve the strain on the cables.

5. Solder cups on thermistor connectors were covered with shrink tubing.

6. On the Flight Model SSU, thermistor connectors and pads were bolted to the structure, in addition to the original bond. This change was made as a result of a connector coming loose during the prototype vibration test and provides positive assurance that a good mechanical connection is made.

7. All bulkhead and interface connectors are lock wired.

In addition, the Prototype and Flight Model SSU harnesses fabrication system was greatly improved by the utilization of exacting layout techniques and extensive in-process quality control.

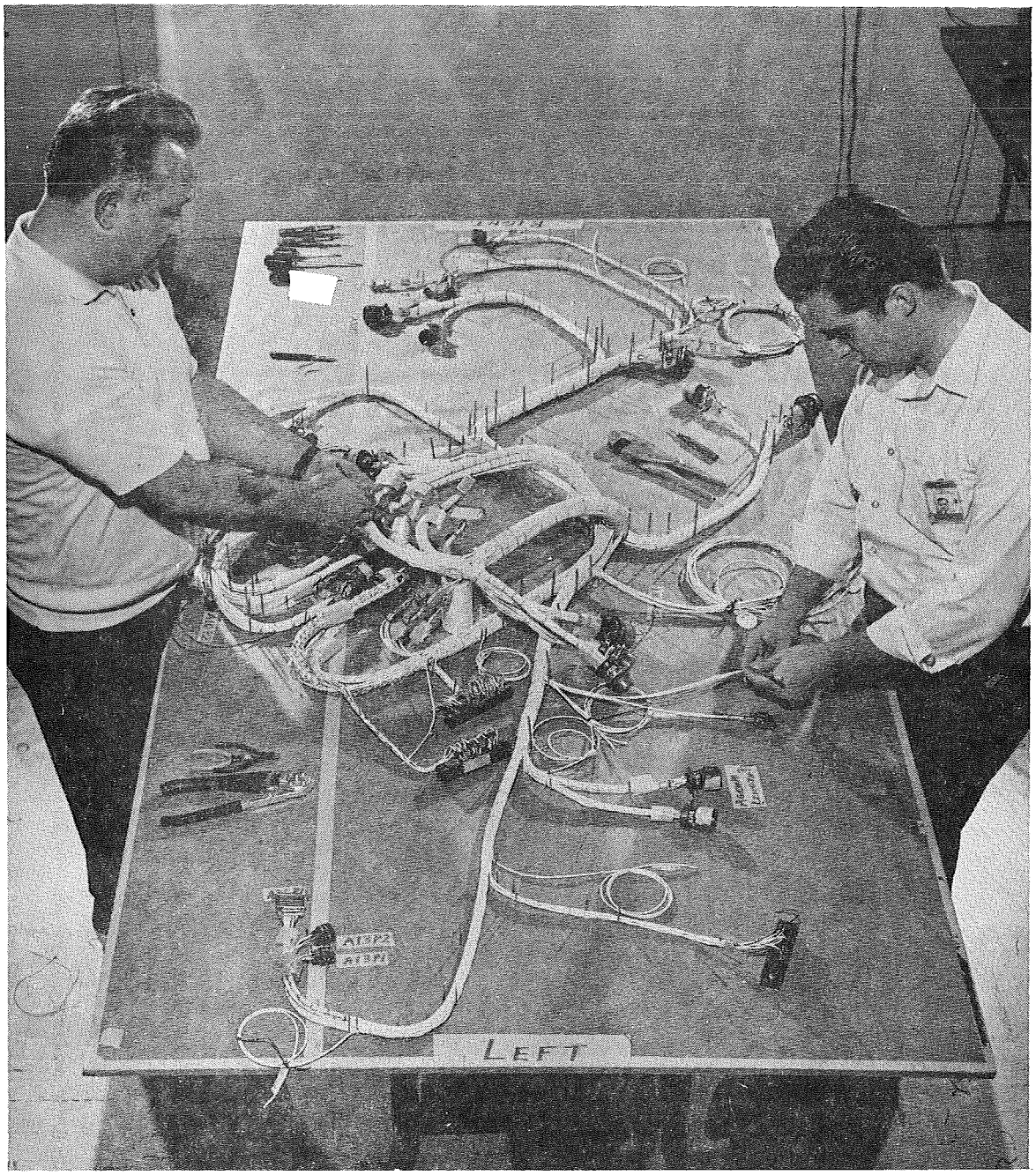

Figure 5.4-1. Large Harness, W2 During Manufacture

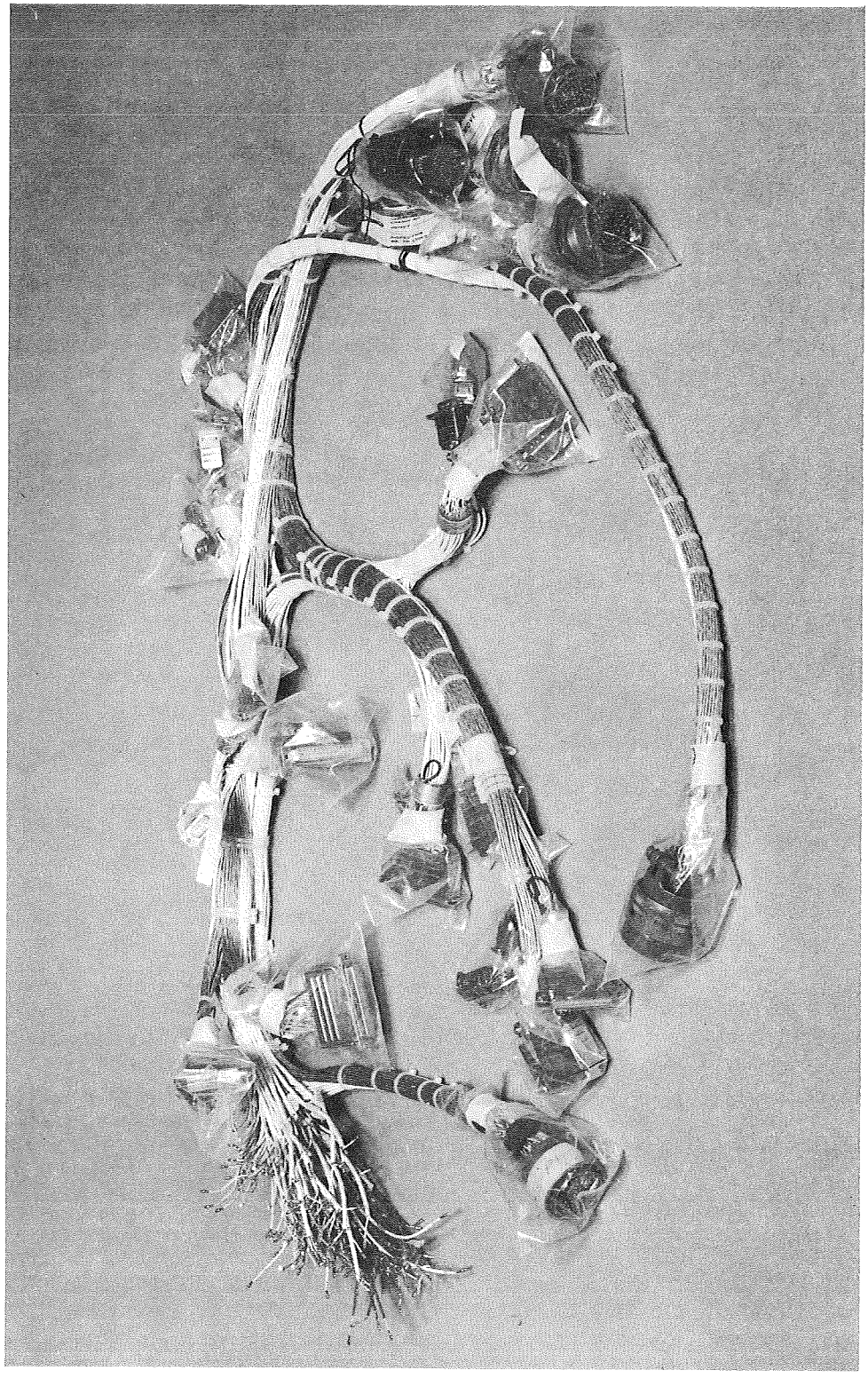

Figure 5.4-2. Small Harness, W2

The Prototype Model harness differed from the Flight Model only in that cadmium plated connectors were allowed to be utilized due to late delivery dates for the approved connectors.

5.4 TEST

Each harness was fully reinspected upon completion. A complete ring-out of each harness and insulation test (at 500 VDC) was performed. The extensive care used during manufacture of the Prototype and Flight Model harnesses resulted in a minimum of rework being required. During the test programs on the Prototype and Flight Model SSU systems there have been no harnessing failures due to poor workmanship or design. Figure 5.4-1 displays the large harness during the final phases of the manufacturing process. Figure 5.4-2 displays the small harness prior to its installation in the SSU structure.

SECTION VI

POWER SYSTEM

6.1 REQUIREMENTS

The power system of the SERT II Spacecraft Support Unit is designed to supply power to the electronic equipment located in the SSU. In addition, AC and DC power is supplied to the SERT II Spacecraft. The power system accepts a solar array input bus from the Agena and provides control of unregulated DC power, regulated DC power, and 400 Hz, 115 VAC power. Under voltage protection, unit failure protection, and redundancy are provided consistent with the SERT II objectives.

6.2 DESIGN

The power system design consists of a configuration of electronic units furnished by various subcontractors. Fairchild Hiller Corporation designed and manufactured a Power Control Electronics Unit whose function was to integrate the subcontractor units into a functioning system. Table 6.2-1 lists the power system components, their manufacturing specification number, and the quantity used per system.

6.2.1 DC POWER SYSTEM

The following section discusses the design of that part of the power system that supplies power to loads connected to the dc power bus. Figure 6.2-1 (sheet 1) displays a block diagram of the power system and may be utilized for reference purposes.

6.2.1.1 Power Requirements

The power system is designed to accept the unregulated power line supplied to the Spacecraft Support Unit from the Agena solar array. The solar array will provide a bus that can vary from 0 to 52 VDC. The switching mode regulators used in the power system are capable of accepting variations on the input bus from 27.5 VDC to 55 VDC, while operating within specification. The input from the solar array can

Table 6.2-1

Power Subsystem Components

Description	No/System	Source	Control Specification
Power Control Electronics Unit	1	FHC	
DC to AC Inverter	2	Gulton Ind. Engrd. Magnetics Div.	833-15403-P001
Switching Mode Regulators	2	Gulton Ind. Engrd. Magnetics Div.	833-15424-P001
Phase Sensitive Demodulators	4	Gulton Ind. Engrd. Magnetics Div.	833-15402-P001
Battery Charger	1	Gulton Ind. Engrd. Magnetics Div.	833-15417-P001
Battery	1	Exide	833-15416-P001
Control Moment Gyro	4	Kearfott	GFE

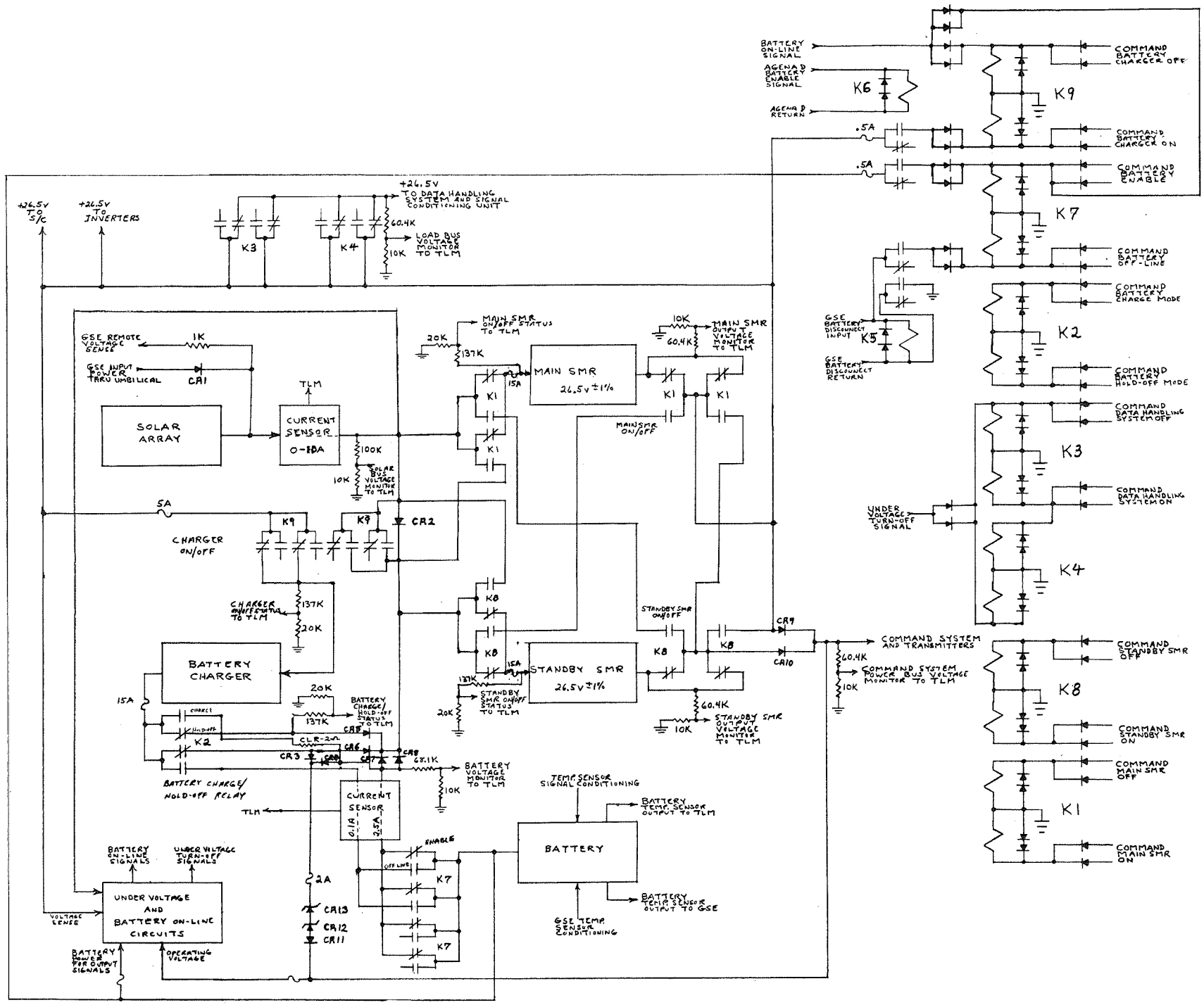

Figure 6.2-1. DC Power System Block Diagram

therefore be coupled to the input of the switching mode regulator without utilizing a power dissipating voltage clamp. The input of the solar array is directly coupled, through switching, to the switching mode regulator. The battery can be placed on-line to support the solar array bus. The power system has been designed to supply approximately 200 watts of dc load, which is better than 50 watts in excess of the maximum expected from the SSU and spacecraft loads.

The output of each switchihg mode regulator is regulated to +26.5 VDC ± 1%. The output current supplied can vary from 0 to 7.5 amperes while maintaining the 1% regulation. Each regulator provides better than 87% efficiency under the specified input voltage and load conditions. Ripple voltage and spikes on the regulated dc bus from the regulators are maintained less than 100 mv.

The SSU Electrical Power Requirements are displayed in Table 6.2-2. The table lists the load placed upon the bus by each of the individual components of the SSU in its operating modes. The maximum power required by each component and its operating voltage range are indicated in the third and fourth columns from the left of the table. Columns 5, 6, 7 and 8 indicate the power drawn by each component of the command system, telemetry system, instrumentation, and control moment gyros during normal modes of SSU operation. The changes in power are dictated, in the most part, by the different modes of operation of the tape recorder and command system. A summary of the ac and dc power requirements, the total dc conditioned power required to supply the ac and dc power, and the total solar array load (unregulated power) is provided for each operating mode. The load placed on the battery for the condition where the solar array output drops is shown in the far right column of Table 6.2-2 and amounts to 21.02 watts of battery power.

6.2.1.2 Battery Design

The use of a silver oxide-zinc battery capable of delivering two amperes at +25.8 to +33.3 VDC for 13 hours with a depth of discharge not to exceed 65% is incorporated into the system design. The battery is capable of a minimum of five discharge cycles after initial activation. This battery is capable of being charged with a constant potential charger, current limited to 2.2 amperes.

The SSU battery charger is essentially a DC-DC converter with a modified output. It operates at an input line voltage range of +22 to +35 VDC with a constant potential output of 34.65 VDC ± 0.5% for output currents from 5 milliamperes to 100 milliamperes and a current limited output of 1.5 amperes ± .5 amperes.

The modes of operation involving the battery system are discussed in the operations section.

SSU ELECTRICAL POWER REQUIREMENTS

REFERENCE DESIGNATION	NOMENCLATURE	MAXIMUM POWER REQUIRED (WATTS)						OPERATING VOLTAGE RANGE				CMG's ON TELEMETRY OFF COMMAND STANDBY		CMG's ON TAPE RECORD, COMMAND STANDBY		CMG's ON TAPE PLAYBACK COMMAND STANDBY		CMG's ON TAPE PLAYBACK, COMMAND INTERROGATE		CMG's ON TAPE PLAYBACK, COMMAND EXECUTE		TELEMETRY OFF COMM. STANDBY CMG'S OFF	
		PEAK		NORMAL		STANDBY		MINIMUM		MAXIMUM													
		AC	DC	AC	DC	AC	DC	AC	DC	AC	DC	AC	DC	AC	DC	AC	DC	AC	DC	AC	DC	AC	DC
A1	Control Moment Gyro 1	40.00		7.00	0.10							7.00	0.10	7.00	0.10	7.00	0.10	7.00	0.10	7.00	0.10	OFF	
A2	" " " 2	40.00		7.00	0.10							7.00	0.10	7.00	0.10	7.00	0.10	7.00	0.10	7.00	0.10	OFF	
A3	" " " 3	40.00		7.00	0.10							←						OFF					→
A4	" " " 4	40.00		7.00	0.10							←						OFF					→
A5	Phase Sensitive Demodulator 1			0.46	1.40				22		35	0.46	1.40	0.46	1.40	0.46	1.40	0.46	1.40	0.46	1.40	OFF	
A6	Phase Sensitive Demodulator 2			0.46	1.40				22		35	0.46	1.40	0.46	1.40	0.46	1.40	0.46	1.40	0.46	1.40	OFF	
A7	Phase Sensitive Demodulator 3			0.46	1.40				22		35	←						OFF					→
A8	Phase Sensitive Demodulator 4			0.46	1.40				22		35	←						OFF					→
A9	Inverter (Main)								22		35												
A10	Inverter (Standby)								22		35												
A11	Power Control Electronics Unit				5.00								2.50		5.00		5.00		5.00		5.00		2.50
A12	Tape Recorder 1				Record 6.00 Playback 12.00		.03		25		31	←	OFF →		6.00		12.00		12.00		12.00	OFF	
A13	Tape Recorder 2				Record 6.00 Playback 12.00		.03		25		31	←	OFF →		0.30		0.30		0.30		0.30	OFF	
A14	Transmitter 1				1.80				24		32		1.80		1.80		1.80		1.80		1.80		1.80
A15	Transmitter 2				1.80				24		32	←						OFF					→

Table 6.2-2. (Sheet 1) SSU Electrical Power Requirements

SSU ELECTRICAL POWER REQUIREMENTS

REFERENCE DESIGNATION	NOMENCLATURE	MAXIMUM POWER REQUIRED (WATTS)						OPERATING VOLTAGE RANGE				CMG's ON TELEMETRY OFF COMMAND STANDBY		CMG's ON TAPE RECORD, COMMAND STANDBY		CMG's ON TAPE PLAYBACK COMMAND STANDBY		CMG's ON TAPE PLAYBACK, COMMAND INTERROGATE		CMG's ON TAPE PLAYBACK, COMMAND EXECUTE		TELEMETRY OFF COMM. STANDBY CMG'S OFF	
		PEAK		NORMAL		STANDBY		MINIMUM		MAXIMUM													
		AC	DC	AC	DC	AC	DC	AC	DC	AC	DC	AC	DC	AC	DC	AC	DC	AC	DC	AC	DC	AC	DC
A16	2 Pt Calibrator Generator				1.20				25		31		OFF		1.20		1.20		1.20		1.20	OFF	
A17	Time Code Generator				3.50				25		31		3.50		3.50		3.50		3.50		3.50		3.50
A18	560 HZ Filters & Isolators	←												NO POWER REQUIRED →									
A19	Command Decoder		9.00		3.50 Inter		0.15		24		32		0.15		0.15		0.15		3.50		9.00		0.15
A20	Diplexer Hybrid	←												NO POWER REQUIRED →									
A21	Hybrid 1	←												NO POWER REQUIRED →									
A22	Hybrid 2	←												NO POWER REQUIRED →									
A23	Antenna Assembly	←												NO POWER REQUIRED →									
A24	Command Receiver 1		0.7		0.40				24		32		0.40		0.40		0.40		0.70		0.70		0.40
A25	Command Receiver 2		0.7		0.40				24		32		0.40		0.40		0.40		0.70		0.70		0.40
A26	VCO-Mixer Assembly																						
	VCO 1 (IRIG #7)				0.26				25		31	← OFF →			0.26		0.26		0.26		0.26	OFF	
	VCO 2 (IRIG #7)				0.26				25		31	←						OFF					→
	VCO 3 (IRIG #10)				0.26				25		31	← OFF →			0.26		0.26		0.26		0.26	OFF	
	VCO 4 (IRIG #10)				0.26				25		31	←						OFF					→

Table 6.2-2. (Sheet 2) SSU Electrical Power Requirements

SSU ELECTRICAL POWER REQUIREMENTS

REFERENCE DESIGNATION	NOMENCLATURE	MAXIMUM POWER REQUIRED (WATTS)						OPERATING VOLTAGE RANGE				CMG's ON TELEMETRY OFF COMMAND STANDBY		CMG's ON TAPE RECORD, COMMAND STANDBY		CMG's ON TAPE PLAYBACK COMMAND STANDBY		CMG's ON TAPE PLAYBACK, COMMAND INTERROGATE		CMG's ON TAPE PLAYBACK, COMMAND EXECUTE		TELEMETRY OFF COMM. STANDBY CMG'S OFF	
		PEAK		NORMAL		STANDBY		MINIMUM		MAXIMUM													
		AC	DC	AC	DC	AC	DC	AC	DC	AC	DC	AC	DC	AC	DC	AC	DC	AC	DC	AC	DC	AC	DC
	VCO 5 (IRIG #2)				0.26				25		31		0.26		0.26		0.26		0.26		0.26		0.26
	VCO 6 (IRIG #2)				0.26				25		31	←						OFF	→				
	Mixer 1				0.28				25		31		0.28		0.28		0.28		0.28		0.28		0.28
	Mixer 2				0.28				25		31	←						OFF	→				
A27	PCM Multicoder				6.00		0.01		25		31	← OFF →			6.00		6.00		6.00		6.00	OFF	
A28	Subcommutator 2				1.70				25		31	← OFF →			1.70		1.70		1.70		1.70	OFF	
A29	" 3				1.70				25		31	← OFF →			1.70		1.70		1.70		1.70	OFF	
A30	" 4				1.70				25		31	← OFF →			1.70		1.70		1.70		1.70	OFF	
A31	" 5				1.70				25		31	← OFF →			1.70		1.70		1.70		1.70	OFF	
A32	Signal Conditioning Unit				2.00										2.00		2.00		2.00		2.00	OFF	
A33	SMR (Main)								22		35												
A34	SMR (Standby) Losses								22		35		4.00		4.00		4.00		4.00		4.00		
A35	PCM Multicoder				6.00		0.01		25		31	← OFF →			0.01		0.01		0.01		0.01	OFF	

Table 6.2-2. (Sheet 3) SSU Electrical Power Requirements

SSU ELECTRICAL POWER REQUIREMENTS

REFERENCE DESIGNATION	NOMENCLATURE	MAXIMUM POWER REQUIRED (WATTS)						OPERATING VOLTAGE RANGE				CMG's ON TELEMETRY OFF COMMAND STANDBY		CMG's ON TAPE RECORD, COMMAND STANDBY		CMG's ON TAPE PLAYBACK COMMAND STANDBY		CMG's ON TAPE PLAYBACK, COMMAND INTERROGATE		CMG's ON TAPE PLAYBACK, COMMAND EXECUTE		TELEMETRY OFF COMM. STANDBY CMG'S OFF	
		PEAK		NORMAL		STANDBY		MINIMUM		MAXIMUM													
		AC	DC	AC	DC	AC	DC	AC	DC	AC	DC	AC	DC	AC	DC	AC	DC	AC	DC	AC	DC	AC	DC
A36	Telemetry Terminal Block and Bulkhead Connectors												NO POWER REQUIRED										
A37	Command Relay Junction Box		1.20		0.03				24		32		0.03		0.03		0.03		1.20		1.20		0.03
A38	Battery								25		35												
A39	Battery Charger Losses								22		35		4.00		4.00		4.00		4.00		4.00	OFF	
	Total AC & DC Loads											14.92	20.32	14.92	45.65	14.92	51.38	14.92	56.77	14.92	62.27		
A9 or A10	Inverter Losses											8.20		8.20		8.20		8.20		8.20		OFF	
	Conditioned Power (DC)											23.12	20.32	23.12	45.65	23.12	51.38	23.12	56.77	23.12	62.27		
	Total Conditioned Power (DC)												43.44		68.77		74.50		79.89		85.39		9.32
A33	SMR (Main) Losses												5.00		6.88		7.45		7.99		8.54		4.00
	Total Solar Array Loads												48.44		75.65		81.95		87.88		93.93		
A34	SMR (Standby) Losses																						5.00
	Total Battery Load																						18.32

Table 6.2-2. (Sheet 4) SSU Electrical Power Requirements

6.2.1.3 Under-and-Over Voltage Protection

Undervoltage protection is provided on the data handling bus and solar array bus. If the voltage on the data handling bus drops below 22 to 24 VDC for greater than 200 msecs., the non-essential loads on this bus will be disconnected. If the voltage on the solar array bus drops below 22 to 24 VDC for greater than 1 second, the battery will be placed on-line. In case of a failure the undervoltage protection permits fault isolation disconnection of the non-essential loads and maintenance of voltage on the solar array bus. The command system (an essential load) is maintained on the bus and can be used to determine and by-pass a faulty component. The undervoltage signals are provided to the spacecraft.

Overvoltage protection is supplied by the switching mode regulators. Only in the case of the failure of both switching mode regulators would the solar array be directly coupled to the regulated bus.

The circuitry required to provide the undervoltage sensing is packaged in the power control electronics unit as is the switching required to control the power system and the power distribution.

6.2.1.4 Instrumentation

The power system provides instrumentation for signal conditioning the power system parameters. The include:

a. Solar Bus Current
b. Solar Bus Voltage
c. Battery Charge/Discharge Rate
d. Battery Voltage
e. Battery Temperature
f. Main SMR ON/OFF
g. Standby SMR ON/OFF
h. Command System Voltage
i. Telemetry System Voltage
j. Battery Charger ON/OFF
k. Battery Charge/Hold Off Status
l. Main Inverter ON/OFF
m. Standby Inverter ON/OFF

n. Main SMR Voltage

o. Standby SMR Voltage

p. CMG ON/OFF Status

q. Constant Current Monitors

The power system also provides constant current to the control moment gyros. The constant current was set to a 10 milliampere nominal value.

The circuitry to provide the conditioning of power system parameters is located in the power control electronics unit.

6.2.1.5 Fusing

In the design of the SERT II SSU power system a ground rule was established that all electrical components would be fused except those whose failure would abort the mission. The fuses utilized and their values are listed in Table 6.2-3. The fuses are placed on plug-in circuit boards in the power control electronics unit.

6.2.2 AC POWER SYSTEM

The following section discusses the design of that part of the power system that supplies the required 115V, 400 Hz power to loads connected to the ac power bus. Figure 6.2-1, sheet two, displays a block diagram of the power system that may be utilized for reference purposes.

6.2.2.1 Power Requirements

The Control Moment Gyro power characteristics that sized the design of the ac power system are listed in Table 6.2-2. The power system is capable of starting two gyros and operating them in running condition. The switching circuitry is arranged so that any single inverter can operate in conjunction with any two control moment gyros.

The dc to ac inverters, utilized to power the attitude control system, operate on an input voltage range of 22 to 35 VDC. The ac output is a three-phase ungrounded delta connection with 115 volts rms, 400 Hz line to line. Over an input of 24 to 32 VDC the output voltage remains within the following limits:

115 VMRS ± 4.5% No load to 10VA

115 VMRS ± 2.5% At 10VA to 40VA

115 VMRS ± 4.5% AT 40VA to 60VA

The ac output frequency is 400 Hz ± 1% for all operating conditions after twenty minutes of warm-up.

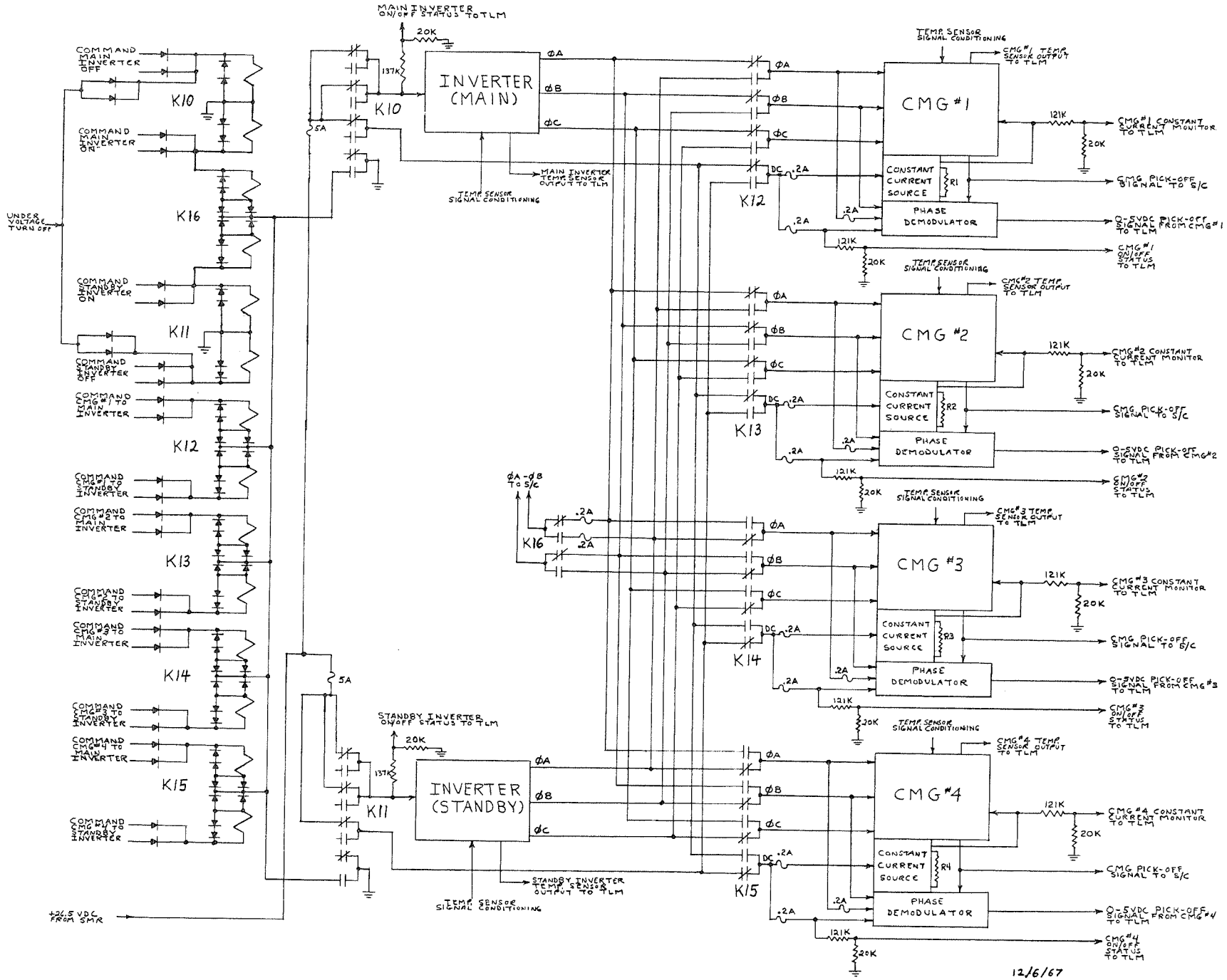
MAIN INVERTER ON/OFF STATUS TO TLM
20K
137K
INVERTER (MAIN)
ΦA
ΦB
ΦC
K10
5A
MAIN INVERTER TEMP SENSOR OUTPUT TO TLM
TEMP SENSOR SIGNAL CONDITIONING
COMMAND MAIN INVERTER OFF
COMMAND MAIN INVERTER ON
UNDER VOLTAGE TURN OFF
K16
COMMAND STANDBY INVERTER ON
K11
COMMAND STANDBY INVERTER OFF
COMMAND CMG #1 TO MAIN INVERTER
K12
COMMAND CMG #1 TO STANDBY INVERTER
COMMAND CMG #2 TO MAIN INVERTER
K13
COMMAND CMG #2 TO STANDBY INVERTER
COMMAND CMG #3 TO MAIN INVERTER
K14
COMMAND CMG #3 TO STANDBY INVERTER
COMMAND CMG #4 TO MAIN INVERTER
K15
COMMAND CMG #4 TO STANDBY INVERTER
+26.5 VDC FROM SMR
STANDBY INVERTER ON/OFF STATUS TO TLM
INVERTER (STANDBY)
STANDBY INVERTER TEMP SENSOR OUTPUT TO TLM
TEMP SENSOR SIGNAL CONDITIONING
CMG #1
CMG #2
CMG #3
CMG #4
CONSTANT CURRENT SOURCE
R1
R2
R3
R4
PHASE DEMODULATOR
DC
.2A
121K
20K
CMG #1 CONSTANT CURRENT MONITOR TO TLM
CMG PICK-OFF SIGNAL TO S/C
0-5VDC PICK-OFF SIGNAL FROM CMG #1 TO TLM
CMG #1 ON/OFF STATUS TO TLM
CMG #2 CONSTANT CURRENT MONITOR TO TLM
0-5VDC PICK-OFF SIGNAL FROM CMG #2 TO TLM
CMG #2 ON/OFF STATUS TO TLM
ΦA - ΦB TO S/C
CMG #3 CONSTANT CURRENT MONITOR TO TLM
0-5VDC PICK-OFF SIGNAL FROM CMG #3 TO TLM
CMG #3 ON/OFF STATUS TO TLM
CMG #4 CONSTANT CURRENT MONITOR TO TLM
0-5VDC PICK-OFF SIGNAL FROM CMG #4 TO TLM
CMG #4 ON/OFF STATUS TO TLM
12/6/67

The ac power system was also sized to supply 24VA of single phase, 400 Hz power to the Spacecraft while running two control moment gyros.

6.2.2.2 Instrumentation

Phase demodulators are incorporated in the ac power system, one for each control moment gyro. The phase sensitive demodulators compare an input signal of zero or one-hundred and eighty degrees phase and a variable amplitude, to a phase reference signal. The input signal is the output derived from a control moment gyro.

The phase demodulators are configured to operate on a 5-18 V full scale input range. Referencing the signals to the input pins on the phase demodulator connector, the output varies from 0 VDC to 2.5 VDC with J1-8 in phase with J1-4 and the output varies from 2.5 VDC to 5.0 VDC when J1-8 is out of phase with J1-4. The units are calibrated for a gain of 0.33 VDC output per volt input (7.5 volts out of phase input results in a 5.0 VDC output).

6.2.2.3 Fuses

The fuses utilized for the non-essential loads of the ac power system are shown in Table 6.2-3. It should be noted that the A of ac power supplied the Spacecraft is not fused within the SSU because the lines within the Spacecraft are fused.

6.3 OPERATION

The power subsystem, integrated and controlled by the power control electronics unit, provides a versatile and reliable system. The power system is capable of operating over an input range of 27.5 to 55 VDC. The system may be operated from ground power, solar array, or on the battery incorporated in the SSU.

6.3.1 DC POWER SYSTEM

The block diagram displaying the dc power system is located on page one of Figure 6.2-1.

During normal operation the solar array will supply power through both the main and standby switching mode regulators (SMR). The main SMR supplies power to the inverters, spacecraft, and data handling system loads (load bus). The standby SMR supplies power to the command system and transmitters. Coupling of the output of the main SMR is provided to the command bus through diode CR9. In the event that the standby SMR fails, loads on the command bus will be picked up by the main SMR. The solar array bus can be routed directly to the load bus and command bus by turning off both SMRs.

TABLE 6.2-3

POWER SUBSYSTEM FUSE VALUES

Unit	Fuse Assembly No.	Fuse Rating (Amps)	Maximum Operating Current (Amps)
1. Rec. #1	A1F1	0.20	.027
2. Rec. #2	A1F3	0.20	.027
3. Decoder	A1F5	0.50	.346
4. Decoder	A1F6	0.50	.346
5. XMTR #1	A1F11	0.20	.069
6. XMTR #2	A1F13	0.20	.069
7. VCO #5	A1F15	0.20	.010
8. VCO #6	A1F16	0.20	.010
9. Mixer #1	A1F17	0.20	.011
10. Mixer #2	A1F18	0.20	.011
11. Time Code Gen.	A1F19	0.75	.216
12. Cmd. Relay Box	A1F20	0.20	.046
13. VCO #3	A2F1	0.20	.010
14. VCO #4	A2F2	0.20	.010
15. VCO #1	A2F3	0.20	.010
16. VCO #2	A2F4	0.20	.010
17. PCM Multi. #1	A2F5	2.00	.422
18. PCM Multi. #1 HO	A2F6	0.50	.0004
19. PCM Multi. #1A	A2F7	2.00	.422
20. PCM Multi. #1A HO	A2F8	0.50	.0004
21. Tape Rec. #1	A2F9	5.00	.453
22. Tape Rec. #2	A2F10	5.00	.453
23. Sub Com #2	A2F11	0.20	.071
24. Sub Com #3	A2F12	0.20	.071
25. Sub Com #4	A2F13	0.20	.071
26. Sub Com #5	A2F14	0.20	.071
27. 2 Pt. Calib.	A2F15	0.20	.053
28. Sig. Cond. Unit	A2F16	0.20	.009
29. Sig. Cond. Unit	A2F17	0.20	.009
30. Batt. Current Sensor	A2F18	0.20	.040
31. Sig. Cond. Unit	A2F19	0.25	.054
32. Current Reg. #1	A3F1	0.20	.010
33. Phase Dem. #1	A3F2	0.20	.062
34. Current Reg. #2	A3F3	0.20	.010
35. Phase Dem. #2	A3F4	0.20	.062
36. Current Reg. #3	A3F5	0.20	.010

TABLE 6.2-3 (continued)

POWER SUBSYSTEM FUSE VALUES

	Unit	Fuse Assembly No.	Fuse Rating (Amps)	Maximum Operating Current (Amps)
37.	Phase Dem. #3	A3F6	0.20	.062
38.	Current Reg. #4	A3F7	0.20	.010
39.	Phase Dem. #4	A3F8	0.20	.062
40.	Phase Dem. #1 (ϕA)	A3F9	0.20	.004
41.	Phase Dem. #2 (ϕA)	A3F11	0.20	.004
42.	ϕ A to SC (MI)	fuse by-passed		
43.	ϕ A to SC (SI)	fuse by-passed		
44.	Fail Safe	A4F1	2.00	.750
45.	UV & BOL Batt. Pwr.	A4F2	2.00	.750
46.	SA Current Sensor	A4F3	0.20	.040
47.	Phase Dem. #3 (ϕA)	A4F4	0.20	.004
48.	Phase Dem. #4 (ϕA)	A4F5	0.20	.004
49.	Batt. Enable (AGENA)	A4F6	0.50	.100
50.	Batt. Charger on (AGENA)	A4F7	0.50	.100
51.	UV & BOL operate	A4F8	0.50	.010
52.	Main Inv.	A10F1	15.00	8.00
53.	Charger Output	A10F2	15.00	2.00
54.	Main SMR	A10F3	15.00	8.00
55.	Stdby SMR	A10F4	15.00	8.00
56.	Stdby Inv.	A10F5	15.00	8.00
57.	Charger Input	A10F6	15.00	8.00
58.	Inv. Temp. Sensors	A10F7	0.20	.010

The battery is connected to the input of the standby SMR through diode coupling. However, in normal operation the diodes (CR7 and CR8) will be back-biased by the battery charger and the battery will not supply any power. In the event that the solar array drops enough so that the battery voltage is higher than that of the battery charger, the battery will start to supply power to the system. Low voltage on the solar bus will be approximately 23 VDC. After a one second delay the battery will be placed in the enable position and the battery charger will be turned off routing the battery up to the input of the main SMR. Under low voltage conditions, 23 VDC on the load bus, non-essential loads will be disconnected from the load bus within 200 milliseconds to minimize the load. The battery may be charged by placing the battery charger in the charge mode. For higher charge rates the battery should be kept in the enable mode. High charge rates (above 440 ma) will result in an erroneous reading (greater than 100 ma discharge) on the low range current sensor. Once the charge rate drops to about 100 ma (the full scale reading on the low range) the battery can be placed in the off-line mode.

The command system switching circuits located in the power control electronics unit provide the following control of the dc power system:

Main SMR	ON/OFF
Standby SMR	ON/OFF
Data Handling System	ON/OFF
Battery to Hold - Off Mode	
Battery to Charge Mode	
Battery Enable	
Battery Off-Line	
Battery Charger	ON/OFF

In addition, status monitors of power system functions are provided (reference section 6.2.1.4).

6.3.2 AC POWER SYSTEM

The block diagram displaying the AC Power System is located on sheet two of Figure 6.2-1.

AC power, instrumentation, and the torquer currents are provided to the control moment gyros by the ac power system. Two inverters are utilized, either of which can provide power to any two control moment gyros and a reference voltage to their associated phase sensitive demodulators. The dc power required by the constant current sources and phase demodulators is switched through common contacts on the ac power relays. Any control moment gyro and its associated components can be placed on either inverter. However, when both inverters are commanded on an interlock inhibits the switching of gyros. The inverters also provide one phase of power to the Spacecraft from the inverter which has been turned on last. The gyro power is wired for a spring launch as follows:

Gyros 1 and 4	ϕB to pin A
	ϕA to pin B
	ϕC to pin C
Gyros 2 and 3	ϕA to pin A
	ϕB to pin B
	ϕC to pin C

The 10 ma constant current is applied to the torquer coil as follows:

Gyros 1 and 3	G (+)
	H (-)
Gyros 2 and 4	G (-)
	H(+)

The phase sensitive demodulators are wired and operate in the following manner:

Demodulator A5 (Gyro A1)

ϕB to pin 4

ϕA to pin 5

A1-D to pin 8

A1-E to pin 15

Demodulator A6 (Gyro A2)

ϕA to pin 4

ϕB to pin 5

A2-D to pin 8

A2-D to pin 15

Demodulator A7 (Gyro A3)

ϕA to pin 5

ϕB to pin 4

A3-D to pin 8

A3-E to pin 15

Demodulator A8 (Gyro A4)

ϕB to pin 5

ϕA to pin 4

A4-D to pin 8

A4-E to pin 15

Voltage from pin 8 in phase with pin 4 results in 0VDC output and out of phase a 5VDC output from the phase demodulator. Figure 6.3-1 displays the mechanical mounting configuration of the gyros.

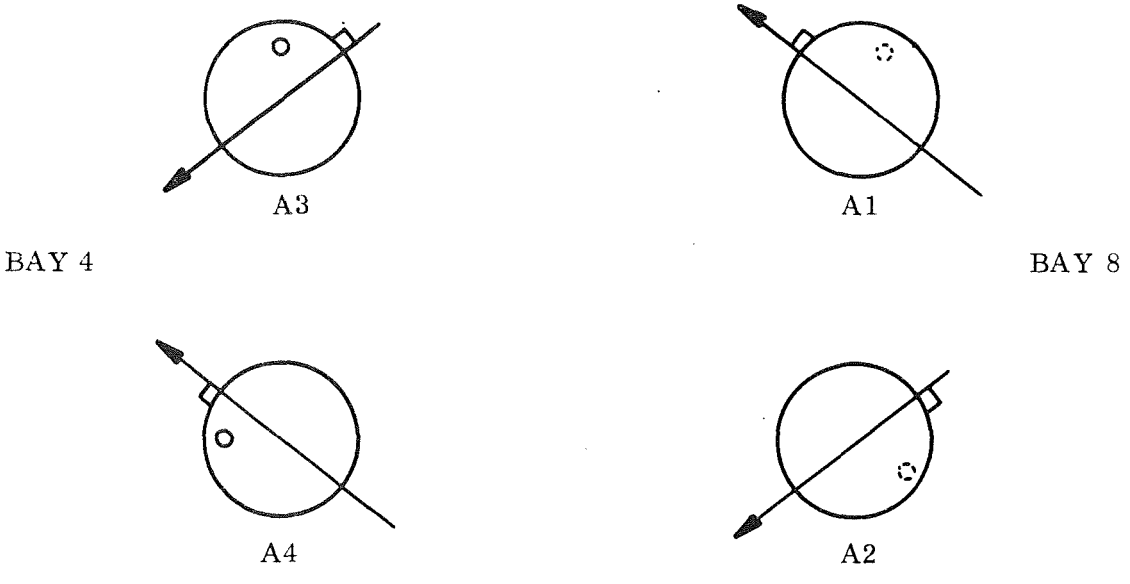

Figure 6.3-1. CMG Mounting Configuration

The command system and power control electronics unit provide switching capability for the ac portion of the power system. The commands include:

Main Inverter ON/OFF
Standby Inverter ON/OFF
CMG #1 to Main Inverter
CMG #2 to Main Inverter
CMG #3 to Main Inverter
CMG #4 to Main Inverter
CMG #1 to Standby Inverter
CMG #2 to Standby Inverter
CMG #3 to Standby Inverter
CMG #4 to Standby Inverter

In addition, status monitors of functions, reference Section 6.2.1.4, are provided.

6.4 DEVELOPMENT

During the design and development of the power system, it became apparent that improvements could be made to enhance the performance of the SSU. The changes are described in the following paragraphs.

6.4.1 POWER SYSTEM REDESIGN

The major change was a redesign of the power system during the initial design phase of the SSU program.

The investigation of redesigning the power subsystem resulted in a proposal to NASA Lewis Research Center that contained the following recommendations:

- Have the battery voltage available on-line at all times.
- Provide current limiting in the battery circuit through the use of a switching mode regulator.
- Cut off all non-essential loads when the battery discharge current exceeds a pre-determined value for a finite period.
- Use a switching mode regulator to replace the zener voltage limiter.

During the design phase for the new configuration it was found desirable to retain undervoltage sensing as was in the original system, however, this was accomplished in a less complex manner.

The following advantages accrued from the new design:

- Reduction of circuitry complexity.
- Substantial weight reduction.
- Removed the series diode from the housekeeping-solar array line and used the voltage drop more effectively with the switching mode regulator.
- Eliminated the undervoltage relays from the solar array line.
- Provided power conditioning for all energy sources.
- Minimized the high current switching transients.
- Eliminated the zener voltage limiter and associated thermal problems.

In the original system, power was supplied to the essential loads, data handling, and signal conditioning circuits by two DC-DC converters.

The selection of the converters was controlled by complex switching circuitry. In the new design, the circuit containing the DC-DC converters and the relay switching logic was removed. The new design incorporated simplicity and flexibility through the utilization of switching mode regulators (SMR) and diodes, providing command capability to bypass failed units. Switching mode regulators (similar to the model EMVR102 manufactured by Gulton Indistries for the Agena) provide a current limited regulated output with a minimum of 1.5 volts between input and output.

The redesigning of the power system resulted in a more efficient system. The zener limiter and series diode on the solar array bus were eliminated. The actual power saving is dependent on the load on the bus and voltage of the bus, but would certainly be greater than four watts under normal operating conditions. The converter no-load loss was 10 watts and the switching mode regulator utilized in the new system has a no-load loss of 3 watts. Both switching mode regulators are maintained on-line in the new system. However, there is still a savings of about 4 watts at no-load.

6.4.2 INVERTER FILTER REDESIGN

The DC to AC Inverter was tested to verify compatibility with the control moment gyros. The purpose of the test was to determine if one inverter could start and run-up to speed two control moment gyros simultaneously. The inverter did start two control moment gyros, but did not drive them beyond approximately half-speed. A contract was given to Engineered Magnetics to study the half-speed lock-up problem. The evaluation of the problem and possible solutions were submitted to Fairchild Hiller in a report from Engineered Magnetics. The results are summarized herein:

The problem was a result of too high an output impedance in the inverter at low frequencies (and dc) causing modulation on the output of the inverter. The low frequencies are produced by the "hunting action" of the gyro motor. DC components can also be generated by a motor due to unbalance of the motor winding and air gap.

To solve the problem, it is necessary to add a dc by-pass to the inverter. This was done efficiently with the addition of a choke in the output filter of the inverter.

All tests indicated that the added choke performed its function. Previously the unit had been unable to run up a gyro without excessive modulation. One, two, three, and then all four gyros were run up without problem although modulation did occur when three and four gyros were run up. High and low temperature tests were also made. Two gyros can therefore, be comfortably run up to speed.

6.4.3 FUSE CHANGES

During integration of the Experimental and Prototype Model Spacecraft Support Units, the inverter and battery charger fuses would sometimes blow on the starting transient. These components have large capacitance inputs and are fed by a source (switching mode regulator) that has a capacitive output. This configuration results in large turn-on transients. The problem was corrected by replacing the 5 ampere fuse with a 15 ampere fuse. The regulated bus is protected by the undervoltage circuit. If a short occurred on these lines the inverters and battery charger would be turned off, allowing the short to be isolated. In the event the battery was on-line, the 15 ampere fuse would protect the battery.

During integrated test with the Spacecraft and Spacecraft Support Unit mated, it was found that the Spacecraft drew more than the 0.2 amperes allowed for the 115 VAC, 400 Hz line. Because the spacecraft adequately fuses all lines, the fuse was bypassed in the power control electronics unit.

SECTION VII

COMMAND SYSTEM

7.1 REQUIREMENTS

The command system provides control functions required by the SERT II Spacecraft, Agena, and SSU systems in the performance of the mission. The command system incorporates the required capability of accepting a serial tone command, amplitude modulated on an r-f carrier. The serial tone command is decoded in the command system decoder. The stored command is then encoded into a serial data word and transmitted back to the ground for controller verification. The ground controller can then issue an "execute" command which causes execution of the stored command. Command storage may be cleared by command or automatically it will clear if no execute command is received within a predetermined time.

7.2 DESIGN

The command system consists of two units, the command decoder and command relay junction box. The command decoder (Spec. No. 833-15409-P001) was purchased from AVCO Corporation Electronics Division; the CRJB was designed and built by FHC. The block diagram of Figure 7.2-1 describes the command system.

7.2.1 COMMAND SYSTEM INPUT

The command decoder accepts simultaneous inputs from two redundant receivers and is capable of operating on either receiver if the other becomes disabled. A serial format is used consisting of an address tone followed by three command tones selected from a field of six tones. The combination of three tones selected from six provides a command capacity of 216 commands.

The command format is compatible with existing STADAN/GSFC command standards and network facilities.

The format of a command is displayed in Figure 7.2-2. The duration of the address tone and command tones is nominally 500 msec, providing an inherent maximum command rate of 1 command per 4.5 seconds but without ground station verification. The decoder will operate at an input signal level of 18 milliwatts and will successfully detect the presence of a valid input signal when the input signal to noise ratio is as low as 3 db (noise bandwidth of 10 kHz).

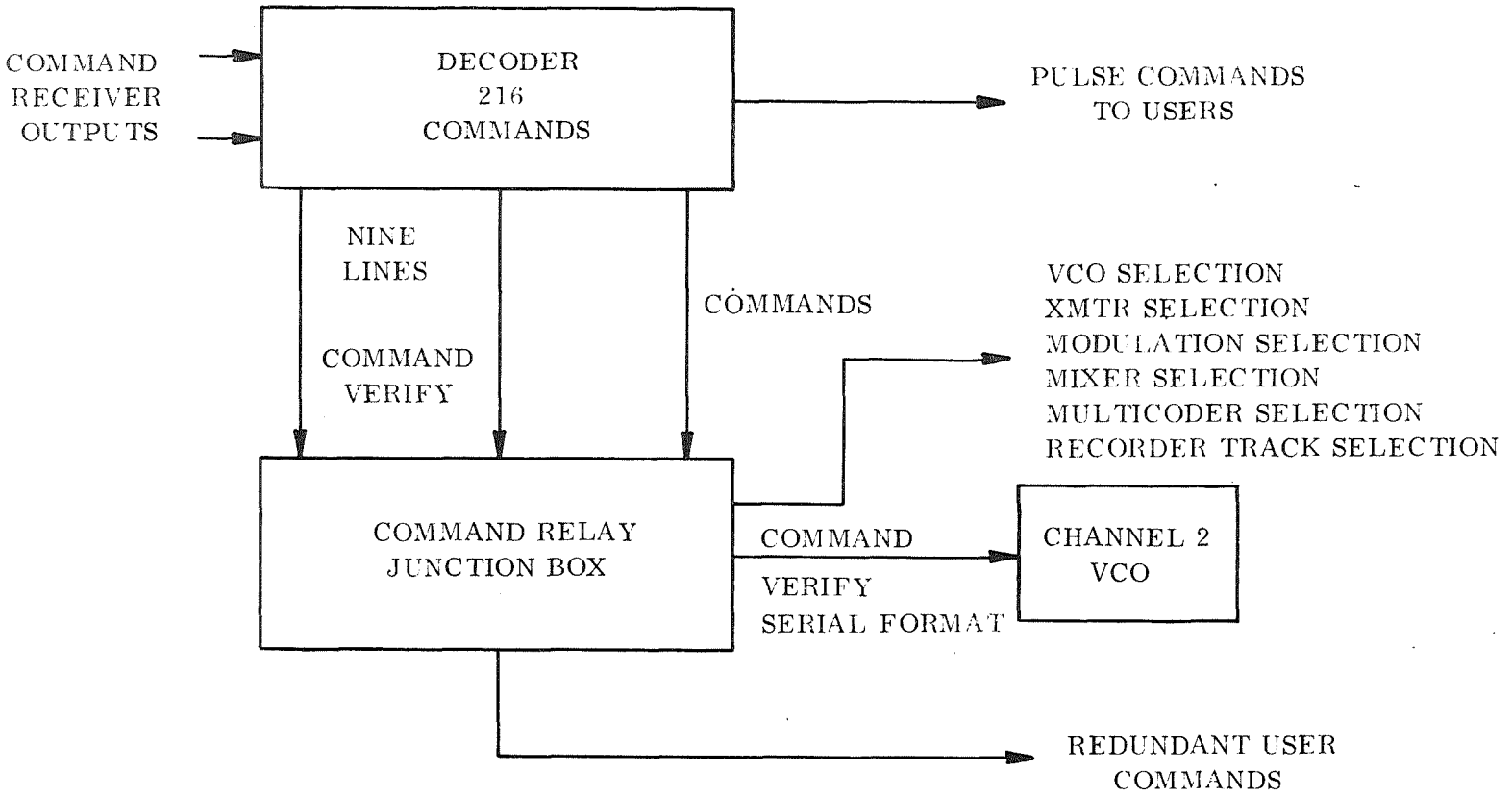

Figure 7.2-1. Command System Block Diagram

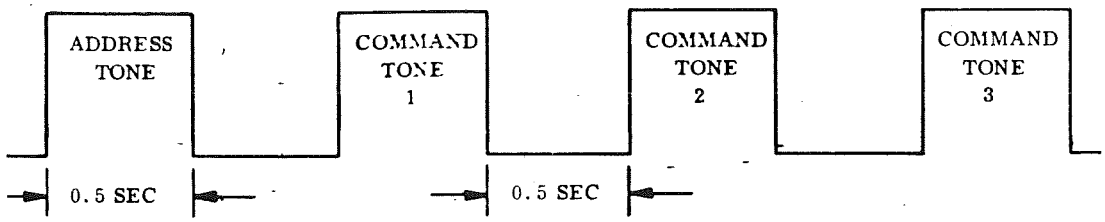

Figure 7.2-2. Command Tone Format

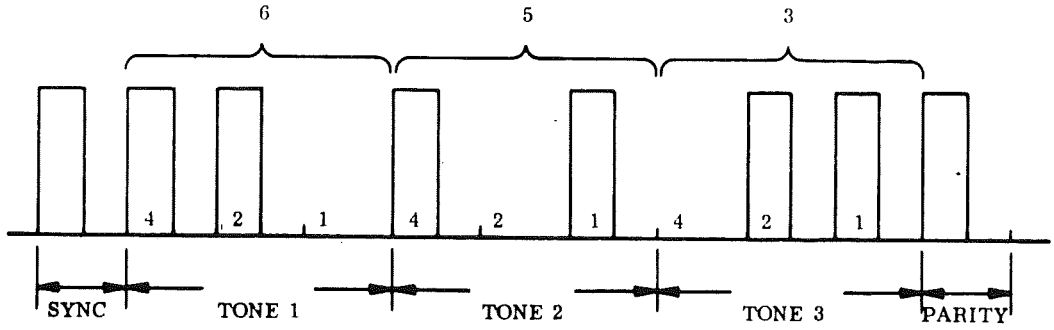

Figure 7.2-3. Typical Command Verify Format

Protection against spurious signals is provided in the command system as follows:

- The decoder accepts command tones which are greater than 400 milliseconds, but less than 600 milliseconds.
- Execute tones between 200 milliseconds and 800 milliseconds are accepted.
- The interval between tones must be between 200 milliseconds and 800 milliseconds.
- All commands having missing tones are rejected.

The decoder "normally" is in a standby state in which the power drawn by the unit does not exceed 150 milliwatts. Reception of a valid address tone activates the decoder to its operating mode, in which 4.5 watts is drawn. Upon transmitting a command, a B+ switch-off circuit is activated returning the unit to the standby state.

The command system will automatically clear itself if execution does not occur within twelve to seventeen seconds after the fourth command tone. The system also will clear itself immediately upon reception of a clear signal, which is any tone other than the address tone.

7.2.2 COMMAND SYSTEM OUTPUT

The command system provides outputs for control of 216 command functions. The control is provided by discrete output pulses with the following characteristics.

Voltage	20 to 30 volts
Voltage pulse width	50 milliseconds minimum
Current	150 ma minimum
Pulse rise time	1 millisecond maximum
Pulse fall time	5 millisecond maximum

Short circuit protection is provided such that a short on any output shall not have any deleterious effect on any other output. In addition, upon removal of the short the command system operates normally.

The output of the command decoder consists of two fully redundant decoder "halves" each capable of decoding 108 commands. Fully redundant commands can be implemented by using a command from each half for the same function.

7.2.3 COMMAND SYSTEM VERIFICATION

Each command received by the spacecraft is stored to allow verification at the ground station prior to execution. The verification function is performed by the decoder, which provides nine readout lines from the memory cells to the command relay junction box (CRJB). The CRJB accepts the nine parallel lines from the decoder, a 17.5 pps clock line from the time code generator and outputs a 8.75 pps serial pulse train to one of two redundant voltage control oscillators (VCO's) on IRIG channel number two.

Figure 7.2-3 displays a typical command verification, (command 653). The command tone identification is encoded in a BCD format and a sync pulse and parity (even) pulse are provided.

7.2.4 COMMAND DISTRIBUTION

Commands are routed from the command system to their respective switching circuits within the SSU and to the Agena and Spacecraft interfaces.

Table 7.2-1 lists the commands utilized by the SSU; their primary tone code, function, and backup tone code where redundancy is required.

Table 7.2-2 lists the commands utilized by the spacecraft and Agena and distributed to their respective interfaces.

In addition to distribution, the command system provides circuits and utilizes commands to perform the following functions:

- Selection of primary or backup voltage controlled oscillators
- Selection of transmitters
- Selection of modulation
- Selection of primary or backup mixer
- Selection of primary or backup PCM multicoder
- Selection of recorder track

A typical switching circuit incorporated in the CRJB is shown in Figure 7.2-4.

The CRJB diode couples redundant commands required by the SSU, Agena, and Spacecraft onto a single line to the user.

7.3 OPERATION

The command system provides control of the SSU functions and commands to the appropriate spacecraft and Agena interfaces.

Table 7.2-1. Command Tone List

SSU Command Tone Code		
Primary	Backup	Function
631	--	CMG 1 to Main Inverter
453	--	CMG 1 to Standby Inverter
254	--	CMG 2 to Main Inverter
226	--	CMG 2 to Standby Inverter
261	--	CMG 3 to Main Inverter
262	--	CMG 3 to Standby Inverter
263	--	CMG 4 to Main Inverter
253	--	CMG 4 to Standby Inverter
111	654	Data Handling System ON
112	564	Data Handling System OFF
113	655	Transmitter 1 ON
663	--	Transmitter 1 OFF
115	622	Transmitter 2 ON
116	--	Transmitter 2 OFF
121	656	Modulation Select 1
122	634	Modulation Select 2
152	364	Select VCO 5 (Command Verify)
153	624	Select VCO 6 (Command Verify)
125	633	Select VCO 1 (Real Time)
126	533	Select VCO 2 (Real Time)
215	643	Select VCO 3 (Playback)
163	524	Select VCO 4 (Playback)
155	642	Select Mixer 1
154	632	Select Mixer 2
145	623	Select Multicoder 1
136	542	Select Multicoder 2

Table 7.2-1. Command Tone List (continued)

SSU Command Tone Code		
Primary	Backup	Function
164	--	Tape Recorder 1 OFF
165	--	Tape Recorder 1 Recond
166	--	Tape Recorder 1 Playback
156	--	Tape Recorder 2 OFF
216	--	Tape Recorder 2 Record
225	--	Tape Recorder 2 Playback
635	--	T.C.G. Zero Reset
235	--	T.C.G. Up Count
236	--	T.C.G. Down Count
554	--	Select Recorder Track 1
555	--	Select Recorder Track 2
131	245	Battery Enable
132	445	Battery Charger OFF
521	446	Main Inverter ON
523	464	Main Inverter OFF
545	621	Standby Inverter ON
436	511	Standby Inverter OFF
531	646	Main SMR ON
535	641	Standby SMR ON
133	456	Battery Charger ON
146	532	Battery OFF-Line
141	525	Battery Charge
135	662	Battery Hold-OFF
246	551	Main SMR OFF
335	461	Standby SMR OFF

Table 7.2-2. Spacecraft and Agena Command Tone List

Spacecraft Command Tone Code					
334	321	536	415	252	626
342	322	614	416	351	661
343	323	562	134	345	114
344	324	433	142	552	123
411	331	316	266	636	124
412	332	325	315	553	515
413	333	326	221	462	522
414	611	463	222	666	526
421	612	434	223	665	556
423	455	422	224	616	566
424	454	441	311	651	615
431	143	442	313	544	652
432	144	443	444	565	653
341	426	352	211	561	
231	435	353	312	644	
232	256	355	512	465	
233	541	356	213	563	
234	543	361	214	645	
241	513	362	212	336	
242	625	363	251	255	
243	514	466	161	613	
244	516	365	425	354	
314	534	366	162	346	

Agena Command Tone Code
151
264

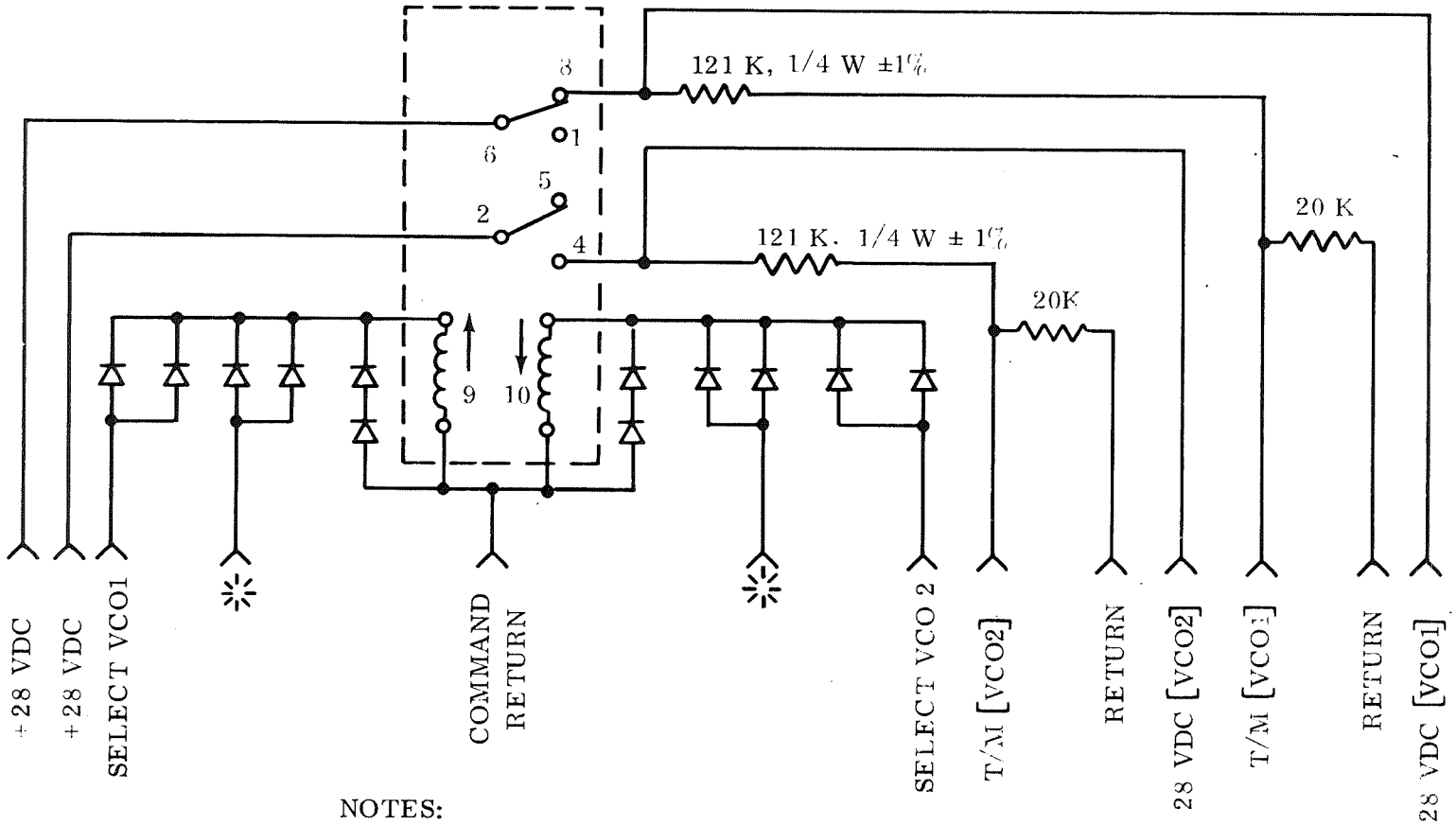

NOTES:

1. ALL DIODES 1N645 UNLESS OTHERWISE SPECIFIED
2. ALL RESISTORS ARE 1/4 WATT
3. THE INPUT INDICATED WITH * REPRESENTS A CAPABILITY TO ACCEPT REDUNDANT COMMANDS IF REQUIRED

Figure 7.2-4. Command Relay Junction Box

The ground operator selects the three tone sequence that corresponds to the command he wishes to send. The command is transmitted to the spacecraft over the 148 MHz command r-f link. The command receiver demodulates the AM signal and provides the serial tone signal to the command decoder. Details on the r-f performance are discussed in section 8.2.2.

The command system accepts and stores the transmitted command. The serial verification signal is telemetered back to the ground, enabling the operator to check the stored command. A clear or execute command may then be sent based on his evaluation. An automatic clear is provided after twelve to seventeen seconds in the decoder and, as a backup, is sent after fifteen seconds to the command encoder. The automatic clear provides two functions. It ensures the command register in the decoder is clear and places the decoder in its standby mode, drawing substantially less power.

Execution of the command results in the transmission of discrete output command pulse to the selected user. Virtually all the systems using commands in the SSU interface with relay circuitry. The low noise level on the command lines and circuitry insensitive to noise precludes the possibility of false commands.

- A resistor in the output strobe monostable multibration was changed to increase the command output pulse duration from 30 to 50 milliseconds.
- The decoder input regulator has an additional series resistor to ensure operation to the maximum input voltage of +32 VDC, without stressing components.
- Memory cells were modified to convert stored commands into nine parallel outputs. These nine lines are brought out of the decoder to external verify circuitry.
- The load capacity of the command output was increased to 150 milliamperes.
- Command execution was modified to allow verification before execution.
- Circuitry was added to clear a stored command automatically if execution does not occur within 12 to 17 seconds.
- Circuitry was added to allow the decoder to accept a ground clear signal.

SECTION VIII

RF SYSTEMS

8.1 REQUIREMENTS

The SERT II SSU r-f system provides the tracking and data transmission link for the spacecraft-to-ground stations of the STADAN network. In addition, commands sent from those ground stations are received and demodulated by the r-f system. The systems implemented are compatible with the STADAN network and were designed to provide:

- In excess of 95 percent coverage for all vehicle orientations.
- Operation of a 5 degree elevation angle.
- Maintenance of error rates to less than 1×10^{-7}.
- Tracking noise of less than 1 degree.

8.2 DESIGN

The system implemented consists of redundant transmitters and receivers coupled to a monopole antenna system by hybrids and diplexers. Table 8.2-1 lists the r-f system components, their manufacturer, specification number and the quantity used per system. Figure 8.2-1 is a block diagram of the rf system.

8.2.1 DATA AND TRACKING LINK

The VHF data and tracking link is implemented through the use of redundant 350 milli-watt transmitters coupled through a hybrid-diplexer system to the -7db monopole antenna system (ref. Figure 8.2-1). The diplexers provide the necessary isolation between the transmission and receiving systems. The hybrids provide distribution of power to the four monopole antennas comprising the antenna system. A requirement of -13 dbw of rf power at each antenna terminal was established as the minimum level allowable. The effective radiated power from the SERT II SSU is therefore -20 dbw.

The space transmission loss or propagation loss between two isotropic antennas can be expressed as follows:

$$L_p = 36.6 + 20 \log f + 20 \log d$$

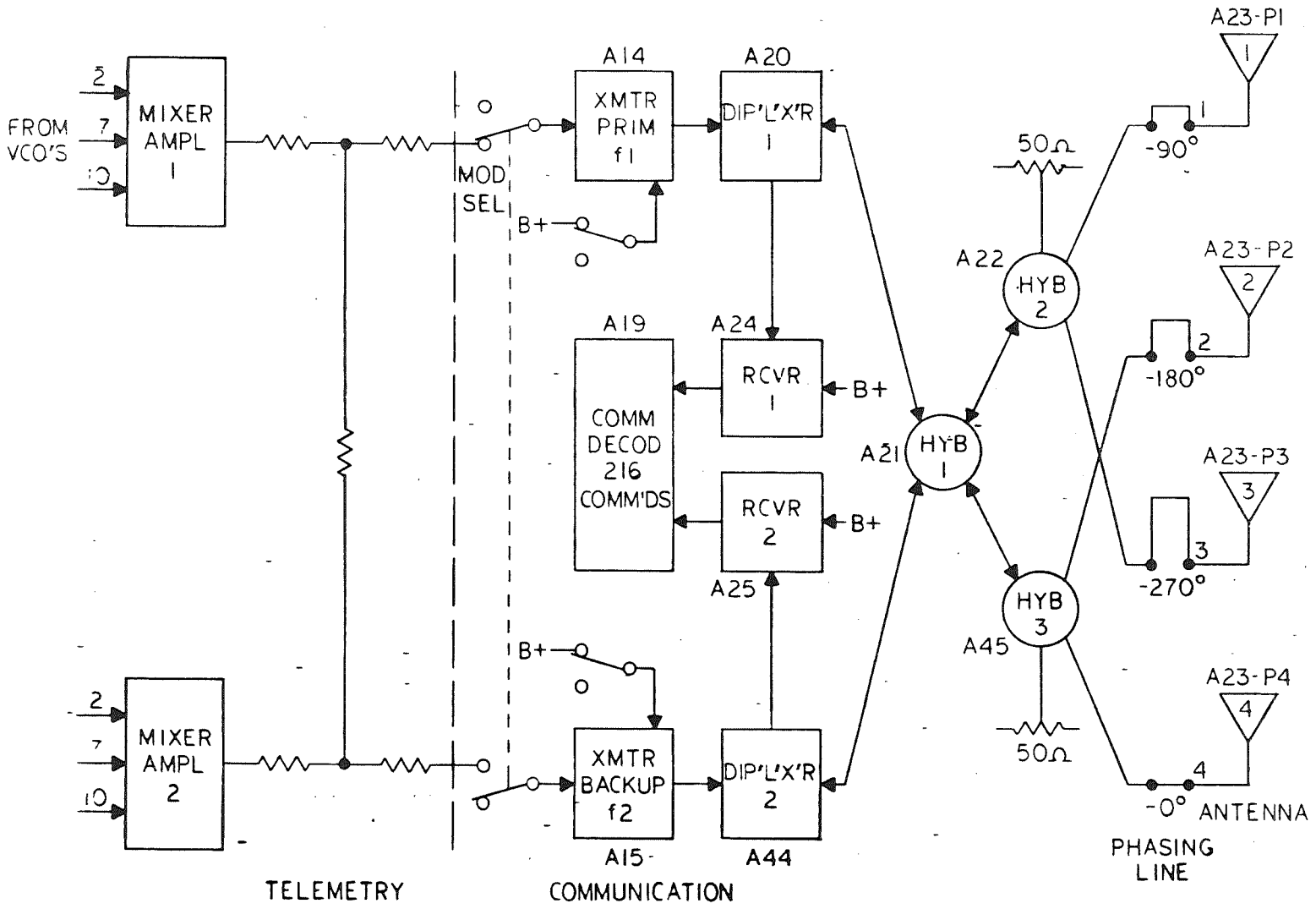

Figure 8.2-1. Communications/RF System Block Diagram

TABLE 8.2-1

RF Systems Components

Description	No./System	Vendor	Control Specification
Command Receiver	2	AVCO Corporation Electronics Div.	833-15401-P-001
Transmitter	2	Spacecraft Inc.	833-15405-P-001
Hybrid	3	Motorola, Inc.	833-15411-P-001
Diplexer	2	Motorola, Inc.	833-15410-P-001
Antenna Assembly	4	FHC	---

where the link is operating at frequency f (MHz) and the antennas are separated by distance d (miles).

The transmitters utilized for the VHF telemetry down link utilize the following frequencies:

Primary Transmitter 136.230 MHz

Secondary Transmitter 136.920 MHz

A frequency of 137 MHz is utilized for the downlink calculations. Range to the satellite will vary from a minimum of 622 s. mile (540 n. mile) at zenith for a circular orbit to a maximum of 2000 s. mile for an inclination angle of 5 degrees above the horizon. Computing the path loss:

L_p	F(MHz)	d (s. miles)
135.2 db	137	622
145.3 db	137	2000

8.2.1.1 Data Link

The STADAN telemetry ground station to be utilized in support of the SERT II mission incorporates a 22 db antenna, selectable polarization, with a system noise figure of 3.5 db. The receiver IF bandwidth is selectable, with 30 KHz recommended for use on SERT II.

The receiving system noise power can be expressed as a noise spectral density (independent of bandwidth), η

$$\eta = k T_E$$

where k is Boltzmann's constant and T_E is the effective noise temperature of the receiving system.

Te = T antenna + T receiver

or

Te = T antenna + (F-1) To

To = 290° and F is the noise factor of the receiving system. For the SERT II data link the receiver noise figure of 3.5 db (η f = 2.24) is equivalent to a noise temperature of 330°K. At 137 MHz the antenna temperature is approximately equal to 700°K, so that the effective noise temperature is 1030°K and the noise spectral density equals -201.5 db.

Figure 8.2-2 and Table 8.2-2 illustrate the data link system and the calculations of the link performance. Table 8.2-2 shows computations of the downlink for the case when SERT is in a zenith position and at its maximum slant range (5 degree elevation).

The power in each subcarrier, discriminator bandwidths, and modulation indices are taken from the analysis performed in section 9.2.5 of this report. The FM improvement factor is related to the modulation index of the channel and can be expressed by the relationship $3B^2$. Figure 8.2-2 relates the computations performed in Table 8.2-2 and shows that the data link performance is more than adequate. The signals transmitted on each of the subcarriers employ a digital format. Error in the system is therefore a function of quantization (ref. section 9.2.2) for the data channels and the bit error rate is negligible ($\ll 10^{-8}$).

8.2.1.2 Tracking Link

The STADAN tracking system capability will be utilized to aid in acquisition and for orbit determination.

Table 8.2-3 shows a link calculation for use of the beacon as an acquisition aid. The SERT II SSU transmission characteristics and the propagation losses were discussed in section 8.2.1.1. The STADAN characteristics are as follows:

- Antenna Gain - 19 db
- Polarization - Linear
- Receive system noise figure - 3.5 db
- Bandwidth - 3 to 300 Hz

The resultant signal to noise ratio varies 20 db as a function of the loop bandwidth. Inspection of the resultant valves show that as the loop is narrowed down equivalent rms error due to the link becomes less than one percent.

The minitrack receiver interferometer used for orbit determination has a noise figure of less than 3.0 db. The antenna gain for fine measurement is 16 db and the antenna gain for ambiguity resolution is 6.5 db. Table 8.2-4 shows the tracking link calculation for orbit determination. A loop bandwidth of 10 Hz is used for the fine system and a bandwidth of 2 Hz for the ambiguity system.

8.2.2 COMMAND LINK

The VHF command link utilizes standby redundant receivers coupled to the antenna system through a system of hybrids and diplexers (ref. Figure 8.2-1)

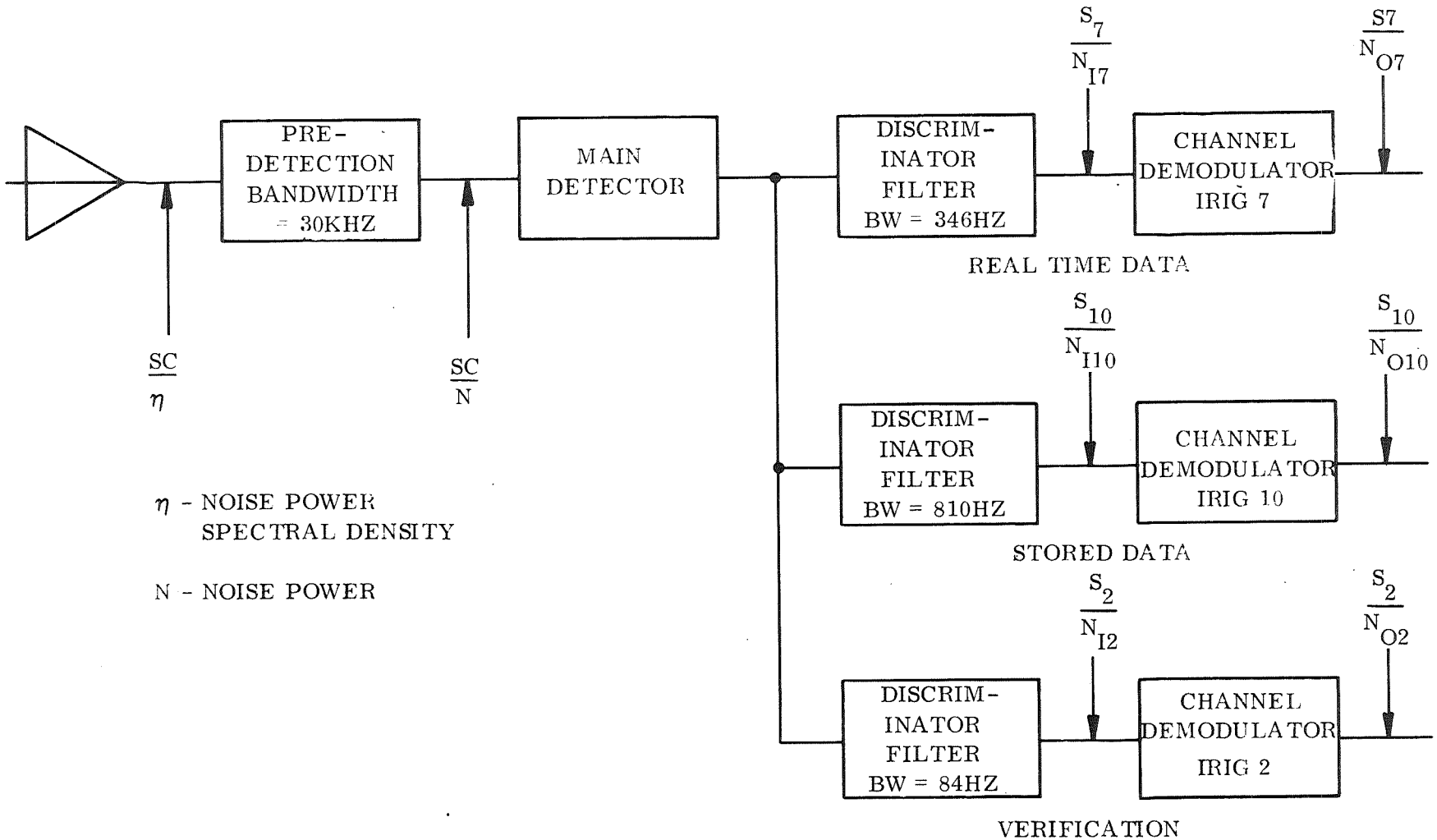

Figure 8.2-2. RF Downlink Block Diagram

Table 8.2-2. RF Downlink Power Budget

Frequency (nominal)	137 MHz	Power Channel 2 Power Channel 7 Power Channel 10	-29.6 db -22.45 db -18.85 db
Minimum Power at the Antenna	-13 db	Discriminator Bandwidth Ch. 2 Discriminator Bandwidth Ch. 7 Discriminator Bandwidth Ch. 10	84 Hz 346 Hz 810 Hz
Propagation Loss (622/2000) (622/2000 s. mi.)	135.2 db/ 145.3 db		
Polarization Loss	0 db	S2/NI2 S7/NI7 S10/NI10	33.3/23/2 db 33.45/22.35 db 33.35/23°25 db
Receiving Antenna Gain	22 db	Modulation Index 2 Modulation Index 7 Modulation Index 10	= 9.6 = 9.9 = 1.45
Received Signal Level	-133.2 db/ -143.3 db	FM Improvement 2 FM Improvement 7 FM Improvement 10	24.5 db 22.0 db 4.3 db
Antenna Noise Temperature	700°K	S2/No 2 S7/No 7	57.8/47.7 db 55.45/44.35 db 37.65/27.55 db
Sc	63.3/ 58.2 db - Hz		
Predetection Bandwidth	30 KHz		
Sc/N	23.5/13.4 db		

Table 8.2-3. Acquisition RF Power Budget

(1)	Frequency (nominal)	137 MHz
(2)	Minimum Power at the Antenna	-13 dbw
(3)	Transmit Antenna Gain	-7 db
(4)	Propagation Loss	135.2/145.3 db
(5)	Polarization Loss	3.0 db
(6)	Receiving System Losses	-----
(7)	Receiving Antenna Gain	19 db
(8)	Received Signal Level	-138.2/-149.3 db
(9)	Receiver Noise Figure	3.5 db
(10)	Antenna Noise Temperature	700°K
(11)	Effective Noise Temperature	1030°K
(12)	C	
(13)	Predetection Bandwidth	10 KHz
(14)	C/N	23.3/12.2 db
(15)	Loop Bandwidth *	3 Hz
(16)	S/N	58.5/47.4 db
(17)	Loop Bandwidth *	300 Hz
(18)	S/N	38.5/27.4 db

*3,300 Hz variable bandwidth

Table 8.2-4. Orbit Determination RF Power Budget

		Fine	Ambiguity
(1)	Frequency (nominal)	137 MHz	137 MHz
(2)	Minimum Power at the Antenna	-13 dbw	-13 dbw
(3)	Transmit Antenna Gain	-7 db	-7 db
(4)	Propagation Loss	135.2/145.3 db	135.2/145.3 db
(5)	Polarization Loss	3.0 db	3.0 db
(6)	Receiving System RF Losses	----	----
(7)	Receiving Antenna Gain	16 db	6.5 db
(8)	Received Signal Level	-142.2/-152.3 db	-151.7/-161.8 db
(9)	Receiver Noise Figure	3.0 db	3.0 db
(10)	Antenna Noise Temperature	700°K	700°K
(11)	Effective Noise Temperature	990°K	990°K
(12)	C	59.2/49.1 db	49.7/39.6 db
(13)	Predetection Bandwidth	10 KHz	10 KHz
(14)	C/N	19.2/9.1 db	9.7/-0.4 db
(15)	Loop Bandwidth	10 Hz	2 Hz
(16)μ	Signal to Noise Ratio	49.2/39.1 db	46.9/36.6 db

The STADAN command system provides amplitude modulated transmitters operating in the 148-149 MHz band at a power level of 2Kw. The antenna gain is 20 db (including transmit system losses) and linear or right circular polarization can be selected.

The SERT II receiver operates at a frequency of 149 MHz. Range to the satellite from a ground station will vary from a minimum of 622 s. mile (540 n. mile) at zenith for a circular orbit to a maximum slant range of 2000 s. miles (inclination of 5 degrees). Computing the propagation losses:

L_p	f (MHz)	d (s. miles)
136.0 db	149	622
146.1 db	149	2000

The SERT II antenna system provides a gain of -7 db, with associated receiving system losses amounting to 7.5 db (maximum). The receiver sensitivity is less than 2.0 microvolts, with a predetection bandwidth of 35 KHz (6 db).

Table 8.2-5 indicates the calculations performed for the SERT II command link. As in section 8.2-1 the effective noise temperature was calculated using,

$$Te = T\ antenna + (F - 1)\ To$$

For the receive system the noise figure of 7.5 db results in a noise factor of 5 and a receiver equivalent noise temperature of 1160°K. The total effective noise temperature is therefore the sum of the antenna noise temperature of 700°K and 1160°K or 1860°K.

The spectral noise density η , can be expressed as:

$$\eta = K\,Te$$

where K is Boltzmann's constant. The noise spectral density equals -204.1 db. Utilizing the computed received signal level and a predetection bandwidth of 35 KHz the resultant signal to noise ratio into the receiver is 76.8/67.1 db.

The output signal to noise ratio of an AM receiver can be expressed as a function of the input signal to noise ratio and the modulation index.

$$So/No = m^2\ Sc/Nc$$
$$So/No = 67.1\ (m^2)\ db$$

It can be seen that for a reasonable modulation index $M \geq .25$, the three db signal to noise ratio required by the decoder is exceeded.

Table 8.2-5. Command RF Link Power Budget

(1)	Frequency (nominal)	149 MHz
(2)	Minimum Power at the Antenna	33 dbw
(3)	Transmit Antenna Gain	20 db
(4)	Propagation Loss (622/2000 s. mi.)	136.0/146.1 db
(5)	Polarization Loss (max)	3.0 db
(6)	Receiving Antenna Gain	-7.0 db
(7)	Received System Losses	7.5 db
(8)	Received Signal Level	-100.5/-110.6 db
(9)	Receiver Noise Figure	7 db
(10)	Antenna Noise Temperature	700°K
(11)	Effective Noise Temperature	1860°K
(12)	C	103.6/93.5 db
(13)	Predetection Bandwidth	35 KHz
(14)	Sc/Nc	76.8/67.1 db
(15)	Output Bit Error Probability	1×10^{-7}

For an evaluation of the design performance of the command verification link, see the analysis of IRIG Channel 2 in section 8.2-1.

8.2.3 ANTENNA SYSTEM

The SERT II SSU Antenna System consists of four monopoles mounted radially around the SSU. The following requirements were incorporated into the Antenna System design:

1. Operation in the region from 136 MHz to 149 MHz.
2. The Monopole Antennas fold parallel to the SERT II SSU when in the shroud. A spring system is used to deploy the antennas into their operating configuration when the shroud is removed.
3. The Antennas have a VSWR less than 1.5.
4. The gain of each monopole is approximately 0 db in the H-plane and +2 in the E-plane.
5. It was desired to maximize coverage and minimize the regions of low signal levels, particularly in the region the earth ground stations will be located.

8.2.3.1 Design

A circularly polarized turnstile configuration of monopole antennas was selected and implemented as shown in Figure 8.2-1. To verify the design antenna pattern measurements were performed at a frequency of 1420 MHz, corresponding to a scale factor 1:10. A one-tenth scale model of the Atena/SSU/SC vehicle was used in making the tests (Figure 8.2-3). The deployed solar panels, the ion engines, and the monopole array are the major features of the model.

The scale model radiating element is a quarterwavelength monopole. Physically, the monopole rod was the extension of the center conductor of the coaxial connector of the monopole. It will be recognized that this arrangement is the same one used in the full-size antenna and hence the scaling of theradiating element is valid. The input VSWR of each of the four monopoles was measured (at 1,420 MHz) and found to be less than 1.4:1.

The feed network for the array must provide equal amplitude and progressive phasing for the four elements. To achieve equal excitation for each monopole, a reactive power divider (Microlab D5-2FT) was used. Proper phasing was achieved by the use of differential cable lengths between the power divider and the antenna elements. The antenna phasing was as follows:

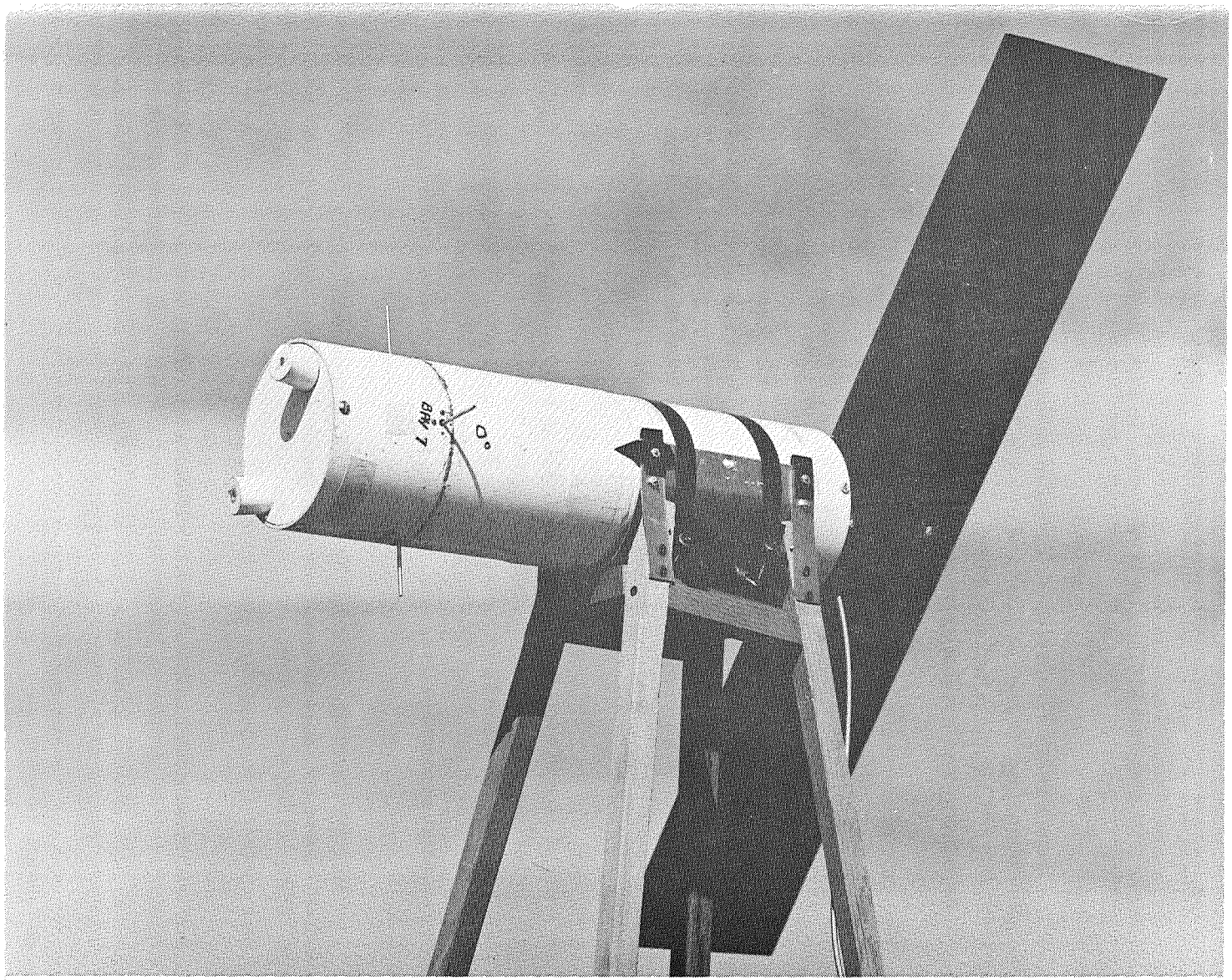

Figure 8.2-3. One-tenth Scale Model Agena/SSU/Spacecraft

Element No.	Location	Phase
1	Bay 1	90°
2	Bay 3	180°
3	Bay 5	270°
4	Bay 7	0°

This phasing is identical with that in the flight systems and, in fact, is achieved in a similar way.

The antenna range facility used for the measurements is located at the Sherman Fairchild Technology Center. Distance betseen the transmitting antenna and the model was 200 feet. The minimum distance, based on the $2D^2/\lambda$ criteria, is 50 feet. The 1420 MHz source was a signal generator, Empire Model No. SG-11.

The gain of the model antenna array was measured by comparison to a standard gain horn (the Polarad CA-L calibrated antenna, with a gain of 10.2 dbi at 1420 MHz was the standard).

The feed distribution losses for the model antenna array were estimated. Total dissipative losses for the array were 2.2 db, with 1.2 db attributed to the coaxial cables and 1 db to the power divider. The full-scale flight system has 0.5 db of cable loss and 1.7 db loss in the diplexers and hybrids, for a total of 2.2 db. Thus the gains of both the full-scale and the model antenna arrays, including feed losses, are identical.

A total of 74 patterns were measured, all at 1420 MHz, as a function of the polar angle θ (see coordinate system in Figure 8.2-4. Such patterns were measured at 5° intervals in azimuth angle φ (= 0°, 5°, . . . , 180°). Thirty-seven patterns were obtained for Eφ polarization and thirty-seven for Eθ polarization. Recordings were in rectangular coordinates, with relative intensity plotted on a db scale.

The antenna coverage afforded by the SERT II monopole array is shown in Figure 8.2-4. Four contours of constant gain (referenced to isotropic) have been plotted: -4db, -7db, -10db and -16 db. The larger of the two linear orthogonal polarizations has been selected in compiling the chart.

The coverage, expressed as a percentage of 4π steradians, has been calculated from Figure 8.2-4 by graphical integration. For the SERT II communication system, a gain level of -7db defines coverage. For this level, the following result was obtained:

$$\left.\begin{array}{l}\text{coverage, at gain} \\ \text{value of -7 db}\end{array}\right\} = 94\%$$

This value compares favorable with the one obtained during the proposal preparation period, wherein a value of 95% was obtained.

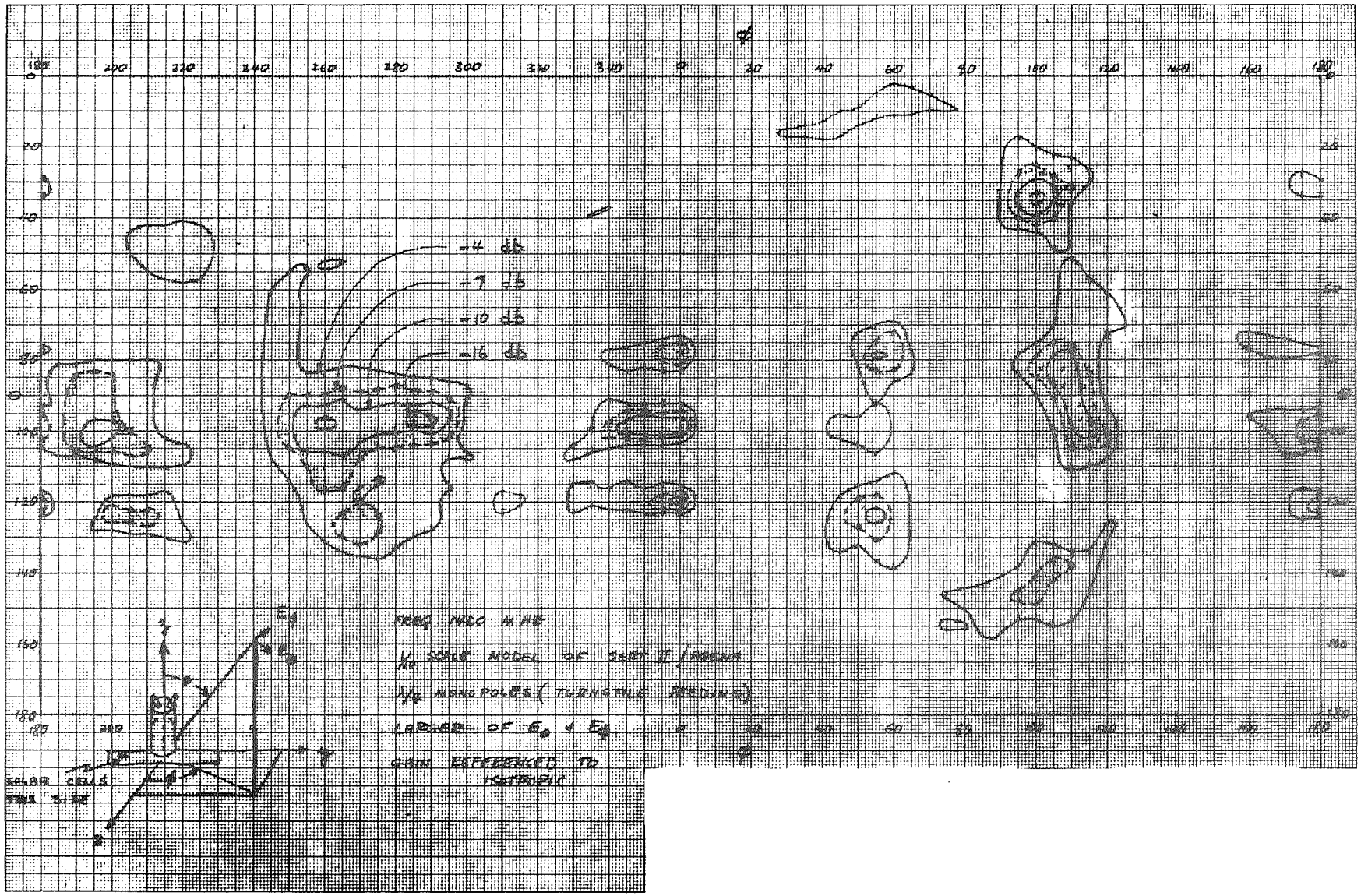

Figure 8.2-4. Monopole Antenna Array Coverage

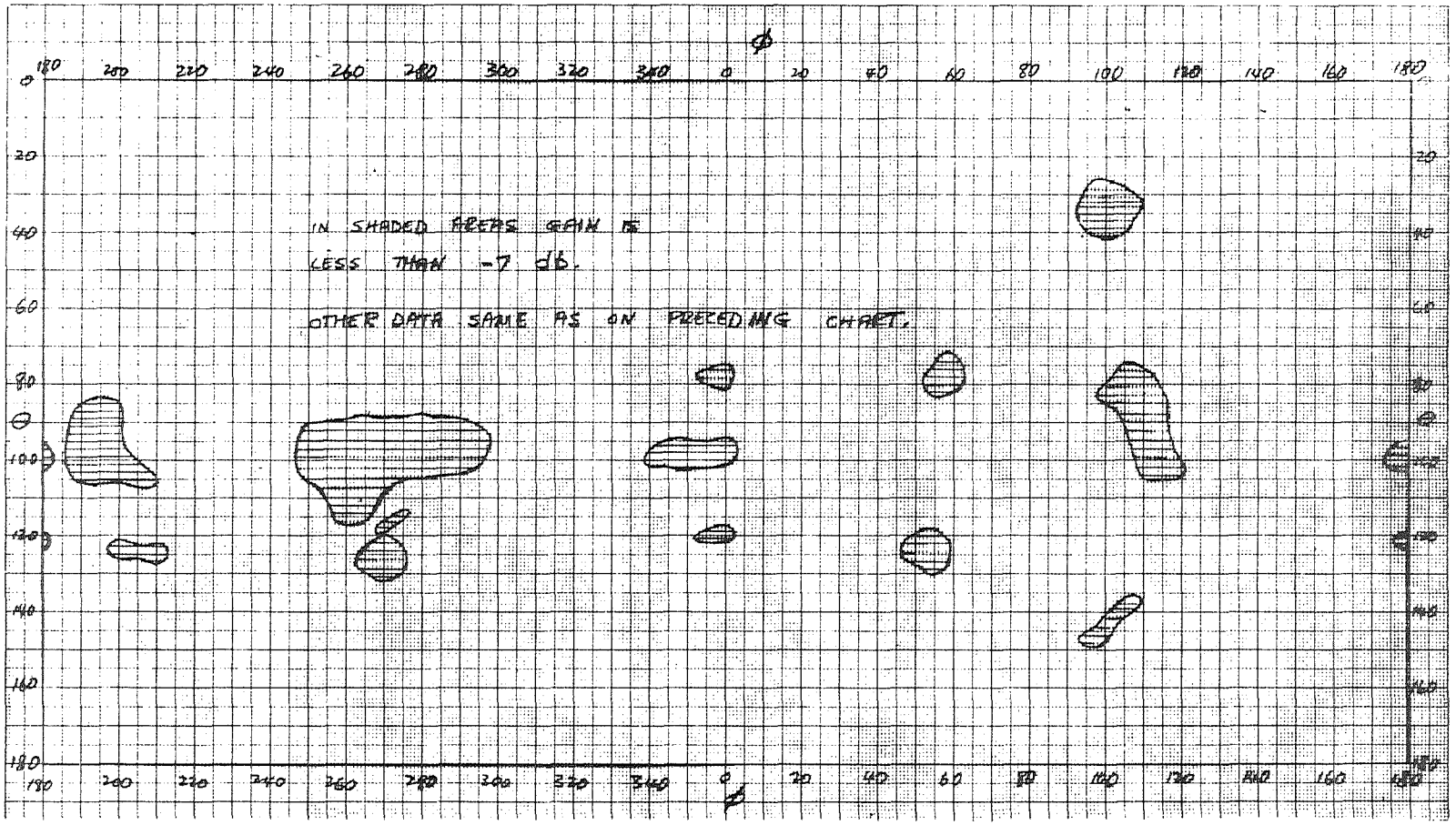

Figure 8.2-4a. Monopole Antenna Array Coverage (-7 db only)

In Figure 8.2-4a only the contour for -7 db has been plotted. This chart clearly shows the regions of low signal levels. For a normal flight, the SERT II ion engines are pointed more or less in the direction of the earth. This means that the earth stations are in the region defined by $\theta = 90°$ (top half of Figure 8.2-3 and 8.2-4). For most of the communication paths, θ is less than 45° or so. A study of the coverage diagram shows that only one region of low coverage exists for $\theta = 45°$. This is the area whose center is located at $\theta = 35°$ and $\phi = 100°$. Because of its small area this low coverage area is not expected to produce any serious "drop-outs".

8.3 RECEIVERS

The First Experimental Model Receiver was an ISIS receiver supplied GFE to AVCO, where it was modified to meet SERT II requirements. The remaining units utilized the basic ISIS design which was modified to change the frequency and power input range. The receiver was specifically manufactured to meet SERT II requirements.

8.3.1 ANTENNA

Antenna Matching stubs were considered for use in the antenna system to minimize the VSWR on each of the four antennas. Tests run on the antennas on the full scale mock-up (Figure 8.2-5) indicated that the measured admittance was significantly better than predicted by calculation. The uncompensated impedance bandwidth is about 15 MHz for a maximum VSWR of 1.5. As a consequence, the use of impedance matching was deleted. The use of such a device would decrease the transmitted power from about 96% to 98%. In view of the weight, size and complexity associated with the matching stubs and the slight power gain, their use is not warranted. No problems were encountered in tuning the Monopole Antennas to VSWR of less than 1.5.

After each antenna was tuned, tipped with a hemispherical insert, and painted it was subjected to an Acceptance Test on the Fairchild Hiller Antenna Range, (Figure 8.2-6). The antennas were checked to the following tolerances:

H-Plane

Maximum gain at 142 MHz, -2db (min)
Maximum gain - minimum gain, 1.5 db (max)

E-Plane

Maximum gain at 142 MHz, 0 db (min)

The standard dipole was utilized as the gain reference.

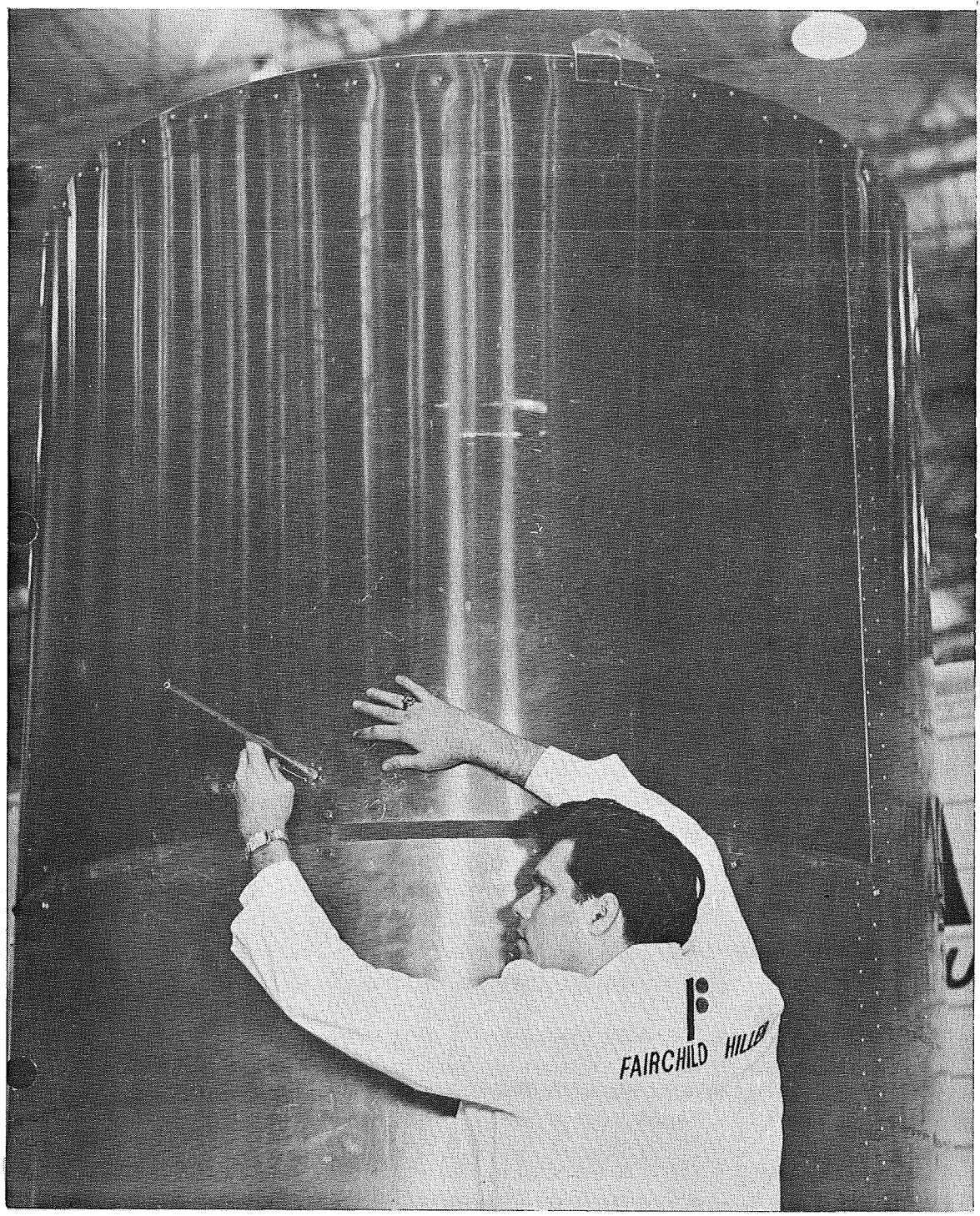

Figure 8.2-5. Antenna Full-Scale Mock-up

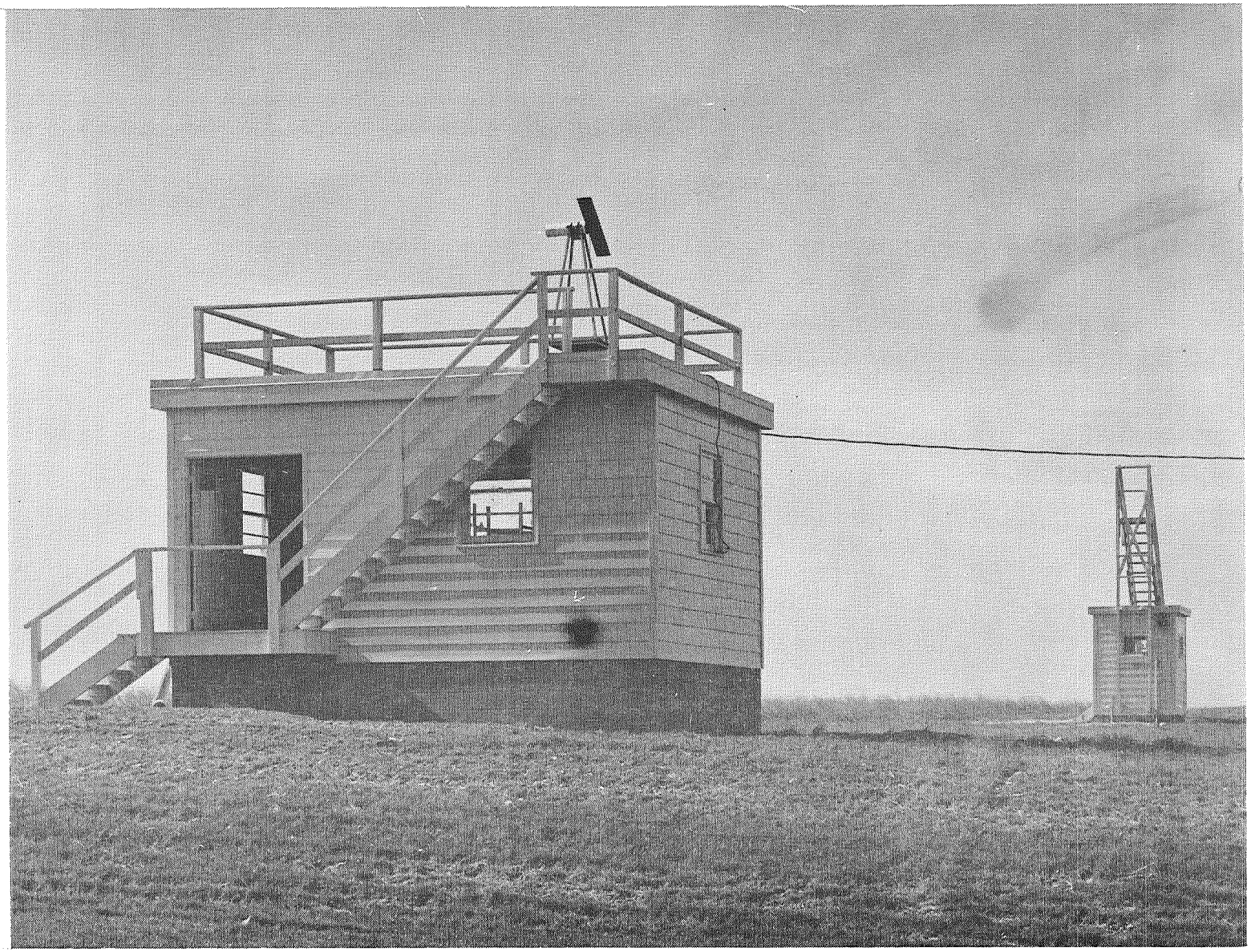

Figure 8.2-6. Fairchild Hiller Antenna Test Range

SECTION IX

COMMUNICATIONS SYSTEM

9.1 REQUIREMENTS

The communications System for the SERT II consists of a PCM telemetry system and ancillary equipment that provide the following functions:

1. Telemetry various data channels from the Spacecraft, Agena, and Spacecraft Support Unit.
2. Provide timing signals for experimenter use.
3. Provide in-flight data calibration.
4. Provide a cumulative indication of elapsed spacecraft time.
5. Provide capability of data storage to allow delayed transmission during periods of acquisition by ground telemetry stations.
6. Allow verification of commands prior to command execution.
7. Be compatible with STADAN facilities and Aerospace Data Systems Standards (NASA document X-560-6302).

The communications system has provisions for accepting and processing analog and digital data signals into a PCM format. Nominally 240 subcommutated and 15 prime data channels are furnished to be utilized for Spacecraft, Agena, and SSU functions. Spare channels are incorporated for growth potential and redundancy. Two independent timing lines are provided the Spacecraft to enable synchronization of the experiments with the sampling of data.

Redundant tape recorders permit up to 129.6 minutes of data to be stored on board the spacecraft for delayed transmission to ground telemetry stations. Playback occurs at a speed sixteen times as fast as the recording rates permitting a relatively fast "dump" of data during periods of acquisition.

A three-point calibration is provided on each subcommutator to ensure high system accuracy. A cumulative elapsed time indication of 277 days in 4-minute increments, is generated by an on-board time code generator. The time code generator has an inherent stability of greater than 0.01% and provides a 17.5 pps clock for the command verification.

The real time data, delay time data, and command verification are multiplexed onto three redundant IRIG subcarrier voltage control oscillators. The subcarriers are frequency division multiplexed through a passive adder and a mixer amplifier and phase modulated on a telemetry transmitter.

9.2 DESIGN

A detailed block diagram of the communications system is presented in Figure 9.2-1. Table 9.2-1 lists the components utilized in the communication system with their manufacturer, specification number and the quantity used per system.

9.2.1 DATA INPUT CAPABILITY

Four subcommutators are employed in the communication system, each capable of handling sixty (60) analog data input lines carrying voltages between 0 and +5 volts. The subcommutator utilizes a single ended configuration with 50 megohms input impedance. Input signal overvoltage protection of $\pm$ 32 volts is incorporated with no degradation of accuracy in adjacent channels. Two subcommutators provide data sampling rates of 60 channels per minute and the remaining two subcommutators provide data sampling rates of 60 channels per 4 minutes. The subcommutators are identical, being synchronized by timing signals obtained from the PCM multicoder.

The PCM multicoder accepts a total of 14 analog channels and 5 digital channels of 6 bits each. The allocations of these channels and their sampling rates are tabulated below:

Channel Allocation	Rate	Type
2 subcommutator	1sp4s	analog
2 subcommutator	1sps	analog
4 time code generator	1sp4min.	digital
1 digital word	1sp12s	digital
2 spacecraft experiment	1sp2s	analog
3 spacecraft experiment	1sp4s	analog
5 SSU (2) and spares (3)	1sp12s	analog

The 2 SSU 1sp12s analog channels are utilized by the command receiver AGC monitors. The digital word is comprised of 4 spare bits and 2 tape recorder ON-OFF monitors. The analog data inputs accept single ended inputs that may vary from 0 to +5.166 volts. The input impedance provided to the analog data is 50 megohms minimum and input signal overvoltage up to $\pm$ 32 volts can be accepted with no degradation of adjacent channels. The digital channel inputs operate with the following logic levels:

Logic 1	+3.5 to 6.0 volts
Logic 0	+0.15 $\pm$0.15 volts

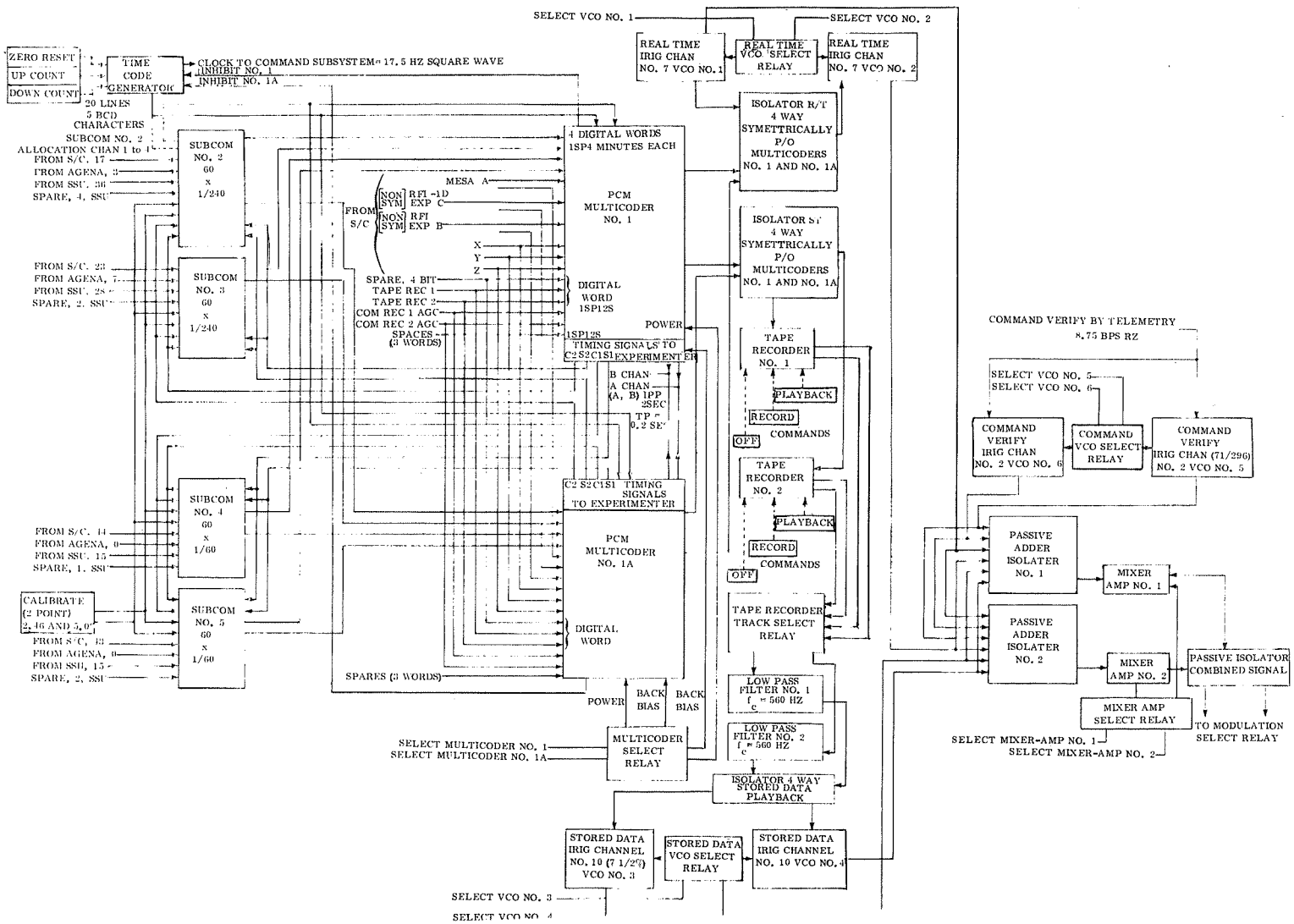

Figure 9.2-1. Telemetry System Block Diagram

Table 9.2-1

Communications System Components

FHC Specification No.	Description	Quantity	Source
833-15404	Tape Recorder	2	Leach
833-15100	2 Pt. Calibrator	1	AEC
833-15100	Time Code Generator	1	AEC
833-15100	Frequency Division Multiplexer	1	AEC
833-15100	PCM Multicoder	2	AEC
833-15100	Subcommutator	4	AEC
----	Signal Conditioner	1	FHC
833-15100	Filter and Isolator	1	AEC

The digital channels also feature the ±32 volt input signal over-voltage protection provided on the other data inputs.

9.2.2 DATA OUTPUT CAPABILITY

The SSU data output will have the PCM frame format shown in Figure 9.2-2. The characteristics of the PCM wavetrain are delineated below:

Word Length	7 bits (6 bits data plus 1 bit parity)
Parity	Odd for logic 1
Bit rate	35 bps NRZ-C
Word Rate	5 words per second
Minor frame	60 words in 12 seconds
Major frame	1200 words in 4 minutes
Frame sync	14 bits
Minor frame ID	Binary count of 0 to 19.

The output of the multicoder provides a bit rate stability of better than 0.02%.

The additional odd parity bit and the requirement for at least one bit transition for each analog word (except all ones)aid in assuring adequate bit synchronization at the PCM decommutator in the ground station. Calibration voltages of 0, 2.46, and 5.00 volts are applied to each of the subcommutators and appear in the PCM wavetrain for in-flight data calibration.

In order to meet the required over-all maximum system error of 2.5% a 6-bit A/D conversion was selected for the SERT II communications system. The 6-bit quantization provides an accuracy of 0.45% $\pm \frac{1}{2}$ LSB (maximum error of 1.2 percent) at the output of the multicoder. The error is a function of the quantization noise and resolution determined by the level of quantization. The rms quantization noise can be expressed theoretically in terms of an equivalent signal to noise ratio. (1)

$$S_o/N_o \text{ db} = 10.8 + 20\ m \log_{10} n$$

where m is the number of pulses in a code group, **n** is the number of code levels selected.

For the SERT II communications system m = 6 and n = 2 (binary).

$$S_o/N_o \text{ db} = 10.8 + 20\ (6)\ 3010$$

$$S_o/N_o \text{ db} - 46.92$$

(1) Schwartz; Information, Transmission, Modulation, and Noise, 1959, p. 330.

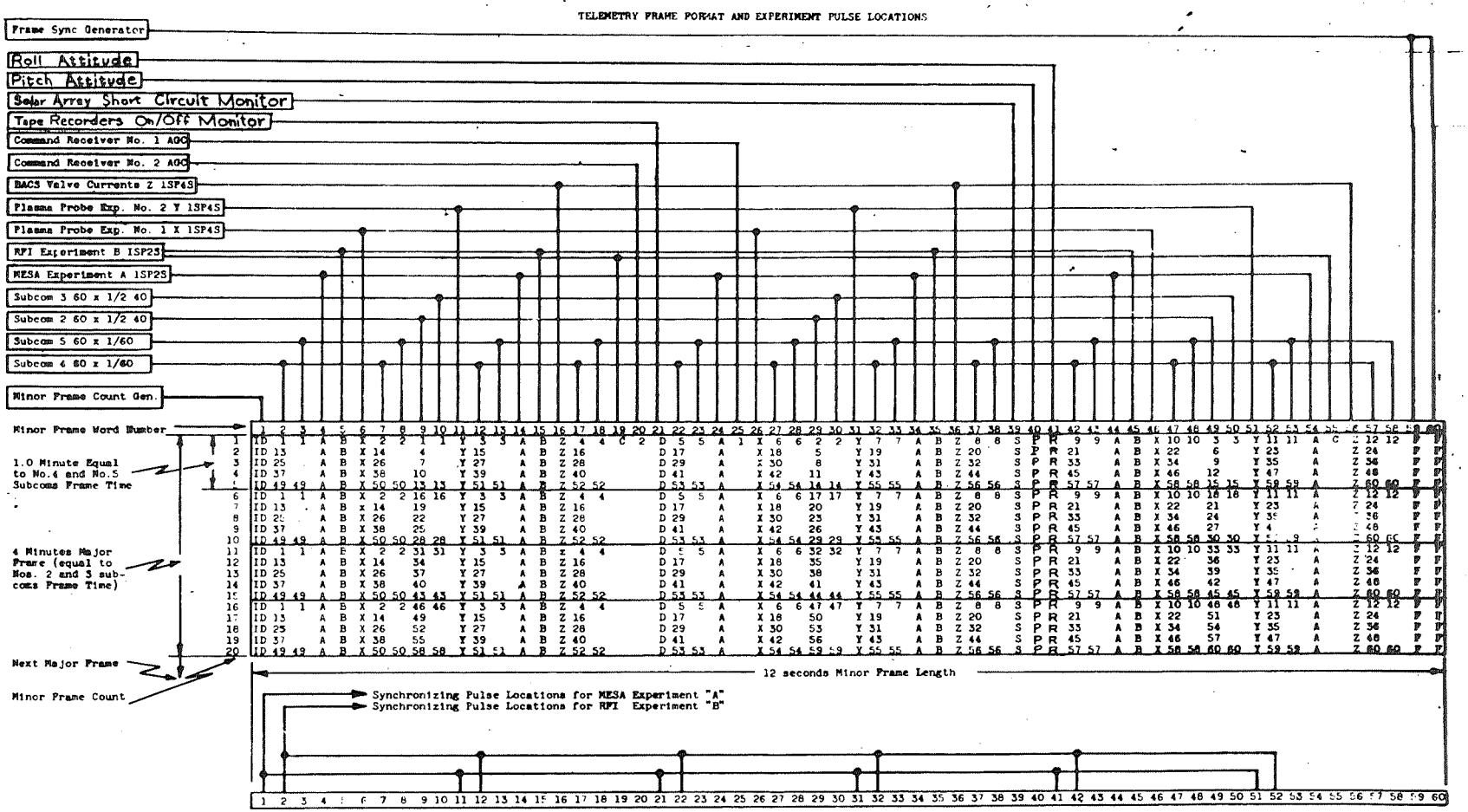

Figure 1

Figure 9.2-2. PCM Frame Format

The error due to quantization can therefore be expressed as .45% of full scale. The error due to the inherent resolution of 80.7 millivolts is $\pm \frac{1}{2}$ LSB, resulting in an error contribution of .757% at the output of the multicoder. The addition of the two error contributions, results in the accuracy of 1.2 percent.

Figure 9.2-3 shows a simplified block diagram of the telemetry system indicating the errors that are present in the system. The telemetry link (ref section 8.2.1) has sufficient margin to support the telemetry function. The link provides a signal to noise ratio of (S/N_{07}) = 44.6 db at the input to the ground decommutator (Pt. C). This signal to noise ratio results in a probability of error much less than $1X10^{-7}$ in the decommutator. The maximum overall error at pt. D on Figure 9.2-3 is therefore essentially the same as at pt. B or 1.2 percent of full scale. This meets the overall maximum system error requirement of 2.5 percent.

9.2.3 TIMING

Two timing lines are provided for use by the experiments located in the Spacecraft. The lines are associated with the two 1sp2s analog data channels on the multicoder. Each timing line provides a strobe pulse that will appear three words prior to the sampling of the respective channel or four words prior to the appearance of the channel in the frame format. The pulses are 0.2 seconds in pulse width and occur at a rate of 1 per 2 seconds. The pulse level is greater than 3.7 VDC with a rise time of less than 1.0 micro-second. Each line is designed to be capable of feeding a load of 4.7k ohms or greater.

A time code generator is provided in the communications system to supply an indication of cumulative satellite elapsed time. The time code generator also provides a clocking signal for the readout of the command system verification.

The time code consists of 5 decimal characters in a BCD format brought out on 20 lines. The count is updated every 4 minutes with an accuracy of better than 0.05 percent providing a maximum cumulative time count of about 277 days. The format of the time code is as follows:

Digital Word

Digital Word		Word Composition							
Minor Frame	Position	Bit No. 1	2	3	4	5	6	7	
				Units					
1	9	Spare	Spare	MSB	X	X	X		Parity
				Tens					
1	29	Spare	Spare	MSB	X	X	X		Parity
		Hundreds				Thousands			
1	49	MSB	X	X	X	X	X		Parity
		Thousands				Ten Thousands			
2	9	X	LSB	MSB	X	X	X		Parity

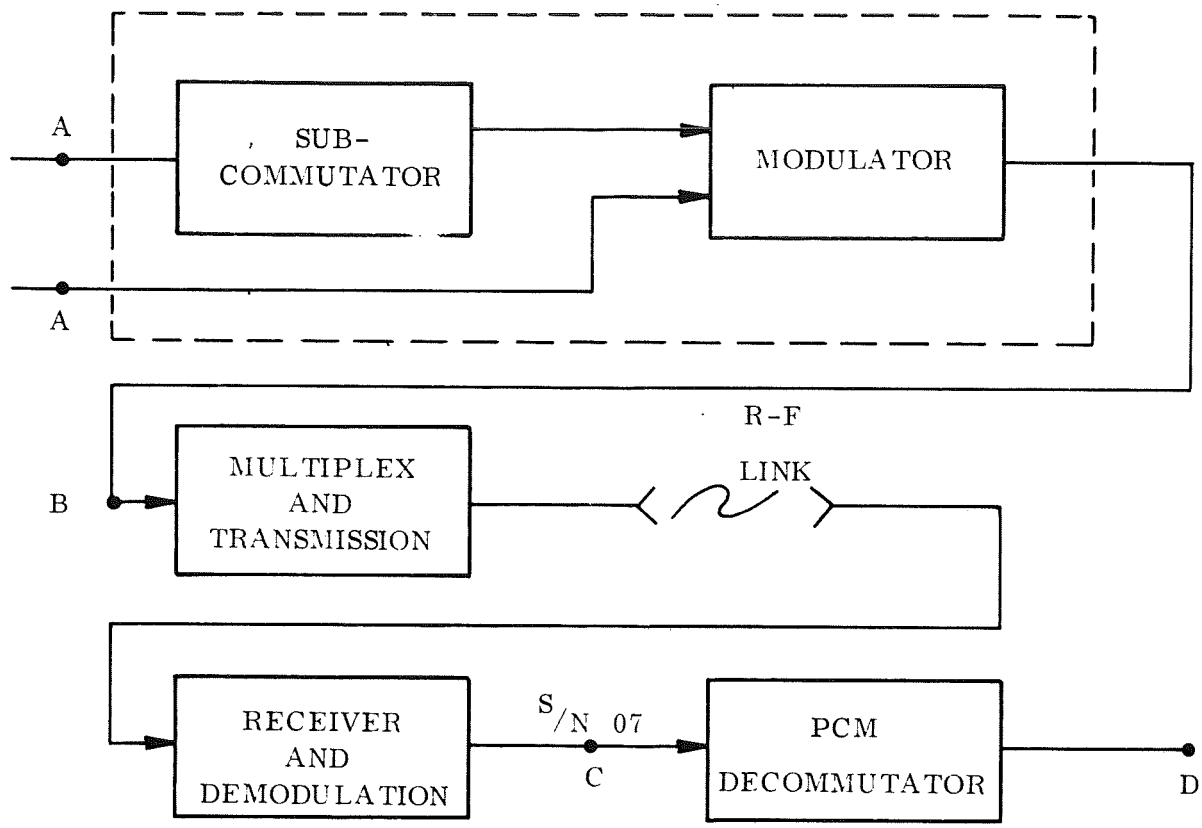

Figure 9.2-3. Data Transmission System Simplified Block Diagram

The time code generator also provides a zero reset, up count (by one), and down count (by one) command capability. If allowed to cycle it will return to zero upon completion of the maximum count. When turned off the time code generator will, when reactivated, start with a zero count.

The clock signal is a 17.5 pulses per second, 4.5 volt peak-to-peak wavetrain that utilizes a 50 percent duty cycle. The clock is provided to the command system and is capable of driving an 18k ohm resistance in series with a type IN916 diode. The stability of the time code generator is better than 0.01 percent.

9.2.4 DATA STORAGE

The data storage capability required for the SERT II mission is implemented through the use of two redundant tape recorders. Each tape recorder provides a nominal 144 minutes (129.6 minutes minimum) of recording time. A playback to-record speed of 16:1 permits readout of stored data within 9 minutes.

The necessary logic for operation via ground command has been implemented in each tape recorder. Operational modes include off, record, and playback. If the recorder reaches its maximum recording capacity of 144 minutes, an end of tape off condition will occur. Under this condition, further advance of the tape or commanding the recorder to an off position is not permitted. It shall permit implementation of the playback mode when the appropriate command is received.

The recorder will be turned off at any position of the tape other than end of tape when the off command is received. In this mode the standby power required is approximately half the required power in the end of tape off mode. Status monitors are provided to permit determination of the tape recorder mode.

The data output obtained in the playback mode is a non-inverted, 560 bps PCM wavetrain. The PCM format utilized minimizes the degradation of data received in the playback mode. The recorders meet the following characteristics:

- Playback time - 16:1 $\pm$ 0.5%
- Stability
  - long term - $\pm$ 1.5% from nominal
  - jitter <100 microseconds
- PCM signal dropout - 1 bit in 10^5

ensuring adequate data quality.

9.2.5 FREQUENCY DIVISION MULTIPLEXING

As indicated in Figure 9.2-1 the three VCO's, with three additional VCO's in standby redundancy, perform frequency division multiplexing of the command verification, real-time data, and stored data. The frequency modulated output signals of the VCO's are mixed and applied through one of two standby redundant mixer

amplifiers to the selected telemetry transmitter. Listed below are the characteristics of the input signals and the VCO's.

Signal	Data Rate	VCO	Modulation Index
Command Verification	8.75 bps	560 ± 42 Hz	9.6
Real Time Data	35 bps	2300 ± 173 Hz	9.9
Stored Data	560 bps	5400 ± 405 Hz	1.45

Each of the data signals are of constant peak to peak amplitude and deviate the subcarrier the full bandwidth.

The amplitude settings of each subcarrier are set to maintain equal signal to noise ratio in each channel. Denoting the peak modulation indices as β_η ;

$$\frac{\beta_2}{(84)^{\frac{1}{2}}} = \frac{\beta_7}{(346)^{\frac{1}{2}}} = \frac{\beta_{10}}{(810)^{\frac{1}{2}}}$$

Setting the composite index at one radian rms;

$$1 \text{ radian} = \frac{\beta_2^2 + \beta_7^2 + \beta_{10}^2}{2}^{\frac{1}{2}}$$

$$\beta_2^2 + \beta_7^2 + \beta_{10}^2 = 2$$

Utilizing the equal signal to noise ratio criterion, the individual indices can be calculated:

$$\beta_{10}^2 (1 + 0.104 \text{ to } 0.428) = 2$$

$$\beta_{10}^2 = 1.3 \qquad \beta_{10} = 1.14$$

$$\beta_7^2 (1 + .241) + 1.3 = 2$$

$$\beta_7^2 = 0.563 \qquad \beta_7 = 0.75$$

$$\beta_2^2 + .563 + 1.3 = 2$$

$$\beta_2^2 = .137 \qquad \beta_2 = 0.37$$

The carrier power retained when these indices are utilized may be calculated as follows:

$$\frac{P\ (carrier)}{P\ (total)} = Jo\ (\beta_2)^2 \quad Jo\ (\beta_7)^2 \quad Jo\ (\beta_{10})^2$$

$$\frac{Pc}{Pt} = Jo\ (.37)^2 \cdot Jo\ (.75)^2 \cdot Jo\ (1.14)^2$$

$$= (.9665)^2 \cdot (.8642)^2 \cdot (.7006)^2$$

$$= (.931) \quad (.747) \quad (.491) \quad = .343$$

With the selection of the indices shown above, 34.3% of the power will be maintained in the carrier (-4.6 db).

The transmitters selected for the SERT II mission also must be considered in determining the alignment of the FM multiplexer. The deviation sensitivity of the transmitter is 1 radian/volt. The maximum deviation of the transmitter is limited as follows:

(1) To 1.5 radians (peak) operates within specifications.

(2) Greater than 1.5 radians operates with two-three percent distortion.

(3) Between 2 and 2.5 volts, the operational limit is reached. It should be noted that this level can be exceeded without damage to the transmitter.

It therefore appears that the peak deviation of the transmitter should be selected to fall between 1.5 and 2.0 radians, with a reasonable guard band at the 2.0 radian end to account for power supply variations, tolerances, etc.

The composite peak index calculated:

$$\beta_c\ (peak) = \beta_2\ (peak) + \beta_7\ (peak) + \beta_{10}\ (peak)$$

$$\beta_c = 1.14 + 0.75 + 0.37 = 2.26 \text{ radians}$$

Selecting a composite peak index of approximately 1.8 radians, the deviation of each is decreased by 2.0 db.

$\beta_{10} = 0.91$ radians peak

$\beta_7 = 0.64$ radians peak

$\beta_2 = 0.29$ radians peak

$$\frac{Pc}{Pt} = \left[Jo\ (.29)^2 \cdot Jo\ (.64)^2 \cdot Jo\ (.91)^2 \right]$$

$$= (.9791)^2 \cdot (.9002)^2 \cdot (.8075)^2$$

$$= (.958) \quad (.81) \quad (.651) \quad = .505$$

With the indices modified by the deviation limitations of the transmitter, 50% of the power will be maintained in the carrier (-3db).

The ratio or power in each subcarrier may be found by utilizing the following expressions:

$$\frac{P\ sc}{P\ t} = 2\ \frac{Pc}{P_T} \left[\frac{J_1\ (\beta_n)}{Jo\ (\beta_n)} \right]^2$$

$$\frac{P_2}{P_t} = 2 \times .5 \left[\frac{.1435}{.979} \right]^2$$

$$= 0.0216 \quad (-16.6db)$$

$$\frac{P_7}{P_t} = 2 \times .5 \left[\frac{.3039}{.9002} \right]$$

$$= .1136 \quad (-9.45db)$$

$$\frac{P_{10}}{P_t} = 2 \times .5 \left[\frac{.4095}{.8034} \right]^2$$

$$= .26 \ (-5.85db)$$

Recalculating the rms index,

$$\beta_c\ (rms) = \left[\frac{(.29)^2 + (.64)^2 + (.91)^2}{2} \right]^{\frac{1}{2}}$$

$$\beta_c\ (rms) = \left[\frac{.0841 + .41 + .828}{2} \right]^{\frac{1}{2}} = \left[\frac{1.3191}{2} \right]^{\frac{1}{2}}$$

$$= (.659)^{\frac{1}{2}} = .81 \text{ radians}$$

In summary, the following parameters are recommended for use in setting the SERT II FM multiplexer bandwidth and pre-emphasis:

VCO	Bandwidth	Amplitude (rms)
2	518 - 602 Hz	0.185 volts
7	2127 - 2473 Hz	0.378 volts
10	4995 - 5805 Hz	0.569 volts

Resulting in an rms index of 0.81 radians, 50% of the power in the carrier, 40% in the subcarrier sidebands, and 10% in higher order products.

For an rms modulation index of 0.81, the third sideband will have a magnitude of approximately one percent. The amount of information that is contained in that sideband is very small (negligible when a digital system is utilized) FM = 5800 Hz is the maximum modulating frequency. In order to detect significant sidebands, a bandwidth of 4 fm would be required for,

$$B = 4 \text{ fm} = 4 (5800)$$

$$= 23.2 \text{ KHz}$$

As a result, a 30 KHz predetection receiver bandwidth is adequate.

9.2.6 SIGNAL CONDITIONING AND INSTRUMENTATION

The PCM communications system for the SERT II SSU requires input signals in the 0 to 5 volt range. For some signals it was necessary to provide special conditioning equipment for the purpose of scaling the inputs to the subcommutators and multicoders to this range.

The following signals are conditioned by the signal conditioner:

1. Tape Recorder End-of-Record
2. Tape Recorder Eng-of-Playback
3. Tape Recorder Command Off
4. Tape Recorder Power Line
5. SSU Temperature Monitors
6. Solar Array Temperature Monitors
7. Open Circuit Cell Voltage (Agena)
8. Short Circuit Cell Voltage (Agena)
9. Maximum Power Cell Voltage (Agena)

Figure 9.2-4 displays the various voltage dividers utilized in the signal conditioners and their function. Figure 9.2-5 displays the amplifiers used to condition the solar cell voltages. Figure 9.2-6 displays the tape recorder temperature calibration curve, Figure 9.2-7 the SSU temperature monitor calibration curve, and Figure 9.2-8 the Agena solar array temperature monitor calibration curve, Figures 9.2-9, 9.2-10 and 9.2-11 display respectively the open circuit cell voltage, short circuit cell voltage, and maximum power cell voltage calibration curves. Where data is shown on the curves, they represent test data taken on the Flight Unit signal conditioner. The SSU temperature monitors are located as indicated below:

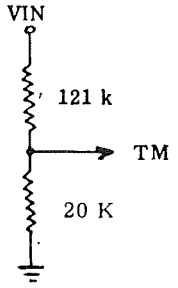

Tape Recorder Power Line

Tape Recorder End-of-record

Tape Recorder End-of-playback

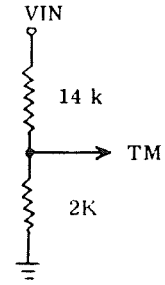

Tape Recorder Command Off

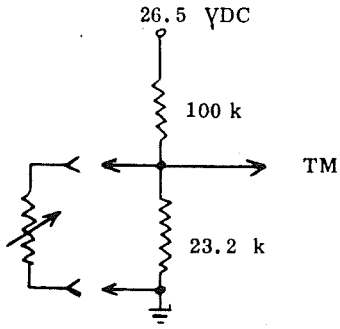

SSU Temperature Monitors

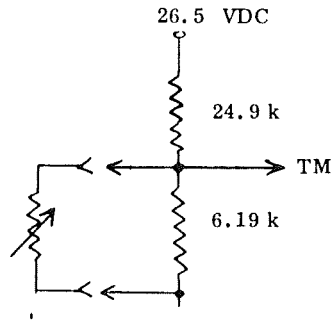

Tape Recorder Temperature Monitor

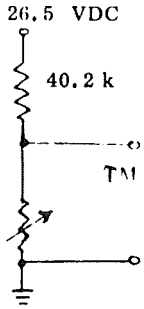

Agena Solar Array Temperature

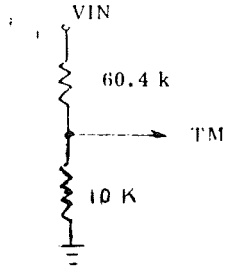

Signal Conditioner Voltage

Figure 9.2-4. Signal Conditioner Voltage Dividers

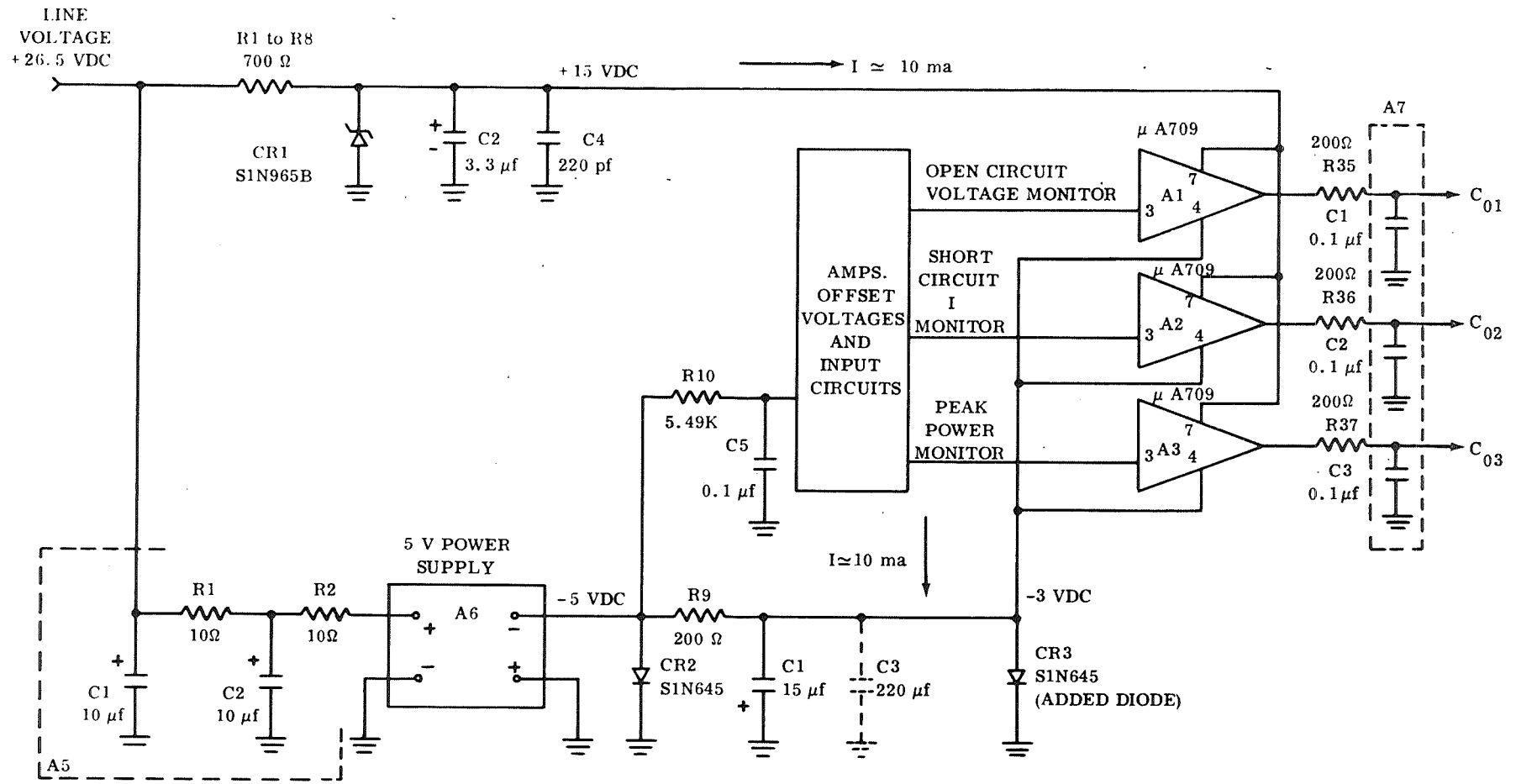

Figure 9.2-5. Solar Cell Voltage Amplifiers

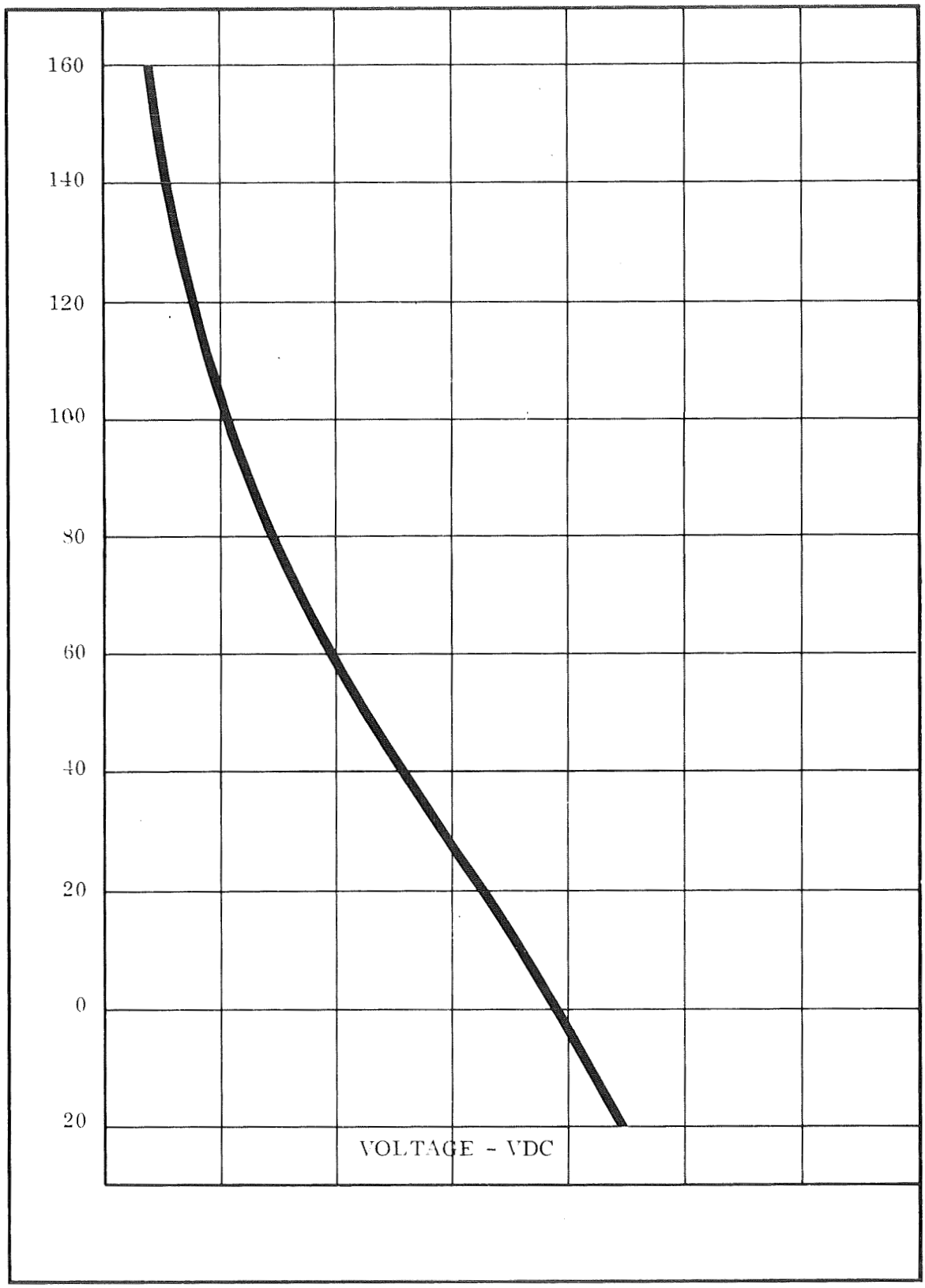

Figure 9.2-6. Tape Recorder Temperatures Calibration Curve

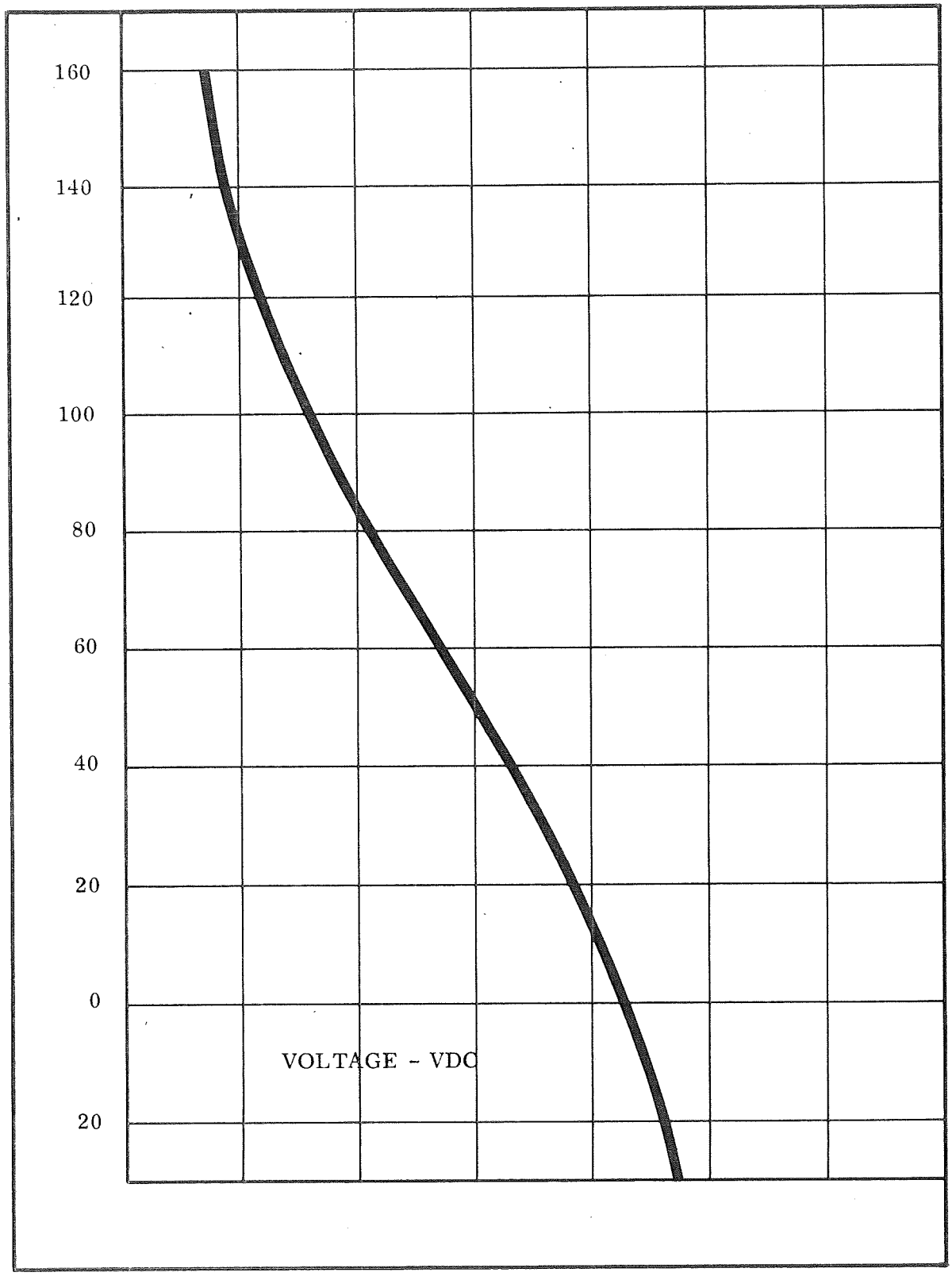

Figure 9.2-7. SSU Temperature Monitor Calibration Curve

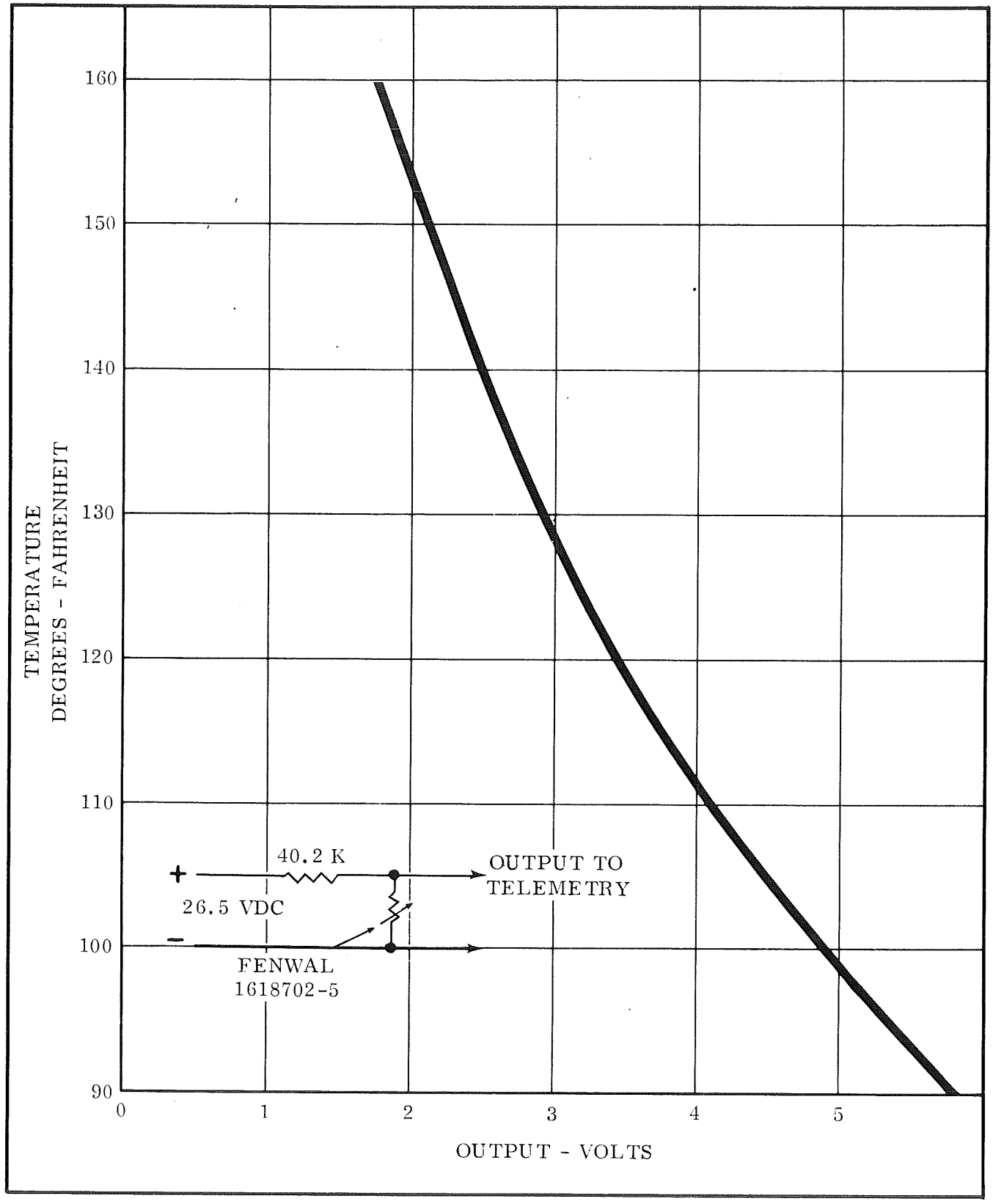

Figure 9.2-8 Agena Solar Array Temperature Monitor

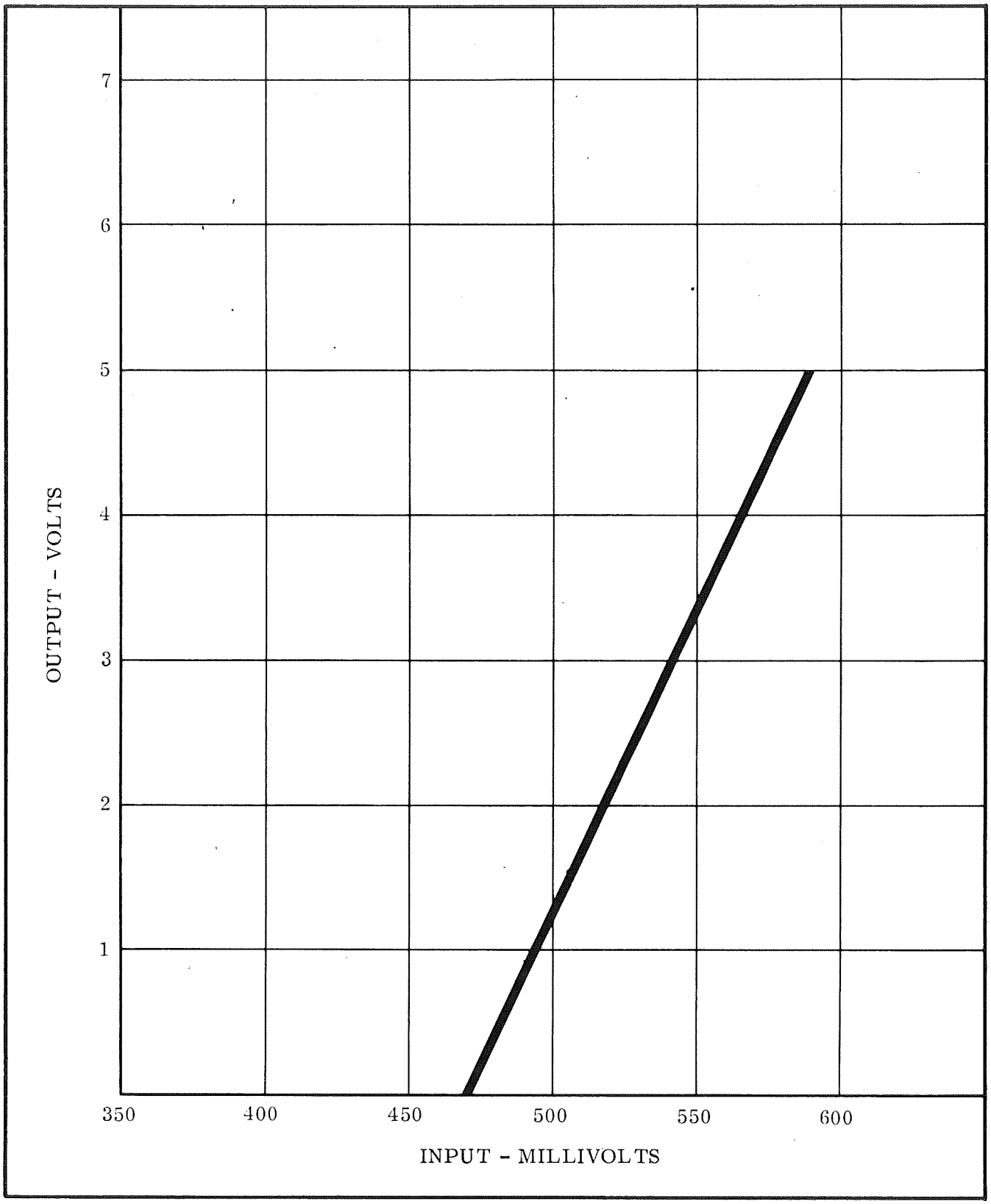

Figure 9.2-9 Open Circuit Cell Voltage

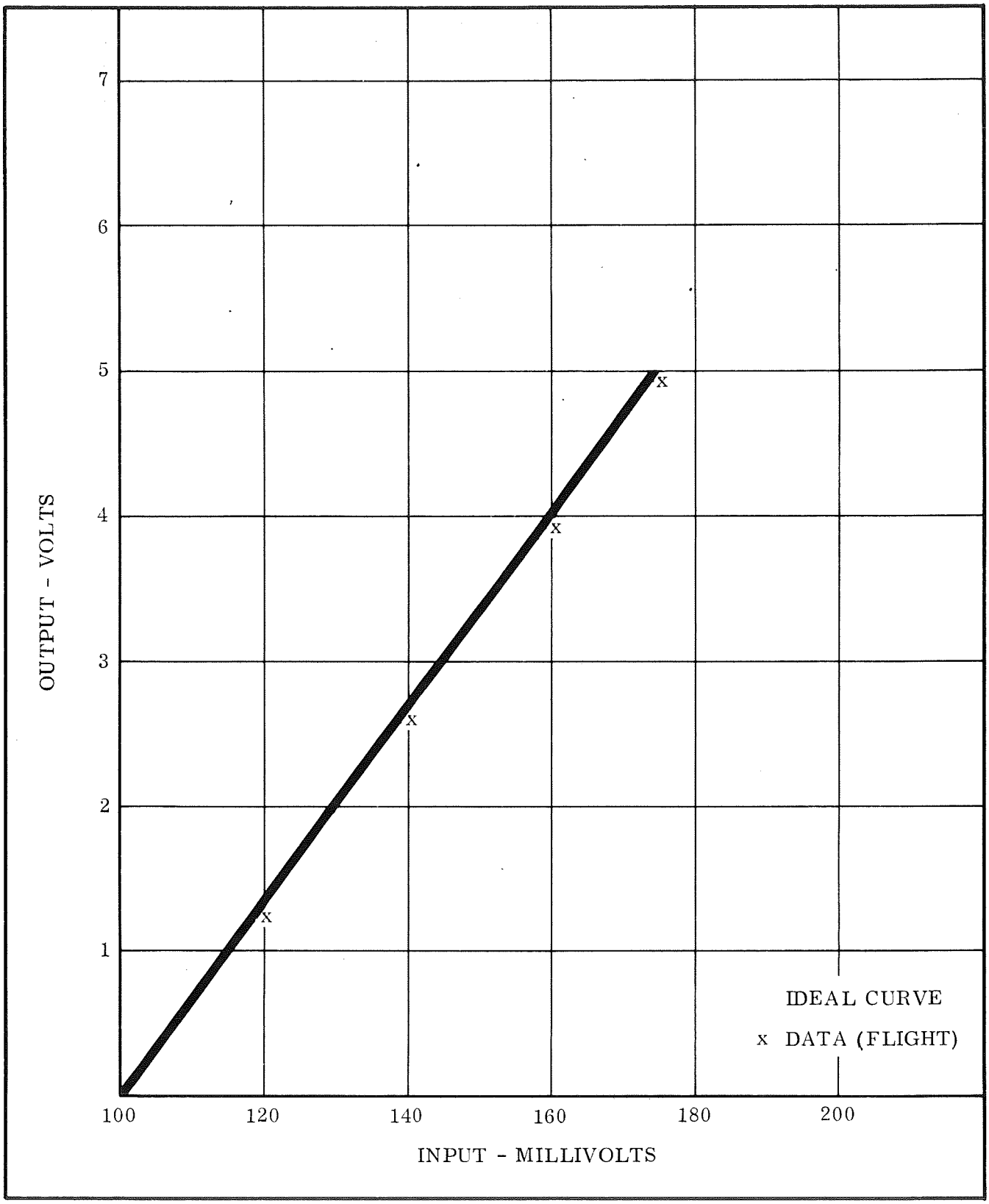

Figure 9.2-10 Short Circuit Cell Voltage

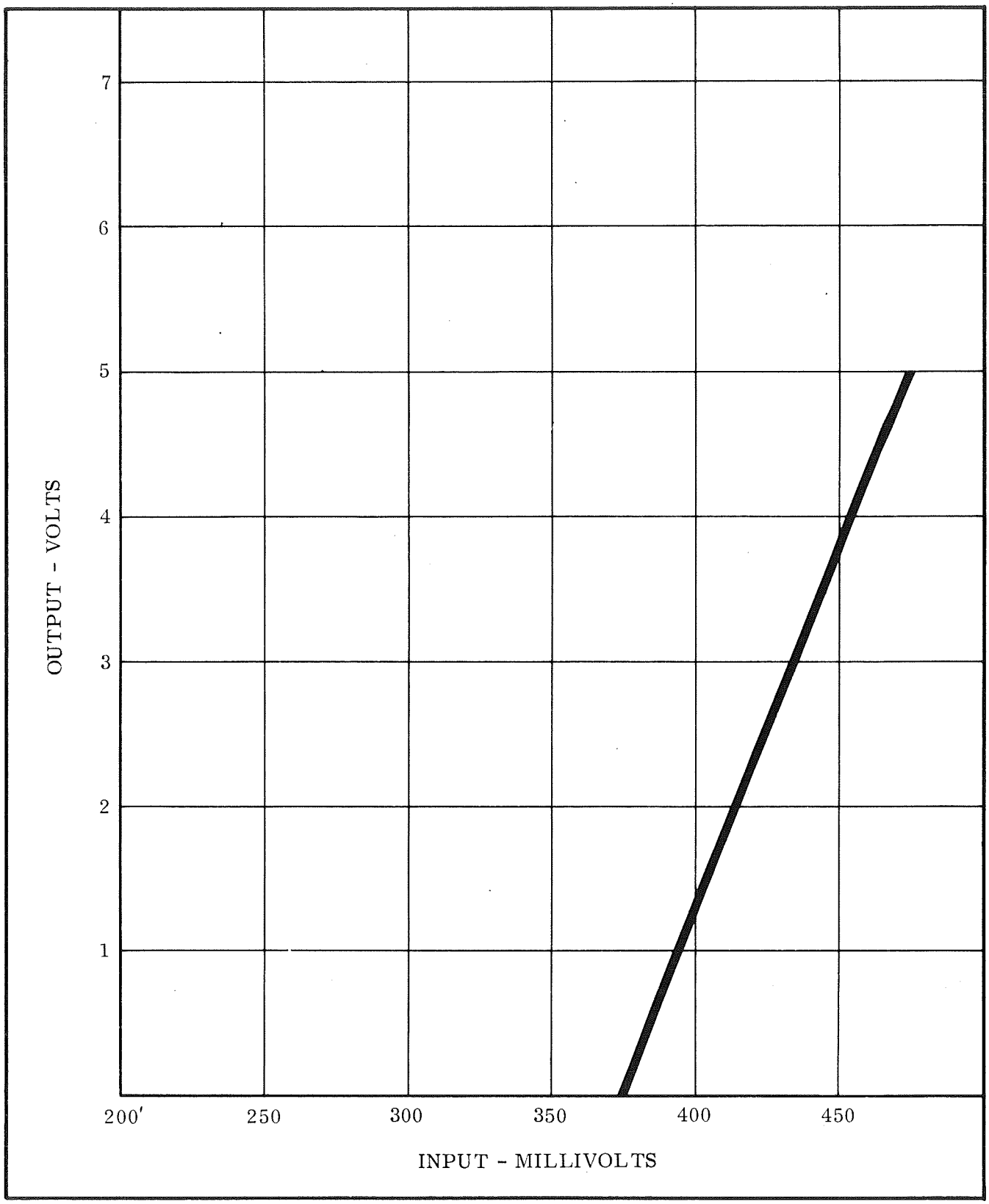

Figure 9.2-11 Maximum Power Cell Voltage

Temperature Monitor	Location
Structural Temp #1	Skin of Bay 1
Structural Temp #2	Skin of Bay 2
Structural Temp #3	Skin of Bay 3
Structural Temp #4	Skin of Bay 4
Structural Temp #5	Skin of Bay 5
Structural Temp #6	Skin of Bay 6
Structural Temp #7	Skin of Bay 7
Structural Temp #8	Skin of Bay 8
Structural Temp #9	Backwall of Bay 2
Structural Temp #10	Backwall of Bay 4
Structural Temp #11	Backwall of Bay 6
Structural Temp #12	Backwall of Bay 8

Fenwall K1313 thermistors were used for these monitors, providing an accuracy of $\pm 3\%$ over the temperature range of -30^{o}F to $+160^{o}$F.

9.3 COMMUNICATIONS SYSTEM OPERATION

The communications system detailed block diagram is presented in Figure 9.2-1. The functional operation of the system is described in the following paragraphs.

Each PCM multicoder accepts output signals from the four subcommutators and time division multiplexes them with analog and digital channel inputs from the Spacecraft and SSU. A clock line and sync line are provided from each multicoder to each subcommutator for synchronization purposes. The "fast subcommutators" utilize a 1 pulse per second clock line and a 1 pulse per minute sync line. The "slow subcommutators" utilize a 1 pulse per 4 minute sync line.

Two isolated outputs, from the multicoder in use, frequency modulate one of the redundant, IRIG channel #7 voltage control oscillators. Two PCM multicoder isolated outputs are also routed to the magnetic tape recorders for data storage and transmission at a later time. The stored data output from each tape recorder is applied to a 560 Hz filter and isolator. The filter and isolator is a passive device that provides two isolated lines, one to each of the redundant IRIG channel #10 voltage control oscillators.

The command verify data signal frequency modulates one of two redundant, IRIG, channel #2 voltage control oscillators. The outputs of the three selected voltage control oscillators are mixed and applied to one of two redundant, mixer amplifiers. The mixer amplifier permits adjustment of the composite signal to match the requirements of the modulation inputs of the transmitters.

A two-point calibrator is supplied in the communications system. The calibrator 2.46 VDC and 5.00 VDC outputs are applied to each of the four sub-commutators to provide end-to-end in-flight calibration of the communications system.

The time code generator provides a cumulative spacecraft time count. The count is updated at the start of each major frame (every four minutes) thus providing a maximum elapsed time of about 277 days. The outputs of the TCG are applied directly to the PCM multicoder, but are allocated to the first four data channels of sub-commutators #2. In addition, the TCG also provides a 17.5 Hz clocking signal for command memory readout.

The communication system design permits independent selection of either multicoder, tape recorder, or mixer amplifier in case of failure. In addition, any combination of the three different voltage control oscillators can be selected out of the two redundant sets of three oscillators supplied.

9.4 COMMUNICATION SYSTEM DEVELOPMENT

During the period the SERT II SSU was being designed and manufactured, a number of design changes were made. Those changes affecting the communications system are listed in the following section.

9.4.1 PCM MULTICODER

During development of the PCM multicoder a number of design changes were implemented.

(1) To minimize noise effects introduced into the PCM system without affecting data accuracy, a two-stage low pass filter was added to the PCM multicoder at the point where incoming analog data has been time division multiplexed into the serial wavetrain. The filter is designed for a 3 db cut-off frequency of 50 Hz from a zero impedance data source.

(2) The vendor experienced difficulty in implementing a Least Significant Bit (LSB) reversal circuit whose function was to provide a bit state transition with analog data at full scale. This circuit in combination with the odd parity for the zero data voltage case would ensure that at least one bit state transition would occur for each word, providing good bit sync capability for the ground station. The requirement was waived for the PCM multicoder since the probability of an all "1's" data word is very low. All data sources are conditioned sotthey will normally be in the 0 to 5-volt range (61 counts maximum) and an all "l's" condition requires 5.125 volts (63 counts).

(3) The requirement to provide a binary count of 1 to 20 for identification of the 20 minor frames was changed to 0 to 19. The bendor interpreted the specification erroneously and the

Experimental Model employed the 0 to 19 count. The PCM Decommutator is compatible with either identification. Since it was desired to have all units operate in the same manner, the requirement was changed.

(4) The warm-up time specification was changed from within 100 msec starting at word 1 of monitor frame 1 to 800 msec starting at the middle of word 57. There is an advantage to this arrangement since it allows the frame sync (words 59 and 60) to be transmitted immediately and will speed up ground station lock-on.

(5) The maximum weight specification was changed from 4.83 to 5 pounds due to additional circuitry.

(6) The maximum power allowable was changed to 12.7w from 6.0 watts. The added circuitry resulted in increased power requirements.

(7) Assignments of the analog data sources to the four transfer gates of the multicoder were modified to allow the interchange of Subcoms #2 and #3 and Spares 1 and 2 between transfer gates one and two. The switch was found in test of the Experimental Model, and since there was no treason not to use the arrangement, the specification was changed to ensure that all SSU Models would have the same configuration.

(8) The specification on the characteristics of the Spacecraft Timing Signals was changed from 5 ± 0.3 volts, 1.0 msec maximum rise and fall time to 4.1 ± 0.4 volts, 0.1 msec maximum rise and fall time. The change in voltage level came when it was found that under system operation, the off multicoder loaded the on multicoder. An evaluation of Spacecraft Experimenter requirements by NASA Lewis Research Center indicated that the lower voltage levels were acceptable and that the faster rise and fall times were required (note, the unit already met the rise and fall time requirements).

9.4.2 560 Hz FILTER AND ISOLATOR

The performance specification of the filter and oscillator was modified as shown in the table below. It should be noted that with the specification change the performance of the unit is more than adequate to meet the communication system operations requirements.

Function	Original Spec. Requirement	Spec. Change
560 Hz Cutoff	3 db (+0, -1 db)	3 db ± 1 db
Filter Rolloff	At least 18 db per octave above cutoff	Nominal 18 db above cutoff
Output Level change with failure of one output line	Alternate line output level constant ± 0.5 db	± 1.0 db
Weight	1.0 lb. approx.	1.25 lb.

9.4.3 FREQUENCY DIVISION MULTIPLEXER

The requirements on the amplitude of the output voltage levels for the VCO's were decreased by a factor of two. The change was made to permit a more effective design of the output isolator and did not affect the system design.

9.4.4 TIME CODE GENERATOR

Two design changes were incorporated into the Time Code Generator:

1. A 2000 mmf capacitor was added to the up-count command line to prevent multiple up-counts from occurring when an up-count command was applied.

2. Two filter capacitors were added in the inhibit circuit to prevent noise from dropping out the inhibit. This problem had exhibited itself on the Flight and Prototype Model time code generators. The change made the circuit far less susceptible to noise. It should be noted that an inhibit drop-out does not affect the prime count and clock function of the time code generator. However, there is a low probability that it could cause erroneous readout of the elapsed time if the multicoder were reading the count during an update.

9.4.5 SIGNAL CONDITIONER

The following design changes were incorporated into the signal conditioner during its development.

1. A zener diode was added to the positive supply voltage line of the amplifiers to allow operation under overvoltage conditions.

2. A two-stage R-C filter was added on the 26.5 VDC line to the power supply in the Signal Conditioner providing approximately 50 db of chopper noise attenuation at the power supply input terminals.

3. Capacitors were added across the three amplifier outputs to prevent oscillations caused by capacitive loading of long lead lengths. The capacitors also reduced power supply noise.

4. Diode CR3 was added to the amplifier circuits to resolve a power supply turn-on problem. A + 0.6 volt level was present on the power supply negative output terminal. The power supply could not overcome this bias derived from line voltage applied through the amplifiers. The diode in conjunction with the 200 ohm isolation resistor produces approximately 6 db reduction in the positive bias voltage. This is sufficient to ensure turn-on.

9.4.6 MAGNETIC TAPE RECORDER

The following design changes were implemented to imrpove tape recorder performance.

1. The checkout of the magnetic tape recorder for the Experimental Unit showed the unit to have a turn-on surge current in the order of 7 amperes peak. This surge occurred each time the recorder turn-on command was issued. The cause of this high surge current was found to be the switching of a capacitor across the power line. The capacitor, which is part of the power line filter, was connected to the power line through the recorder switching circuit. To reduce the surge current the filter was located directly across the power line. This still requires a heavy charging current, but only when the tape recorder is first energized, which occurs when the SERT II power subsystem is initially turned on.

2. In the tape recorders supplied for SERT II, it was planned to use an "Apollo" type clutch. This was a Vogue #372 clutch which incorporated a larger shaft and bearings for longer life.

   During the testing of the Experimental Unit tape recorder, a failure of the Apollo type clutch occurred during low temperature tests. The recorder would not start in the reproduce mode after soad at 0°F. A number of engineering tests utilizing various clutch and tape transport configurations were therefore conducted. As a result of these tests, which

consisted of performance testing over temperature ranges, a Dynamics #372 clutch with a 4-belt transport was selected for use on the Prototype and Flight Units.

SECTION X

GROUND SUPPORT EQUIPMENT

10.1 INTRODUCTION

Ground support equipment (GSE) was required during the test program of the SERT II Spacecraft Support Unit. This equipment consists of the following units:

1) Solar Array Simulator

2) Agena Simulator

3) Battery Charger

4) Ground Station

5) Spacecraft Simulator

10.2 REQUIREMENTS

The above equipments were required for use in supporting the SSU or in providing an interface simulation. The battery charger is required to permit ground charge of the SSU battery and the ground station is required to strip out data from the telemetry link and to provide required command capability. The Solar Array, Agena, and Spacecraft interfaces were simulated by separate units designed for that purpose. The following paragraphs give a brief description of each unit.

10.3 SOLAR ARRAY SIMULATOR

The Solar Array Simulator, designed and manufactured by Fairchild Hiller Corporation, provides a power source that simulates the characteristics of the Agena Solar Array. The Simulator operates on three characteristic current curves - high, nominal and low. The short circuit currents are 8 amps, 7 amps, and 6 amps. for the respective current curves. Figure 10.3-1 describes the characteristics of the unit.

Two modifications were made to the original design of the Solar Array Simulator. The first modification provided for the incorporation of diode isolation in the Simulator output line. This permits the SSU battery to be placed on-the-line while the Solar Array Simulator is in operation without loading down the SSU battery, as would be the case in an operational system.

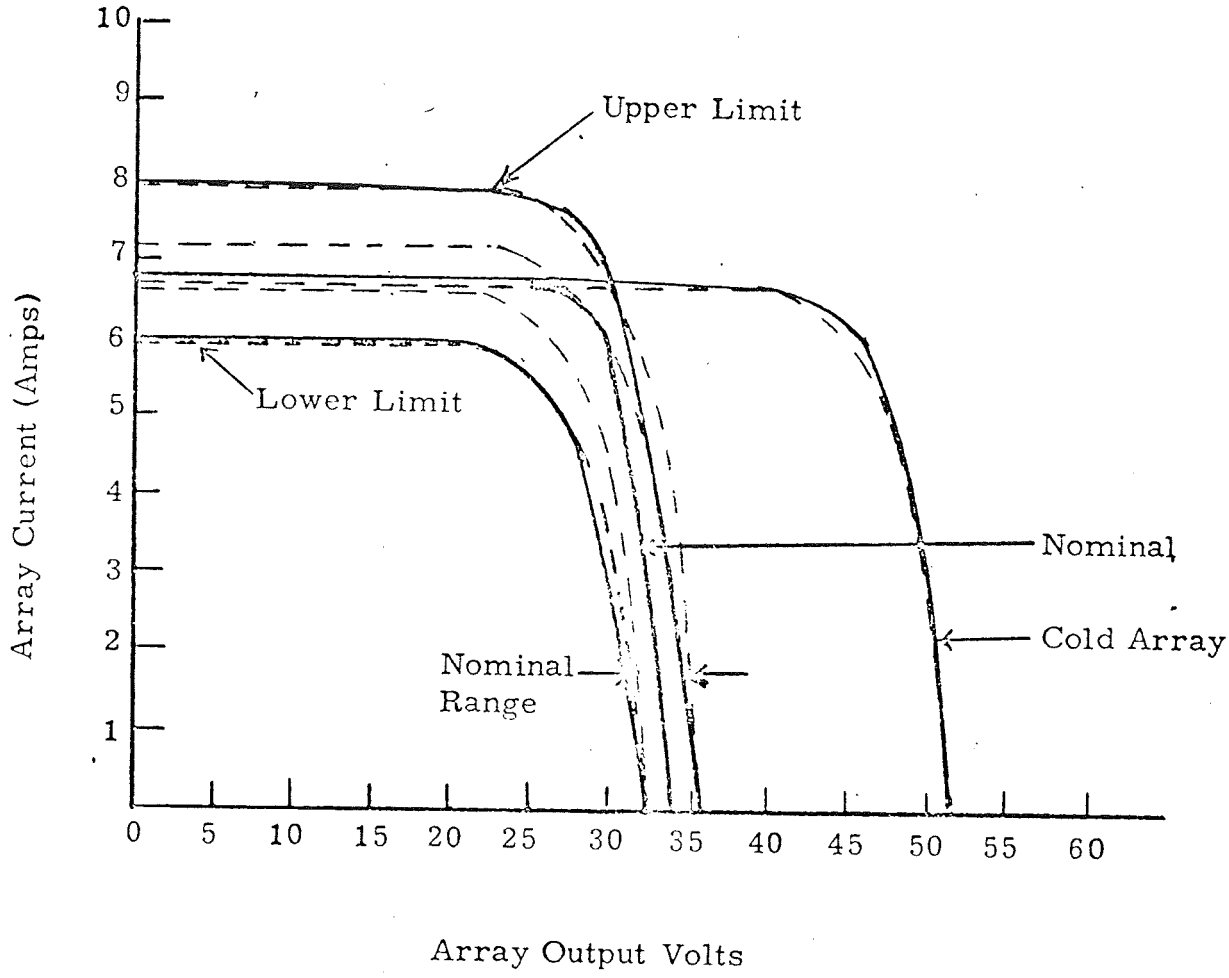

Figure 10.3-1. Solar Array Simulator Characteristics

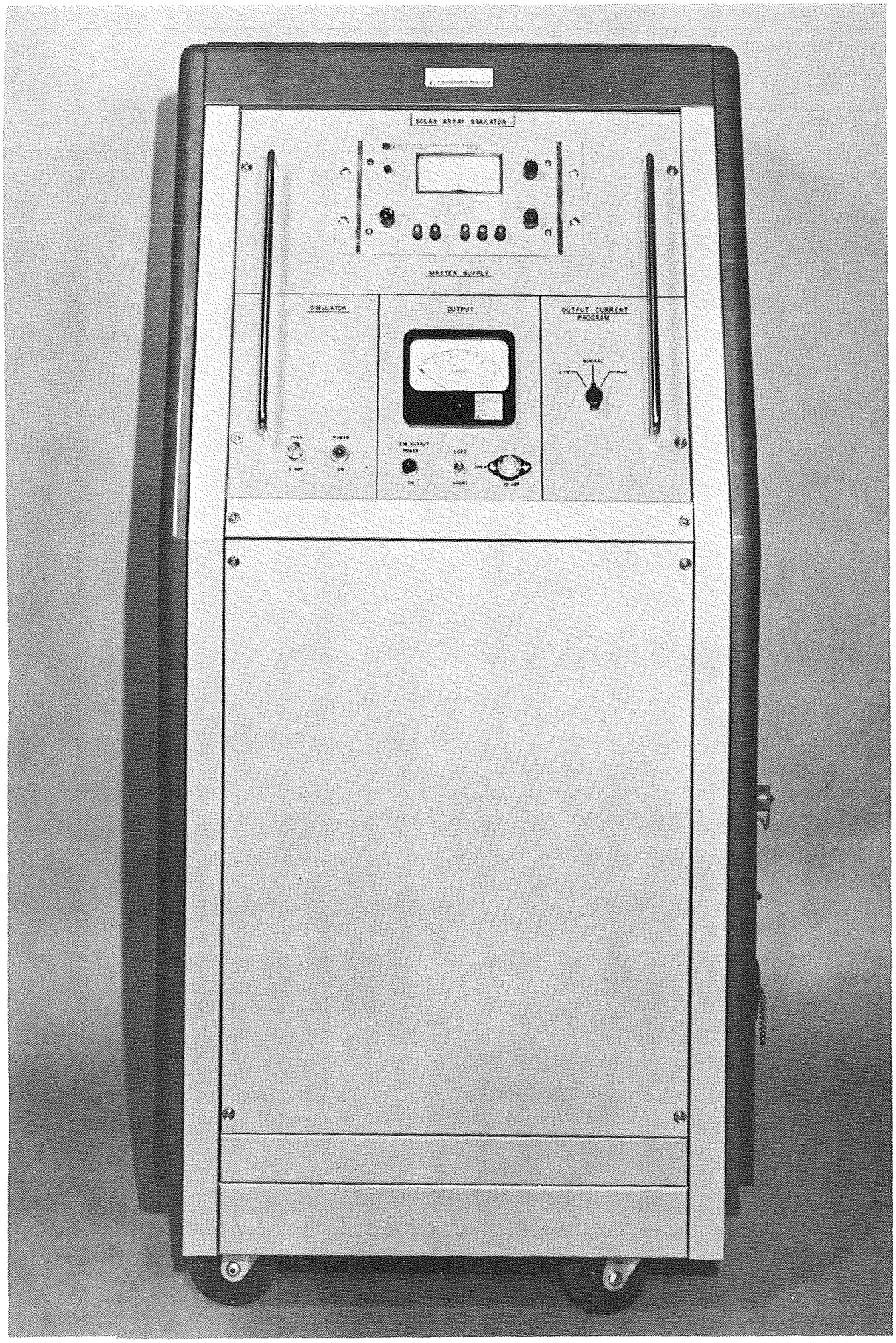

Figure 10.3-2. Solar Array Simulator

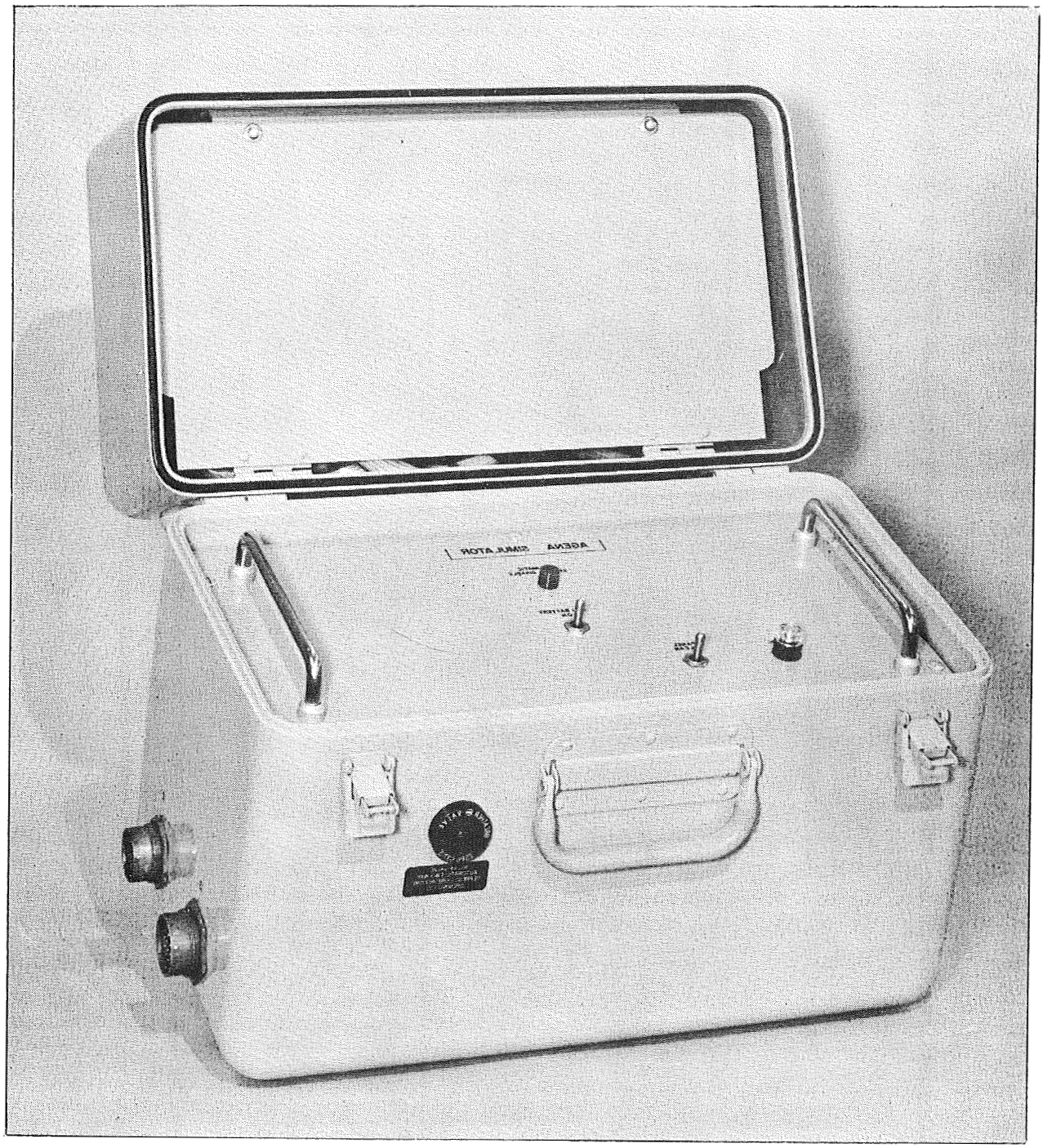

Figure 10.4-1. Agena Simulator

The second change added two monitoring jacks to the front panel of the simulator, to permit the monitoring of the simulator output voltage. The Solar Array Simulator is shown in Figure 10.3-2.

10.4 AGENA SIMULATOR

The Agena Simulator was designed and manufactured by Fairchild Hiller Corporation. The simulator provides the SSU with an interface that simulates the actual signals that pass across the Agena/SSU interface. The solar array thermistor and control cell output signals are simulated as a constant mid-scale telemetry voltage. The simulator provides a momentary signal to energize the "Battery ON" magnetic latching relay. The Agena Simulator also provides the loads associated with the Agena commands sent from the SSU. Provisions are incorporated in the simulator for the distribution of 28 VDC ground power to the SSU through the Agena/SSU interface. The Agena Simulator is shown in Figure 10.4-1.

10.5 BATTERY CHARGER

The Battery Charger allows the SSU battery to be charged without energizing the SSU system. The charger was purchased from Electro-Development Corporation.

10.6 GROUND STATION

The primary tool for monitoring tests and obtaining systems data is the telemetry ground station. Two telemetry ground stations were provided to support the SSU system test program. The first station is a complete, self-supporting telemetry van. The second station is a mobile, rack-mounted telemetry receiving and processing station. The equipment in both stations is the same and consists of the following units:

a) Telemetry Receivers (2)

b) Command Encoder

c) 560 Hz Discriminator

d) 2300 Hz Discriminator

e) 5400 Hz Discriminator

f) Signal Conditioner

g) Decommutator

h) Data Distributor

i) Digital to Analog Converter

j) Printer

k) PCM Simulator

All of the above equipment, with the exception of the PCM Simulator and Command Encoder, are used in the reception and processing of the data from the SSU telemetry system. The PCM Simulator is used in the test and calibration of the EMR Data Processing Equipment. The Command Encoder is used to obtain command control of the SERT II Spacecraft. The verification signal is also decoded and compared to the transmitted command in the encoder.

Both the RF link and coaxial hard line connections were used to obtain data during the test programs. The telemetry van and the mobile ground station are shown in Figures 10.6-1 and 10.6-2, respectively.

10.7 SPACECRAFT SIMULATOR

The Spacecraft Simulator was supplied to FHC by the Lewis Research Center. The simulator provides the SSU with an interface approximating that provided by the Spacecraft. Voltages which simulate data from the spacecraft are provided to the telemetry system. The a-c and d-c loads, associated with the SERT II Spacecraft, are provided to the SSU power system. Receipt of the spacecraft commands is indicated by the indicator lamps on the front panel.

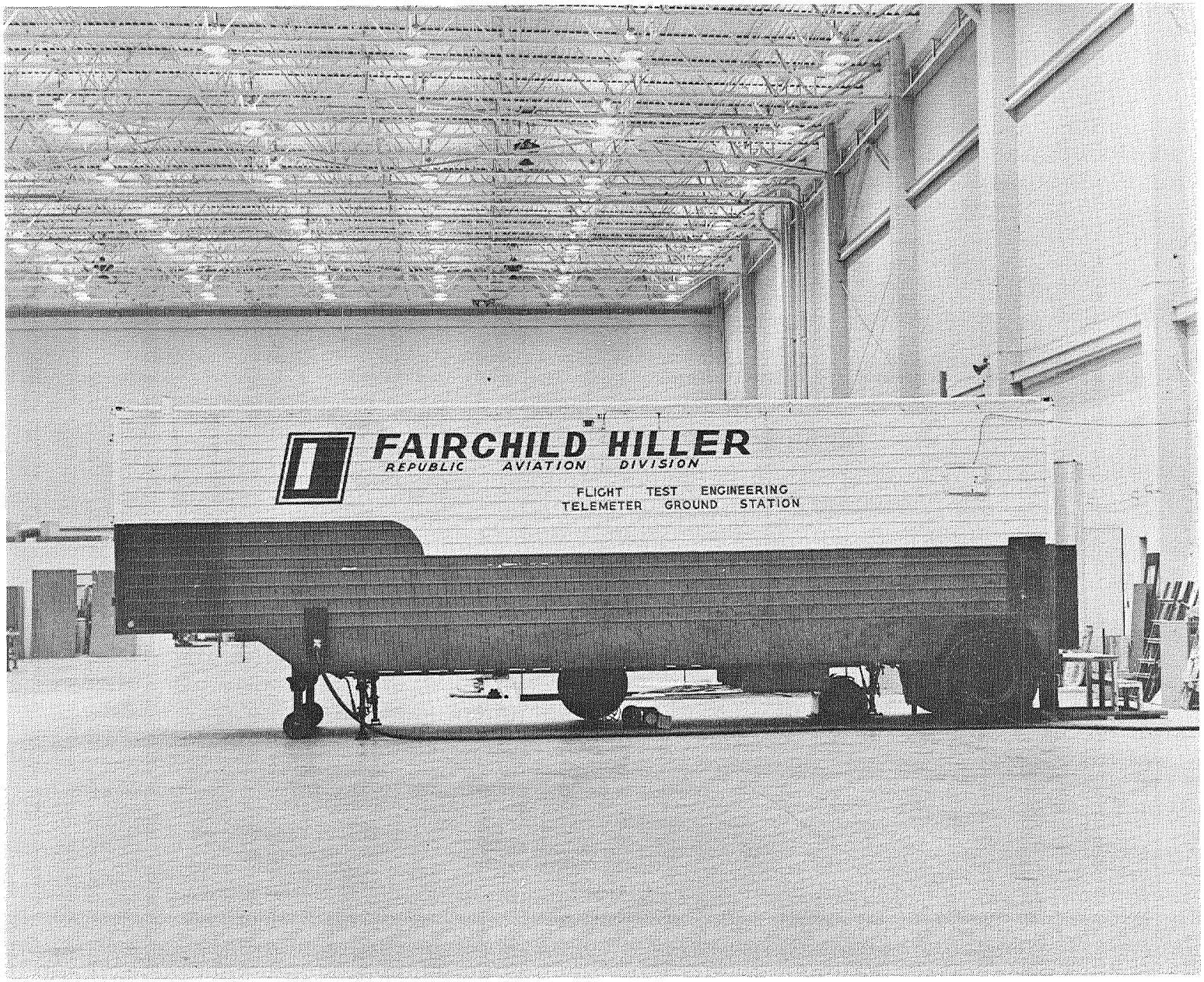

Figure 10.5-1. Telemetry Van

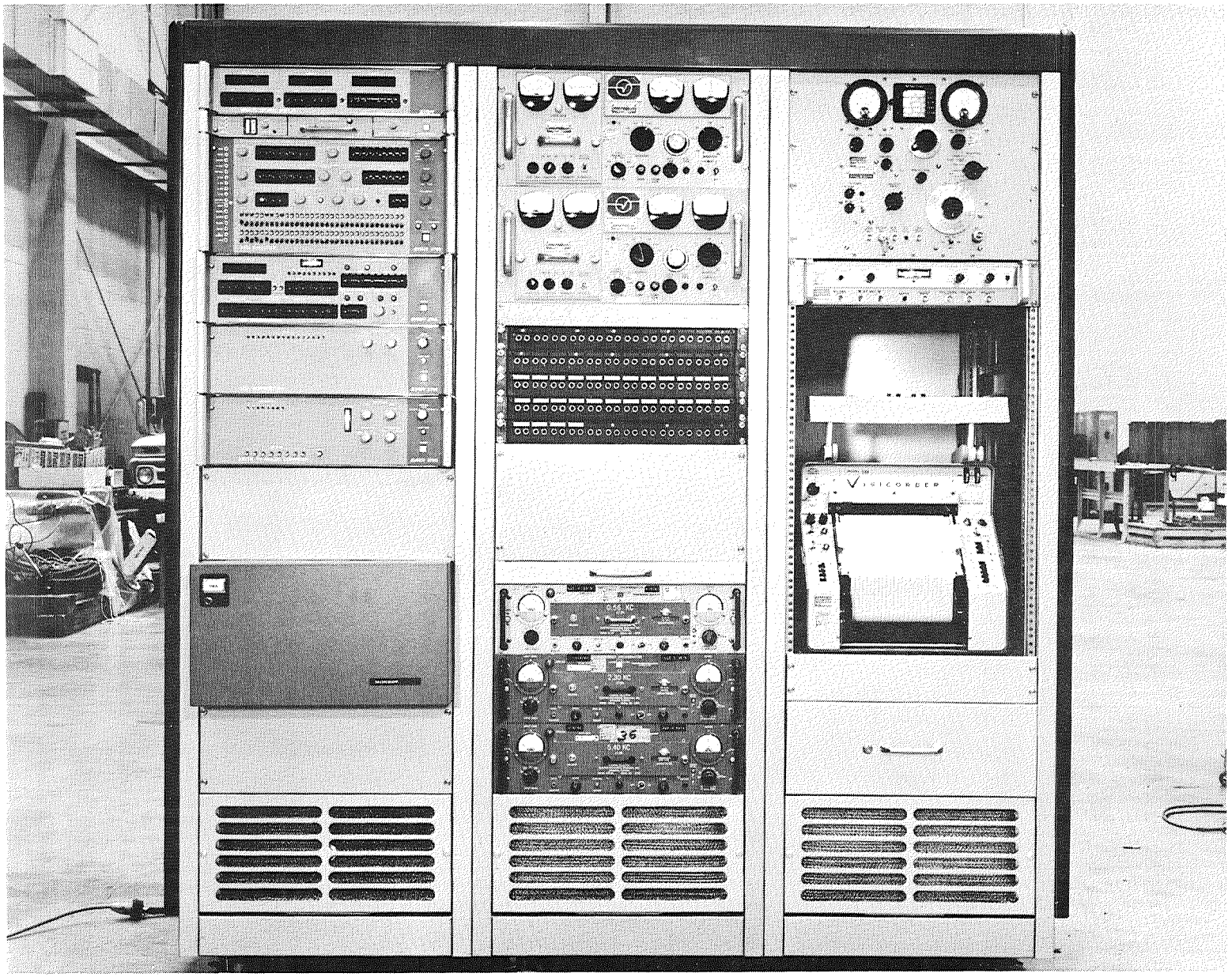

Figure 10.5-2. Mobile Ground Station

SECTION XI

TEST

11.1 INTRODUCTION

This section contains a description of the component testing performed for the SERT II Spacecraft Support Unit Program and the SSU system level testing performed at FHC.

The component test program was established to demonstrate the compliance of equipment to the following requirements:

- o Qualification to environmental levels established in Appendix D of Exhibit A of the contract for those components not previously qualified.
- o Flight acceptance to the environmental levels established as being consistent with SERT II objectives.

Component testing has been performed by the supplier or FHC, depending on the cost or delivery involved. Component testing was planned and conducted by the SERT II Test and Evaluation Group and monitored by Quality Assurance Personnel.

The SERT II SSU system test program at FHC determined the following:

- o The functional integrity of the SSU systems through performance of an Integrated Electrical Systems Test on the Experimental, Prototype, and Flight SSU systems.
- o A preliminary verification of the adequacy of the SERT II thermal control system through performance of a preliminary thermal vacuum test.

Spacecraft testing was performed by the SERT systems test group and monitored by Quality Assurance personnel.

11.2 COMPONENT TESTING

Component tests consisted of functional performance tests at ambient and under simulated environmental conditions. All components of the experimental,

prototype and flight units were subjected to complete functional performance test. Prototype and flight components were subjected to both performance and environmental tests.

In instances where schedule and/or cost savings could be effected, environmental tests of components were performed at Fairchild Hiller.

All components were subjected to vibration, thermal vacuum (thermal at ambient pressure on flight batteries) and mechanical shock test. With the exception of previously qualified components, all prototype components were subjected to prototype design qualification test levels. Flight components and all prototype components not subjected to design qualification test were tested to flight acceptance test requirements. A matrix of components, test performed and previous qualification status is shown in Table 11.2-1.

11.2.1 ENGINEERING UNIT COMPONENT TESTS

Engineering unit components were not required to meet design qualification or flight acceptance level environments. The primary purpose of these components were to verify functional design requirements and interfaces prior to prototype assembly. Therefore, these units were subjected only to functional performance test to verify operational performance of the component, and compatibility with test equipment and software.

11.2.2 QUALIFICATION TESTS

The purpose of the component qualification test is to demonstrate that the techniques used in the manufacturing and design of the components provide sufficient margin for the spacecraft to withstand successfully qualification and subsequent flight acceptance and orbital environment. Components which have a history of previous qualification and flight performance were not subjected to requalification. Qualification test consisted of the following tests in sequence:

- o Functional Performance
- o Vibration
- o Functional Performance
- o Thermal Vacuum
- o Functional Performance
- o Mechanical Shock
- o Functional Performance

11.2.2.1 Functional Performance

Each component was subjected to a functional performance test at the completion of its manufacturing and inspection process at the manufacturer's

Table 11.2-1. Component Test Summary

COMPONENTS	MANUFACTURER	TEST CONDUCTED	VIBRATION	THERMAL VACUUM	SHOCK	COMMENTS
Power Control Unit	FHC	FHC	X	X	X	
Command Relay Junction Box	FHC	FHC	X	X	X	
Signal Conditioner Unit Assembly	FHC	FHC	X	X	X	
DC to AC Inverter	Gulton	FHC	X	X	X	Qualified on Agena
Switching Mode Regulator	"	FHC	X	X	X	Qualified on LEM
Phase Demodulator	"	FHC	X	X	X	Qualified on Agena
Battery Charger	"	FHC	X	X	X	Qualified on Agena
Battery	Exide	FHC	X	X	X	Qualified on Mariner
Command Decoder	Avco	Avco	X	X	X	Qualified on ISIS
Command Receiver	Avco	Avco	X	X	X	Qualified on Pegasus
Transmitter	S/C	FHC	X	X	X	Qualified on FR-1
Hybrid	Motorola	M	X	X	X	Qualified on Pegasus
Diplexer	"	M	X	X	X	Qualified on Pegasus
Tape Recorder	Leach	L	X	X	X	Qualified on Classified Programs, extensive flight history.
2-Point Calibrator	AEC	AEC	X	X	X	
Time Code Generator	AEC	AEC	X	X	X	
Frequency Division Multiplexer	AEC	AEC	X	X	X	
PCM Multicoder	AEC	AEC	X	X	X	
Subcommutator	AEC	AEC	X	X	X	
Filter & Isolator	AEC	AEC	X	X	X	

facility. All performance tests were conducted under Fairchild Hiller Quality Assurance and DOD surveillance in accordance with written procedures approved by Fairchild Hiller. Functional performance tests were also conducted prior to, during (thermal vacuum only) and after each environmental exposure.

11.2.2.2 Vibration

The components were attached to a vibration generator via a rigid fixture designed and fabricated to accept the test unit at the specified mounting planes. Prior to the test, the fixture was vibrated at the component vibration levels shown in Table 11.2-2 to ensure its freedom from significant resonances below 600 cps and that no greater than a 2:1 amplification factor existed at frequencies from 600 to 2000 cps.

Vibration control was provided by an accelerometer mounted on the test fixture immediately adjacent to the components attachment point with the sensitive axis aligned with the axis of vibration. Two other accelerometers with their axes mutually perpendicular to the axis of vibration were located on the fixture to monitor uncontrolled lateral coupled modes.

After the fixture was thoroughly evaluated, the test component was secured to the fixture. A low level resonance search of the fixture-test component combination was then conducted to the following sinusoidal vibration schedule:

Frequency Range	Acceleration Level
5 - 2000 cps	0.5 g's (0-pk)

Sweep rate: one octave per minute

The components were then subjected to independent sinusoidal and random vibration tests according to the schedule shown in Table I. Sinusoidal tests were performed by sweeping the applied vibration from the lowest to the highest frequency once for each range specified.

Gaussian random vibration was applied with g-peaks clipped at three times the rms acceleration. With the test unit installed, the control accelerometer response was equalized such that the specified power spectral density values are within $\pm$ 3 db everywhere in the frequency band.

TABLE 11.2-2

SINUSOIDAL SWEEP FREQUENCY TEST

Axis of Vibration	Frequency Range	Acceleration Level
Three Mutually Perpendicular axes	5-19 cps	0.50 inch D.A.
	19-2000 cps	9.0 g's (0-pk)

Sweep Rate: 1.0 octave per minute or approximately 22.4 degrees per minute.
Sweep Time: for 5-2000 cps approximately 9.0 minutes.

TABLE 11.2-2 (continued)

RANDOM NOISE VIBRATION SCHEDULE

Axis of Vibration	Frequency Range CPS	Acceleration Level rms	Spectral Density	Overall Level rms	Time
3 Mutually Perpendicular Axes	20-400	6.5 g's	.112 g^2 cps	20 g's	9 min/ per axis
	400-2000	18.9 g's	.223 g^2 cps		

11.2.2.3 Thermal Vacuum

The components were mounted to a base plate in the same manner in which they are mounted in the spacecraft. Thermocouples were installed on the base plate, temperature critical areas and the components major mass.

A functional performance test of the component was then performed to verify the integrity of the test set up through the vacuum chamber penetration. The internal chamber pressure was then reduced from ambient pressure to 25 mm Hg in approximately 90 seconds and evacuation of the chamber continued until a pressure of 10^{-5} mm Hg or less was achieved.

Simultaneously with pressure reduction the temperature of the base plate was reduced to minus 30°F over a period of not less than 35 minutes. Conditions were maintained for four hours after the component reached temperature stabilization as indicated by a change of less than 2°F in 15 minutes of the component major mass. At the conclusion of the four-hour cold soak the component was energized for a 2-hour period, during which time a performance test was conducted. The component was then placed in its maximum heat dissipation mode and the base plate temperature raised to 160°F. These conditions were maintained for a period of 48 hours. During the last two hours of the 48-hour soak, the functional performance tests were performed.

The chamber pressure and base plate temperature were then slowly returned to ambient conditions and another functional performance test was conducted.

11.2.2.3 Mechanical Shock

The component vibration fixture was mounted to the shock machine. Component mounting was as described for vibration testing. A monitoring accelerometer was attached to the fixture adjacent to the component mounting with its sensitive axis aligned with the direction of applied shock. Additional accelerometers were attached to measure the induced accelerations along the two transverse axes. The unit was then subjected to three half sinc pulses of plus and minus 30 g's peak amplitude for a duration of 8 milliseconds in each of three orthogonal axes.

At the conclusion of the shock test a functional performance test was conducted to ensure the absence of component degradation due to the environment.

11.2.3 FLIGHT ACCEPTANCE TEST

Component acceptance tests were identical to qualification test with the exception of the environmental test levels. These levels were established based on expected launch and operational environmental conditions to verify freedom from latent workmanship defects and prove quality of performance.

11.2.3.1 Vibration

Flight components were subjected to a vibration environment as shown in Table 11.2-3.

TABLE 11.2-3

SINUSOIDAL SWEEP FREQUENCY TEST

Axis of Vibration	Frequency Range	Acceleration Level
Three Mutually	5 - 15 cps	0.50 inch D.A.
Perpendicular Axes	15 - 2000 cps	6.0 g's (0-pk)

Sweep Rate: 2.0 octaves per minute or 44.8 degrees per minute.

Sweep Time: for 5 - 2000 cps approximately 4.5 minutes

RANDOM NOISE VIBRATION SCHEDULE

Axis of Vib.	Frequency Range cps	Acceleration Level rms	Spectral Density	Overall Level rms	Time
3 Mutually	20 - 400	4.3 g's	$.05 g^{2}/cps$	13.3g's	4.5 min/
Perpend. Axes	400 - 2000	12.6 g's	$.10 g^{2}/cps$		per axis

11.2.3.2 Thermal Vacuum

Flight acceptance thermal vacuum tests were conducted identically as described for qualification tests except the high temperature soak was with the baseplate temperature held at 130^{O}F.

11.2.3.3 Mechanical Shock

Flight acceptance mechanical shock tests were identical to qualification tests in every respect.

11.3 SYSTEM TEST

The SERT II Spacecraft Support Unit (SSU) system test was performed by a SERT II Systems test group and monitored by Quality Assurance personnel. Each SSU underwent an integration and test program. The program, its objectives and results are discussed in the following paragraphs.

11.3.1 INTEGRATION PROGRAM

An integration program was instituted for each of the SERT II SSU models to ensure a timely integration of components into the spacecraft with a maximum of safety. A brief description of the integration program follows.

11.3.1.1 Factory Test Equipment

To accomplish the integration program it was necessary to design and use special factory test equipment to supplement the Agena, Spacecraft, Solar Array Simulators, and capital equipments. The factory test equipment manufactured includes a Test Control Unit, Command and Power Control Panels, and Component Breakout Boxes.

The Test Control Unit was designed to interface with the AG Agena simulator umbilical connector. Functionally, the Test Control Unit controls ground power and monitors and controls battery signals that are brought to the umbilical. The Test Control Unit is also utilized during system test.

The Command and Power Control Panels allow manual command of the SSU system. The panels were used exclusively during the integration phase of the test program, primarily for testing power distribution.

Component breakout boxes were utilized to check parameters and functions that could not be tested with the components connected directly into the system harness. Component breakout boxes include:

- Gyro Breakout Box
- Time code generator breakout box
- Multiplexer breakout box
- Tape Recorder breakout box
- 2 Pt. Calibration Breakout Box

Breakout boxes were used for system test and integration.

11.3.1.2 Integration

The Integration Program was conce ed to optimize incorporation of equipments into the spacecraft. The Integration Program minimized the time for spacecraft assembly and maximized the safety of equipments as well as demonstrated the following design characteristics.

- Component/SSU structural interface
- Subsystem/System performance

- o Component/spacecraft harness interfaces
- o Ground station compatibility
- o Interface compatibility with Agena and spacecraft simulators

The sequence of tasks performed to accomplish the integration of the SSU follow. The structure of the SSU had the harness and a majority of the components mechanically installed. A power distribution check was performed on the harness. The power subsystem components were then integrated into the harness, with checks of the remaining power distribution performed. The remaining equipments were then installed as subsystems and their operation tested and verified. An informal Integrated Electrical Systems Test (Acceptance) was then performed to fully verify operational performance.

11.3.2 TEST PROGRAM

The SSU System Test Program performed at Fairchild Hiller was designed as an integral part of the overall SERT II Test Program coordinated and directed by LeRC. Following is a brief description of Fairchild's in-house SSU system test program. Except for thermal design verification tests on the Experimental Unit, environmental testing was performed at the Lewis Research Center with FHC support provided for the Electromagnetic Interference Test.

11.3.2.1 Experimental Unit Thermal Vacuum Test

The objective of the SERT II SSU Thermal Vacuum Test for the Experimental Unit (EU) was to provide preliminary data to show that the EU functions properly under passive thermal input and vacuum conditions. The EU was operated in simulated orbital conditions and temperatures of the EU were monitored by thermocouples during the test.

11.3.2.1.1 Test Configuration

The EU Thermal Vacuum Test was performed after satisfactory completion of an Integrated Electrical System Test (ref. 11.2.2.2). Thermocouples were installed and set up to monitor SSU temperatures. For each of the component boxes, a thermocouple was placed on the box and underneath the box and/or on the shelf. The SSU and the required test equipments were connected as shown in Figure 11.2-1.

11.3.2.1.2 Test Procedure

The thermal vacuum test was performed in the following sequence. Chamber and SSU depressurization was followed by SSU power application. Once the SSU temperature stabilized, an SSU functional test was performed. Pertinent test parameters are listed below:

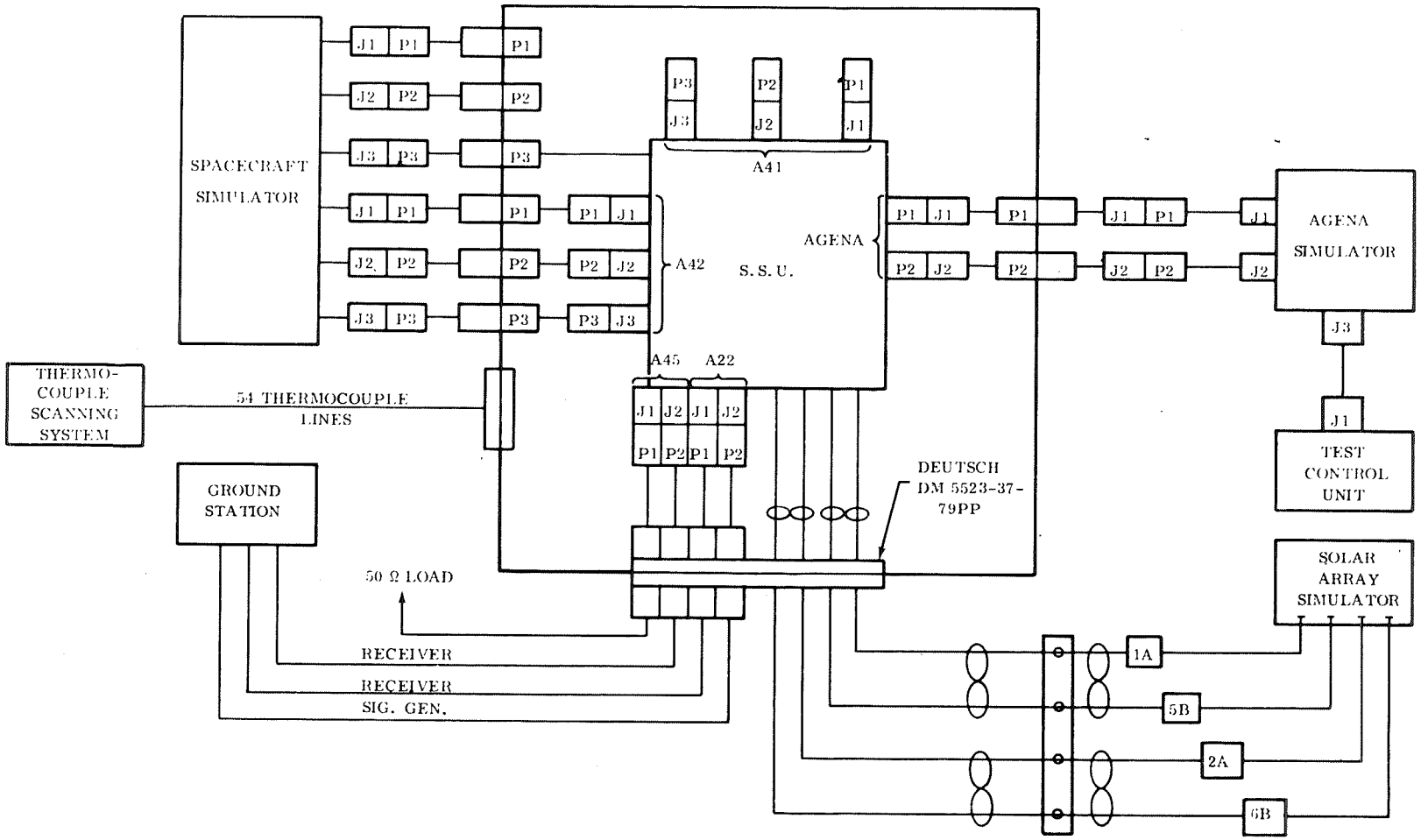

Figure 11.2-1. Integrated SSU Test Set-up

- o Depressurization 1 x 10^{-5} mm Hg
- o Power Application - Start of data acquisition. SSU to a full on condition. Thermocouple scan taken prior to every fifteen minutes thereafter.
- o Temperature Stabilization. The point where each temperature point has a variance of $\pm 1^{o}$F or less within the fifteen-minute sampling period.
- o Upon reaching stabilization, thermal vacuum functional test was performed to verify system performance.

11.3.2.1.3 Test Results

The test verified adequate passive thermal control of the SSU components except for the two-point calibrator. It was noted during performance of the test that this unit was running too hot. On the basis of these results, the mounting bracket of the unit was redesigned to increase the contact area on the dissipating surface. Later tests verified adequacy of the redesign.

The experimental unit thermal vacuum test was successfully completed with no degradation in SSU functional performance noted during test.

11.3.2.2 Acceptance Test

The Acceptance Test, revised to incluce the Integrated Electrical Systems Test, was performed on each of the SSU models. The objectives of the test were as follows:

- o Demonstrate satisfactory systems integration of the SSU under test.
- o Demonstrate functional performance for the full range of orbital operational modes and command sequences.
- o Demonstrate the functional performance for extreme solar array power conditions.
- o Demonstrate the system calibration.
- o Demonstrate compatibility on the Agena and spacecraft interfaces.

11.3.2.2.1 Test Configuration

The SERT II SSU Acceptance Test made extensive use of capital equipment. In addition, use was made of the breakout boxes listed in section 11.2.2.1, Government Furnished Equipment and Ground Support equipments. Figure 11.2-1

illustrates the prime SSU test set-up. The Spacecraft Simulator was provided GFE by the Lewis Research Center. The Test Control Unit was a piece of factory test equipment. The Agena Simulator, Solar Array Simulator, and Ground Station are pieces of Ground Support Equipment.

The SSU Acceptance Test was performed in the clean room located in the Paul Moore Test Building at Germantown. The test was performed under ambient conditions. Figure 11.2-2 illustrates the SSU undergoing final acceptance test.

11.3.2.2.2 Test Procedure

The following paragraphs describe the scope of the SSU Acceptance Test and the objectives of the procedures involved. The Acceptance Test has been organized into four basic sections:

1. Calibration and measurement of telemetry system parameters, particularly those that require breakout boxes.

2. Verification of command system performance and command distribution.

3. Verification of gyro system performance.

4. A plugs-in, simulated flight with the exercise of orbital modes, particularly power, and command sequences.

The calibration and performance test of the telemetry system constituting the first section of the acceptance test verified the following:

- Calibration of the voltage control oscillators (deviation and pre-emphasis).
- Transmitter deviation and frequency.
- Two-point calibrator levels.
- Timing signal characteristics.
- Time code generator performance.
- Tape recorder performance.
- RF power to the antennas.

The command system test verified the following:

- Command Link sensitivity (of each receiver)

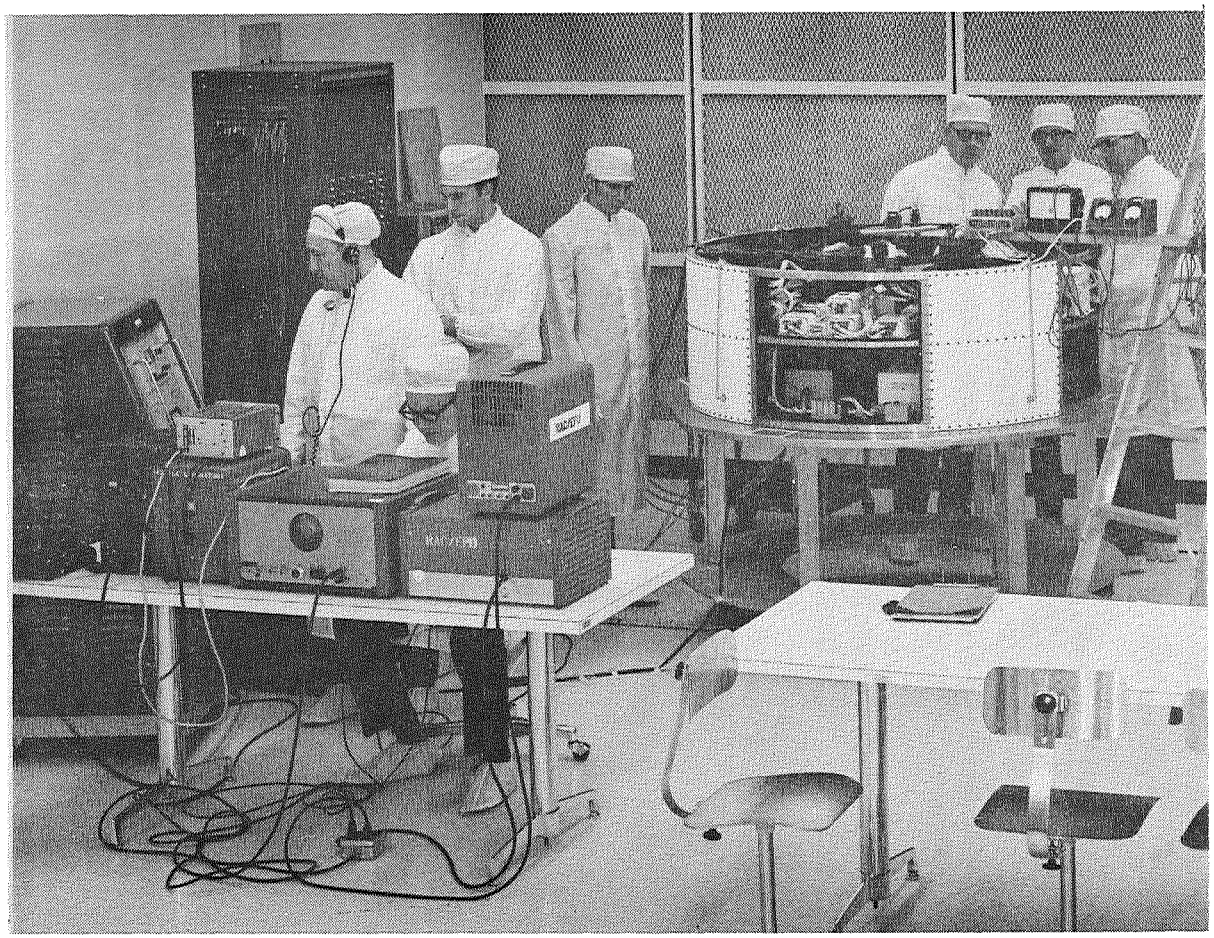

Figure 11.2-2. SSU Undergoing Final Acceptance Test

- Command distribution to the Agena and spacecraft.

The gyro system test verified the capability of the SSU power system to start and run the control moment gyros (CMGS) in accordance with SERT II requirements. The constant current supplied to the CMG's was measured and the phase demodulator performance verified.

The simulated flight test approximated in-flight functional conditions for evaluation of the SSU performance. Items tested included

- Agena Battery-ON command interface.
- High, nominal, low current conditions on the solar array.
- Performance on main and standby conditions.
- Telemetry system accuracy and telemetry points.
- Commands to Agena.
- Timing signals.
- Delay-time channel data quality.
- Power system performance under various load conditions to full load with battery, without battery support, and on battery.
- Failure mode test of protective circuitry.
- Power system mode configurations.
- Instrumentation system.

The Acceptance Test confirmed the performance of the SSU on the system level, complementing the tests performed on the component level. Data recorded on magnetic tape during performance of the Acceptance Test was reduced at the completion of the simulated flight.

SECTION XII

RELIABILITY

12.0 INTRODUCTION

The section presents the reliability analysis and the failure mode, effect, and criticality analysis for the SERT II SSU.

12.1 RELIABILITY MODEL AND PREDICTION

The reliability model is defined in block form in Figure 12.1-1. The diagram is punctuated with equations defining the complex systems reduced to individual series components. The reliability of the SSU is the product of the reliability of these individual series-reduced blocks. The six month reliability prediction for the SSU is .8849. This excludes the command verification system which can be considered nonessential to mission success. When command verification is considered essential, the six month reliability becomes .8112. Table 12.1-1 presents the system calculated reliability.

Table 12.1-1. System Reliability Summary	Reliability
Power Subsystem:	.93621
Telemetry Subsystem:	.95002
Communications Subsystem:	.99495
SSU W/O Command Verification	.8849
Command Verification	.91673
SSU W/Command Verification	.8112

12.1.1 GENERAL CONSIDERATIONS

The trestment of switches, fuses, wires, and connectors in the prediction is discussed in the following paragraphs.

12.1.1.1 Switching

Figure 12.1-2a shows a typical switching network. The dotted portions are variations also used on SERT II SSU. The diode redundancy is such that if any single diode fails in any mode, the switch or the associated command system will not fail. Thus the reliability of the switch becomes the reliability of the relay as follows:

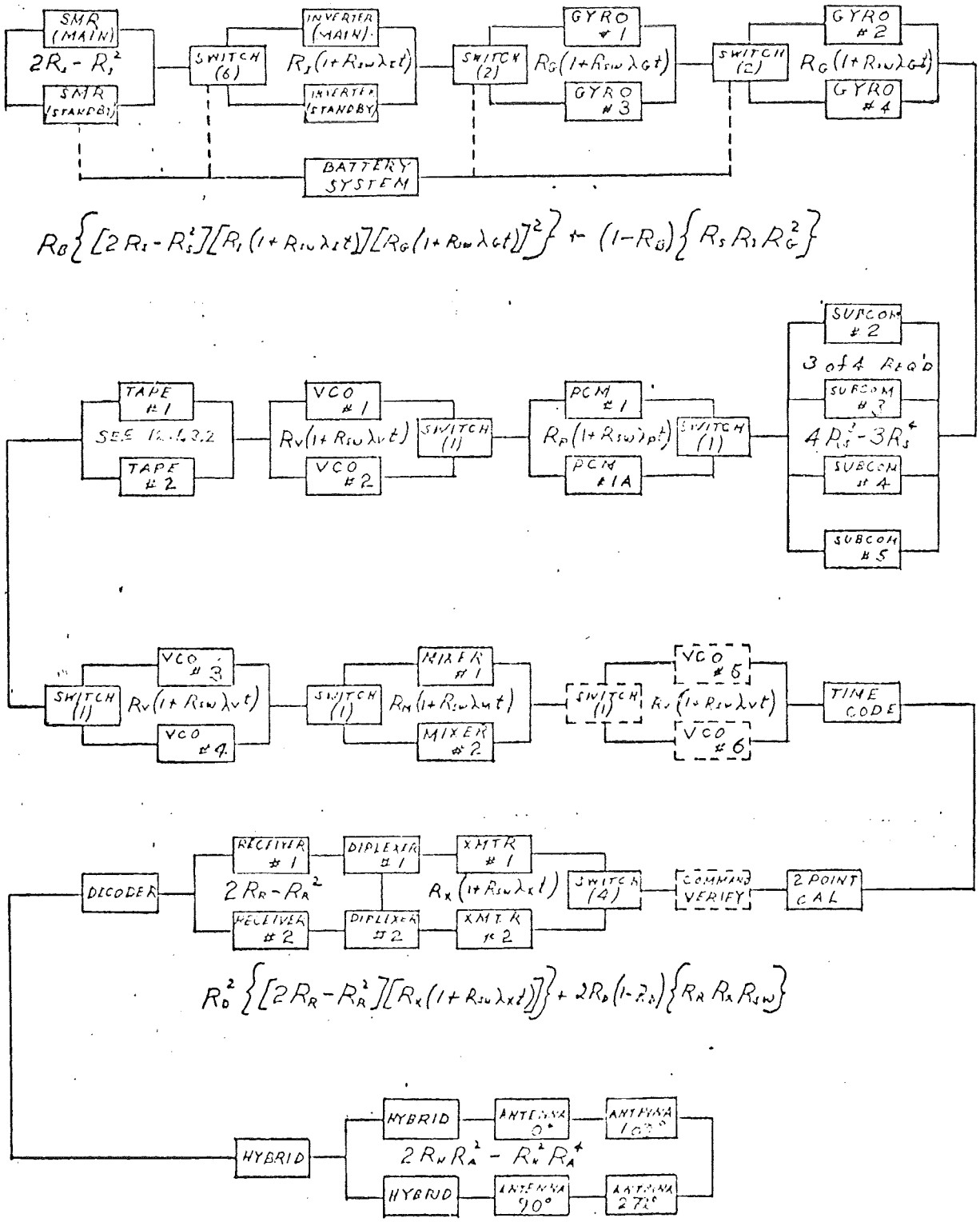

Figure 12.1-1. System Reliability Model

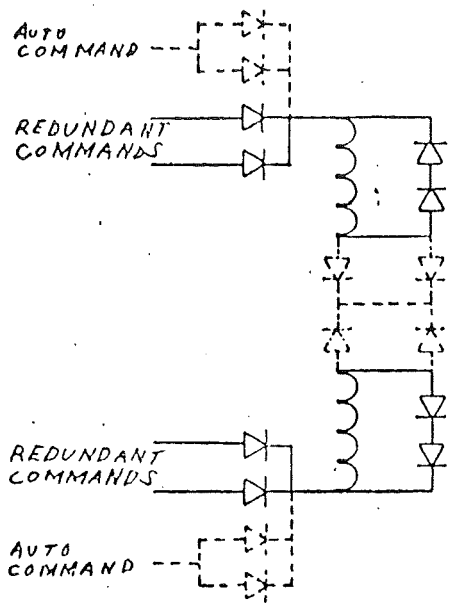

a) Standard Switch with Typical Variations

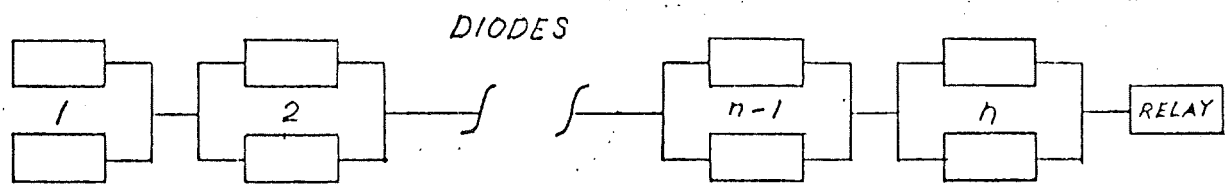

$$R_{SW} = R_R\left[1 - Q_{CR}^2\right]^n \simeq R_R\left[1 - \lambda_{CR}^2 t^2\right]^n \simeq R_R\left[1 - n\lambda_{CR}^2 t^2\right] \qquad n = 4, 5, 6, 7, 8$$

b) Switch Reliability

Figure 12.1-2. Reliability Model

$$R_s = R \text{ (diodes) } R(\text{relay}) = R_D R_r$$

where R_D is the reliability of all the diodes in their redundant combinations. The reliability diagram for the switch is presented in Figure 12.1-2b. The failure rate (λd) for individual diodes is a .03 parts per million hours. This is a factor of 10 better than the MIL HDBK 217A value. This factor is applied for screening and burn in. For six months,

$$\lambda_d t = (.03)\ (.004380) = .0001314 \quad Q = 1-R$$

where Q is the six month unreliability and the following approximation was made:

$$R = e - \lambda_d t \quad 1 - \lambda_d t$$

The reliability of each redundant pair of diodes is $1 - Q^2$ and the maximum number of diodes used in any one switch in the SSU is 8 redundant pairs. The reliability of that combination is

$$R_D = (1 - Q^2)^8 = (1 - 1.73 \times 10^{-8})^8 \quad 1 - (1.73 \times 10^{-8})$$
$$= 1 - 1.38 \times 10^{-7} = .999999862$$

This is legitimately approximated to 1. Thus the switching reliability is the relay reliability.

. The relay failure rates are taken from MIL HDBK217A. They range from 0.1 to 0.15 parts per million hours depending on the stress and type of load. In this analysis the figure 0.15 parts per million hours is used. Thus the relay reliability and, hence, the switch reliability is:

$$R_s = R_r = e^{-0.15\ (.00438)} = e^{-.000657} = .99934$$

12.1.1.2 Fuses

The individual components of the SSU are fused with Bussman, type GFA fuses. Available test data covers such blow characteristics as required overload, repeatability among lots, blow time for various amounts of overload. Life test data for fuses operating below rated current are not available. The short circuit current available in the SSU to cause a fuse to blow is at least 200% of rating. This figure is in excess of the "all-blow" overload current. Life test data for the fuses operating as series elements in a normally operating circuit would give information on the random opening of fuses. Reliability calculations for the SSU application should be based on this random type of open failure rather than the failure of a fuse to open under its specified overload rating.

The failure rate for fuses in MIL-HDBK-217A is 0.1 parts per million hours. This failure rate is used in the analysis although the failure rate for the high rel GFA fuse is probably much lower. The six month reliability of a fuse is

$$e^{-(0.1)\ (.004380)} = 0.99956.$$

12.1.1.3 Wire and Connectors

The failure of wires can generally be traced to design and workmanship. The most common failure mode is a break at the termination. This is caused by improper stripping, improper termination (solder, crimp, etc.), or a sharp bend at the termination. All of these causes are obviated by strict quality control and inspection during assembly and proper wire routing to relieve stresses. This failure mode is included as part of the connector failure rate.

Harness connectors, in this analysis, are generally considered a part of the component they are attached to. This works out very well for components like the gyros, transmitters, and receivers. However, when one considers the command decoder, PCU, and command relay junction box, the situation is more complicated. These components perform support functions and are really part of the systems they support. In order to get around this, the connector failure rates on single function components are doubled. While this is not strictly precise, it is a good estimate. This will be considered further in discussion of the telemetry subsystem and the command decoder.

12.1.2 POWER SUBSYSTEM

The purpose of the power subsystem is to deliver regulated DC power to the SSU components and the spacecraft. It also delivers AC power to the gyros and the spacecraft. In this analysis the gyros are considered part of the power subsystem. The functional flow diagram of the power subsystems is presented as Figure 6.2-1.

12.1.2.1 Assumptions

The following assumptions are made about the operation of the power subsystem:

1. If, for any reason, the gyros lose power, the satellite will lose its orientation and the arrays will lose the sun.
2. A gyro failure will have the same effect as in assumption 1.
3. Two adjacent gyros are required to stabilize the satellite.

Assumptions 1 and 2 are worst case assumptions.

12.1.2.2 Power Subsystem Reliability

Assumptions 1 and 2 of 12.1 2.1 above lead to the necessity of the battery in case an SMR, an Inverter, or a gyro fails; that is the battery will be required to switch out the failed component, switch in its redundant replacement and reorient the satellite. Thus the battery effects redundancy of the SMR's, inverters, and tyros. Without the battery, redundancy is lost.

Singling out the battery systems and applying Bayes theorum leads to:

$$R_{PS} = R_B R_{PS}(B) + Q_B R_{PS}(\bar{B})$$

where $R_{PS}(B)$ is the reliability of the power subsystem given the battery system is good and $R_{PXS}(\bar{B})$ is the reliability of the power subsystem given the battery system has failed. With the battery operative there is redundancy, thus,

$$R_{PCU_{PS}}(B) = (2R_S - R_S^2) \quad R_I (1 + R_{sw}\lambda_I t) \quad R_G (1 + R_{sw}\lambda_G t)^2$$

The square on the last term indicates that there are two sets of redundant gyros. With the battery failed, redundancy is lost, thus

$$R_{PCU_{PS}}(\bar{B}) = R_S R_I R_G^2$$

The SMR's both operate full time and so are actively redundant; hence the $2R_S - R_S^2$ term. The inverters and the gyros are standby redundant, i.e., the redundant component does not operate until there is a failure. For such a system, the reliability of the combination is: $R_R = R(1 + R_{sw}\lambda t)$ where λ is the failure rate of the single component. In order to switch from one inverter to the other, 6 relays (K10 thru K15) must be switched to retain the same two gyros in operation. This is the (6) in the inverter switch block of Figure 12.1-1. R_{sw} in that calculation is the reliability of six switches. The same was done with the gyros and the transmitters. This analysis is again not exact, however, the reliability of the switch appears as a second order term and the error is small.

Not included in Figure 12.1-1, but included in the calculation are the relay (K_{16}) and fuses which supply 2 phases of AC power to the spacecraft.

The battery charger, steering diodes, fuses and switches relating to the battery and charger are included as part of the battery system. Diodes CR9 and 10 are considered part of the main and standby SMR's respectively.

The power subsystem reliability calculations for six months are presented as Table 12.1-2.

12.1.3 TELEMETRY AND DATA HANDLING SUBSYSTEM

The Telemetry and Data Handling Subsystem consists of those components which collect, condition, store, and multiplex data from the spacecraft, the SSU, and the Agena. The functional flow diagram of the Telemetry and Data Handling Subsystem is presented as Figure 9.2-1.

Table 12.1-2. Power Subsystem Calculations (6 months)

Component	Reliability	Redundancy	λt	Series		Contribution
SMR	.99206	Active		$2R-R^2$	=	.999937
Inverter	.97483	Standby	.0255	$R(1-R_{SW}\lambda t)$	=	.999589
Gyro Network	.76914	Standby	.2620	$R(1-R_{SW}\lambda t)$	=	.970388
Gyro Network (2 sets)				$\left[R(1-R_{SW}\lambda t)\right]^2$	=	.941652
Battery System						
Battery	.99748					
Connector	.99982					
Charger	.99900					
Connector	.99991					
4 Fuses	.99825				R_B =	.98926
5 Relays	.99672				O_B =	.01074
9 Diodes	.99803					
Product	.98926					

$$P_{PS} = R_B \left\{\left[2R_S - R_S^2\right] \left[R_C (1 + R_{SW}\lambda_I t)\right] \left[R_G (1 + R_{SW}\lambda_G t)\right]\right\}^2 + O_B \left\{R_S R_G^2 R_I\right\}$$

$$= (.98926)(.999937)(.999589)(.941652) + (.01074)(.99206)(.76914)^2 (97483)$$

$$= .931097 + .006144 = .937241$$

Include 2 phases to spacecraft, Relay (K16) and fuses R = .9989

$R_{PS} = (.937241)(.9989) = .936210$

12.1.3.1 Assumptions and Analysis

The data from the spacecraft experiments are fed directly to the redundant PCM multicoders. All other data collected are considered to be non-essential to mission success. However, certain decisions affecting the mission may be made on the basis of "housekeeping" data; thus, this data cannot be entirely overlooked in a reliability prediction.

While it is impossible to evaluate the essentiality of every piece of data collected, the assumption is made that any three of the four subcommutators will lead to mission success. The connectors of the harness are included as part of the individual subcoms. Signal conditioning is overlooked since the data are generally taken from redundant subsystems, are generally non-essential, and the signal conditioning circuits have a high individual reliability.

The other two components about which there may be some question are the two point calibration system and the time code generator. The calibration system is required only in case of failure or degradation of other components in the system; the PCM, the tape recorder, the VCO, etc. The calibrator is included in the analysis as a series element, a sine qua non. To analyze the effect of the calibrator on the reliability could add a maximum of .4% to the prediction. Similarily, the time code generator, if excluded, would add .5% to the prediction.

The isolation systems between the PCM's and VCO's and Mixers, etc. are considered part of the subsystem on the input end of the isolator. This is valid because the isolators individually have a high reliability causing the error generated by this assumption to be very small.

The tape recorders are standby redundant with active redundancy between the two tracks on each recorder. The two record and two reproduce amplifiers are redundant through the track select relays in the command relay junction box. The analysis of the tape recorder reliability is discussed in 12.1.3.2 below.

The six month reliability calculation for the telemetry and data handling subsystem is presented as Table 12.1-3.

12.1.3.2 Tape Recorder Analysis

The two tape recorders are standby redundant with active redundancy between the two tracks on each recorder. The reliability block diagram for such a system is as in Figure 12.1-3.

Table 12.1-3. Telemetry Subsystem Calculations (six months)

4.2 Telemetry and Data Handling Subsystem

4.2.1 Subsystem Calculation

Component	Reliability	Redundancy	λt	Series		Contribution
Subcom	.989946	Active (3 of 4)		$4R^3 - 3R^4$	=	.999402
PCM	.984111	Standby	.01601	$R(1 \pm R_{SW}\lambda t)$	=	.999855
VCO (1 & 2)	.972655	Standby	.02773	$R(1 \pm R_{SW}\lambda t)$	=	.999608
VCO (3 & 4)						.999608
Tape (See Section 12.1.3.2)						.959585
Mixer	.984658	Standby	.01547	$R(1 + R_{SW}\lambda t)$	=	.999879
Time Coder Generator						.995438
Calibrator						.996212
Reliability of Telemetry Subsystem						.950022

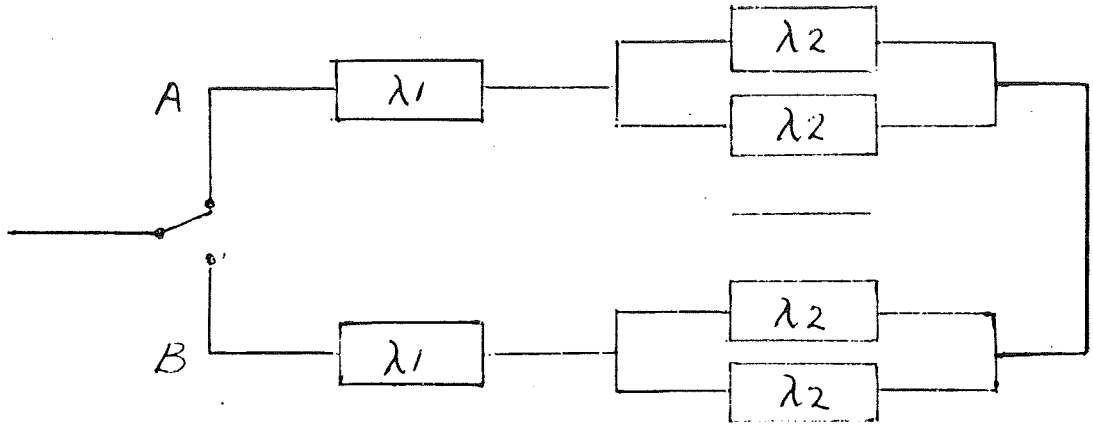

Figure 12.1-3. Standby Redundant System with Individual Active Redundancies

The system will be successful for time t if either of the following conditions are met:

1. Leg A operates to time t

or

2. Leg A fails at time t_1 t and leg B operates from time t_1 to time t.

The probability of success is P (1) + P (2).

The probability that leg A will operate to time t is

$$P(1) = e^{-\lambda_1 t} \quad 2e^{-\lambda_2 t} \quad -e^{-2\lambda_2 t}$$

P(2) can be expressed as follows:

$$P(2) = \int_{t_1 = 0}^{t} \left[2(\lambda_1 + \lambda_2)\, e^{-(\lambda_1 + \lambda_2)\, t_1} \quad -(\lambda_1 + 2\lambda_2)\, e^{-(\lambda_1 + 2\lambda_2) t_1} \right]$$

$$0 \left[2e^{-(\lambda_1 + \lambda_2)\,(t - t_1)} \quad -e^{-(\lambda_1 + 2\lambda_2)\,(t - t_1)} \right] d\, t_1$$

The first bracket multiplied by dt_1 is the probability that leg A will fail between t_1 and $t_1 + dt_1$. The second bracket is the probability that leg B will operate from time t_1 to time t. The expression is integrated on t_1 between 0 and t since t_1, the time at which leg A fails, can occur anytime between 0 and t.

Multiplying the brackets and adding P (1) and P (2) leads to:

$$R = P(1) + P(2) = 2e^{-(\lambda_1 + \lambda_2)t} - e^{-(\lambda_1 + 2\lambda_2)t}$$

$$+ 4(\lambda_1 + \lambda_2)\, e^{-(\lambda_1 + \lambda_2)t} \int_0^t dt_1 + (\lambda_1 + 2\lambda_2) e^{-(\lambda_1 + 2\lambda_2)t} \int_0^t dt_1$$

$$- 2(\lambda_1 + \lambda_2)\, e^{-(\lambda_1 + 2\lambda_2)t} \int_0^t e^{\lambda_2 t_1}\, dt_1$$

$$- 2(\lambda_1 + 2\lambda_2)\, e^{-(\lambda_1 + \lambda_2)t} \int_0^t e^{-\lambda_2 t_1}\, dt_1$$

Performing the integrations:

$$R = e^{-(\lambda_1 + \lambda_2)t} \left[2 + 4(\lambda_1 + \lambda_2)t\right] + e^{-(\lambda_1 2\lambda_2)t} \left[(\lambda_1 + 2\lambda_2)t - 1\right]$$

$$- \left[2(\lambda_1 + \lambda_2)\, e^{-(\lambda_1 + 2\lambda_2)t}\right] \left[e^{\lambda_2 t} - 1\right]$$

$$- \left[2(\lambda_1 + 2\lambda_2)\, e^{-(\lambda_1 + \lambda_2)t}\right] \left[1 - e^{-\lambda_2 t}\right]$$

$$R = 4\, e^{-(\lambda_1 + \lambda_2)t} \left[(\lambda_1 + \lambda_2)t - \lambda_1/\lambda_2 - 1\right]$$

$$2\, e^{-(\lambda_1 + 2\lambda_2)t} \left[(\lambda_1 + 2\lambda_2)t + 4\lambda_1/\lambda_2 + 5\right]$$

For the tape system,

$\lambda_1 = 71.70$ PPM hours

$\lambda_2 = 9.32$ PPM hrs.

$\lambda_1 + \lambda_2 = 81.02$ PPM hrs.

$$\lambda_1 + 2\lambda_2 = 90.34 \text{ hrs.}$$

$$e^{-(\lambda_1 + \lambda_2)t} = -.35487 = .701266 \quad \lambda_1/\lambda_2 = 7.6931$$

$$e^{-(\lambda_1 + 2\lambda_2)t} = e^{-.39569} = .673215 \quad t = 4380 \text{ hours}$$

$$R(t) = 4\left[0.35487 - 1 - 7.6931\right]\left[.701266\right] + .673215\left[5 + .39569 + 30.772\right]$$

$$= (.673215)(36.168) - (.701266)(33.3529) = .959585$$

12.1.4 COMMUNICATIONS SUBSYSTEM

The communications subsystem consists of those components which effect the transmission of data and the reception, verification and execution of commands from earth. Figure 8.2-1 presents the functional block diagram for the communications subsystem.

12.1.4.1 Assumptions

The following assumptions are made about the operation of the communications subsystem.

1. Failure of a diplexer means loss of one transmitter and one receiver.

2. Failure of a hybrid ring means loss of both its outputs.

3. Degraded output resulting from failure of two opposed antennae is not considered a system failure.

12.1.4.2 Analysis

Using assumption 1 of 12.1.4.1 and applying Bayes' theorem to the pair of diplexers leads to

$$R_{XRD} = R_D^2\left\{\left[2R_R - R_R^2\right]\left[R_X\left(1 + R_{SW}\lambda_X t\right)\right]\right\} + 2R_D Q_D R_{SW} R_R R_X$$

as the reliability of the transmitters, diplexers, and receivers. This equation states that with both diplexers working (R_D^2), there are active redundant receivers ($2R_R - R_R^2$) and standby redundant transmitters $R_X(1 + R_{SW}\lambda_X t)$. With one diplexer

failed ($2R_D Q_D$), redundanty is lost and the transmitter switch is required ($R_{SW} R_R R_X$).

Assumptions 2 and 3 of 12.1.4.1 lead to the model defined by the bottom section of Figure 12.1-1.

The command decoder is itself a redundant system capable of handling 108 sets of redundant commands. The reliability figure on the decoder was derived by using 5% duty cycle on parts stressed during command only. The assumption about the output, however, is that if one command output fails then all 108 commands of that redundant leg are lost. It is clear that this is not strictly the case. The output system is really part of the switch rather than part of the decoder. The 108 outputs transistors can be discounted much the same way the steering and suppression diodes for switches in paragraph 12.1.1.1 are discounted. The same is the case with command system connectors and harnesses. The power connectors, and fuses are redundant and were included in the prediction as part of the redundant legs of the decoder.

Table 12.1-4 presents the calculation of the communication subsystem reliability.

12.2 FAILURE MODE, EFFECT, AND CRITICALITY ANALYSIS

This section presents the Failure Mode, Effect, and Criticality Analysis (FMECA) of the Spacecraft Support Unit for SERT II. The SSU subsystems in this analysis are as follows:

- Power Control Subsystem
- Communications Subsystem
- Telemetry Subsystem

The possible failures are categorized according to their system effect as follows:

Failure Category I -	Critical failures of equipment or component where the SSU can no longer perform its mission.
Failure Category II	Major failures as in Category I, except provisions are available to compensate for the failure.
Failure Category III	Minor failure other than critical or major, including those failures which would have no significant effect on the reliability or performance of the SSU.

Table 12.1-4. Communications Subsystem Calculations (six months)

4.3 Communications Subsystem Calculations

Component	Reliability	Redundancy	λt	Series		Contribution
Transmitter	.944449	Standby	.0571	$R(1 \pm R_{SW}\lambda t)$	=	.998234
Receiver	.979430	Active		$2R - R^2$	=	.999576
Diplexer	.99408					
Switch (4 relays)	$.99934^4$ = .997361					

$$R_{XRD} = R_D^2 \left\{\left[R_X \left(1 + R_{SW}\lambda_X t\right)\right] \left[2R_R - R_R^2\right]\right\} + 2R_D Q_D \left\{R_X R_R R_{SW}\right\}$$

$$= (.988195)\ (.998234)\ (.999576) + 2\ (.99408)\ (.00592)\ (.944449)\ (.979430)\ (.997361)$$

$$= .986032 + .010859 = .996890$$

Decoders	.999142					
Hybrid	.998912					
Antenna	.9999					

$$R_{ANT} = 2R_A^2 R_H - R_A^4 R_H^2$$

$$= 1.997424 - .997425 = .999998$$

$$R_{COMM} = R_{XRD}\, R_{DEC}\, R_H\, R_{ANT} = .994948$$

Command Verification

VCO 5 & 6		.999608
AVCO Parts λ = 14.207 PPM hrs	λt = .06223	.939666
FHC Parts λ = 5.552 PPM hrs	λt = .02432	.975972
Reliability of Command Verification		.916729

Failure Category III (cont) The system will function and perform its intended purpose, but possibly not within specified limits. These failures do not constitute system breakdown.

The FMECA for the SSU discloses two category I failures within the Power Subsystem. These are cases #39 and 40. A study of the power subsystem schematic, Figure 6.2-1, shows that the possible causes of these failures are highly improbable. They involve the shorting of a harness wire to ground or the breakdown of diode mounting insulation.

The diodes within the power control unit (PCU) have their cathodes connected to their cases. A category I failure will thus result if the case of CR1, 2, 5, 6, 7, 8, 9, 10, or 11 shorts to the chassis of the PCU. The same is true if the harness wires connecting to the cathodes of these diodes short to ground. As discussed earlier, these failures are highly improbably and extreme care was taken in assembly of the PCU to insure that the fabrication was proper and did not degrade the inherently high reliability of wiring assembly and diode insulation.

The FMECA worksheets are presented in the following pages.

FAIRCHILD HILLER
SPACE SYSTEMS DIVISION

FAILURE EFFECTS ANALYSIS

SYSTEM SSU REFERENCE

COMPONENT Power System

Mode	Failure		Case No.	Symptoms & Consequences		Compensating Provisions	Failure Category
	COMPONENT	MODE		Immediate	System		
(1) Solar Energy and battery normal operation	Housekeeping solar array	Low output <27.5V	1	(a) Conditioned power line voltage to non-essential load drops	(a) System operation may be degraded due to low line voltage (b) Main SMR no longer regulates	(a) Solar array voltage increases if non-essential loads are removed. (b)battery may supply part of the load. (c) Main array may be commanded "ON" to support housekeeping array.	II
		Low output <24V	2	(a) Conditioned power line voltage drops, under voltage sense turns OFF non essential loads, and battery-on-line signal turns off charger after 1 second	(a) Draws battery current and removal of nonessential loads plus battery charger	(a)Battery supplies essential loads. (b)Battery may be recharged when array can support charge cycle (c)Main array may be commanded "ON" to support housekeeping array	II
		High output >35V but <55V	3	(a) Input voltage to both SMR's increases	(a) Input power to SMR (Standby) is supplied by array instead of charger.	(a) None required	III
		No output (Open)	4	Same as case 2	Same as case 2	(a) Use battery until exhausted (b) or command main array on to support housekeeping array	II

FORM 550-[illegible]

FAIRCHILD HILLER
SPACE SYSTEMS DIVISION

FAILURE EFFECTS ANALYSIS

SYSTEM SSU REFERENCE

COMPONENT Power System

Mode	Failure		Case No.	Symptoms & Consequences		Compensating Provisions	Failure Category
	COMPONENT	MODE		Immediate	System		
(1) (Cont.)	Housekeeping Solar Array (Cont.)	No output (Shorted)	5	Same as case 2	Same as case 2	Same as case 4	II
(2) Battery Charger in "hold-off" mode and housekeeping array 24V	Battery	Low output <27V	6	All conditioned power line voltages drop	System may not function properly when voltage drops	(a)System may function with reduced loads on housekeeping array (b)Main array may be commanded "ON" to support housekeeping array	II
		No output (Fail to charge)	7	Same as case 6	Same as case 6	Same as case 6	II
(3) Array voltage nominal >27.5V	SMR (Main)	No output (Open)	8	Same as case 2	Same as case 2	(a)Stand-by SMR can supply loads by commanding main SMR "OFF" (K1) (b)Command battery "OFF" to conserve life (K7)	II
		No output (output short)	9	Same as case 2	Same as case 2	Same as case 8	II
		No output (input short)	10	Same as case 2 plus fuse flows at input to SMR	Same as case 2	Same as case 8	II
		Low output <23V	11	Same as case 2	Same as case 2	Same as case 8	II
		High output >31V	12	Voltage increases on all conditioned power lines.	Possible damage to system due to overvoltage condition	(a)Same as case 8 (b)Command "ON" additional loads which will lower voltage	II

FORM SSD-0607 1/--

FAIRCHILD HILLER
SPACE SYSTEMS DIVISION

FAILURE EFFECTS ANALYSIS

SYSTEM SSU REFERENCE

COMPONENT Power System

Mode	Failure		Case No.	Symptoms & Consequences		Compensating Provisions	Failure Category
	COMPONENT	MODE		Immediate	System		
(4) Array voltage nominal >27.5V and charger in "HOLD-OFF" mode	SMR(Standby)	No output(Open)	13	SMR output voltage drops	Lose standby power to command system	(a)Command stand-by SMR"OFF" (K8) to reduce power loss (b)Command battery "OFF" to conserve life (K7)	II
		No output (out short)	14	Same as case 13	Same as case 13	Same as case 13	II
		No output (in short)	15	Same as case 13 and fuse blows at input to SMR	Same as case 13	None required	II
		Low output <25V	16	Same as case 13	Same as case 13	Same as case 13	II
		High output >31V	17	Command powerline voltage increases	Same as case 12	(a)Main SMR can supply loads by commanding standby SMR "OFF" (K8) (b)Command battery "OFF" to conserve life	II
(5) Main SMR Output Nominal 26.5V	Battery charger	Low output 27V < V_o < 33V	18	SMR (Standby) input voltage will drop to solar array voltage	Draws battery current to support power loss in SMR(standby) and unable to charge battery fully	(a)Command battery "OFF" to conserve life (K7)	II
		High output >35V	19	SMR (Stand-by) input voltage will increase	(a) No effect when in "HOLD-OFF" mode	(a)None required	(a) III
					(b) Possible degradation to battery when in "charge" mode	(b)Command battery to "enable" mode to current-limit charger (K7)	(b) II
		No output (Open)	20	Same as case 18	Same as case 17	Same as case 17	II

FAIRCHILD HILLER
SPACE SYSTEMS DIVISION

FAILURE EFFECTS ANALYSIS

SYSTEM SSU REFERENCE

COMPONENT Power System

Mode	Failure		Case No.	Symptoms & Consequences		Compensating Provisions	Failure Category
	COMPONENT	MODE		Immediate	System		
(5)(Cont.)	Battery Charger(Cont)	No output (Shorted input)	21	Same as case 18 and fuse to the charger blows	(a)Draws battery current and removal of non-essential loads (b) Unable to charge battery	(a)Command non-essential loads "ON" when required. (b)Command battery "OFF" to conserve life. (K7)	II
		No output (Shorted output)	22	Same as case 18 and fuse blows at output of charger when in "charge" mode	Same as case 18	(a)Command battery "OFF" (K7) to conserve life, and (b)Command charger "OFF" (K9) to reduce power loss.	II
(6) Conditioned Power line voltage nom. 26.5V	Inverter (Main)	No output (Open)	23	Main AC power line voltage drops	No main AC supply to CMG's, phase demodulators or S/C.	Command CMG's from main to stand-by" inverter - AND- Command "Main" inverter OFF (K10) to reduce power loss. (Redundant inverter)	III
		No output (two phases)	24	Same as case 23	Same as case 23	Same as case 23	II
		No output (input short)	25	Same as case 23 and fuse blows out input of inverter.	Same as case 23	Same as case 23	II
		Low Output	26	Same as case 23	Same as case 6	Same as case 23	II
		High Output	27	Main AC power line voltage increases	May cause CMG's connected to main inverter to overheat	Same as case 23	II
	Inverter (Standby)	No output (Open)	28	Standby AC power line voltage drops	No backup AC supply to CMG's, Phase demodulators or S/C	Redundant Inverter	II
		No output (two phases)	29	Same as case 28	Same as case 28	Same as case 28	II

FORM SSD-

FAIRCHILD HILLER
SPACE SYSTEMS DIVISION

FAILURE EFFECTS ANALYSIS

SYSTEM SSU REFERENCE

COMPONENT Power System

Mode	Failure		Case No.	Symptoms & Consequences		Compensating Provisions	Failure Category
	COMPONENT	MODE		Immediate	System		
(6)Cont.)	Inverter Standby (Cont)	No output (input short)	30	Same as case 28 and fuse blows at input to inverter	Same as case 28	Same as case 28	II
		Low output	31	Same as case 28	Same as case 6	Same as case 28	II
		High output	32	Standby AC power line voltage increases	Same as case 27	Same as case 28	II
	Constant Current Source	No Output (Open	33	No DC current supply to CMG	CMG of failed current source will malfunction	Command Alternate CMG "ON" and Command Failed CMG "OFF"	II
		No output (Input short)	34	Same as case 33 and fuse blows at input to constant current source.	Same as case 33	Same as case 33	II
		Improper regulation	35	Incorrect supply to CMG	Same as case 33	Same as case 33	II
	Phase Demodulator	No output (Open)	36	No reference voltage to telemetry.	Unable to detect phase difference of CMG	Redundant Unit	II
		No output (shorted input power)	37	Same as case 36 and fuse blows to input of phase demodulator	Same as case 36	Same as case 36	II
		Improper output	38	Produces error signal from CMG to TLM	Same as case 36	Same as case 36	II
(1)	Power Control Unit	No conditioned power output all lines (short)	39	Unable to control system by command and no input voltage to the system.	System will be inoperable	None	I
		Low conditioned power output all lines (<23V)	40	Unable to control system by command and low input voltage to the system	Same as case 39	Same as case 39	I
		No output to nonessential loads	41	All systems inoperative except command and transmitters	Same as case 2	Same as case 8	II
		Low output to nonessential loads (<23V)	42	Same as case 41	Same as case 2	Same as case 8	II

FORM SSD-

FAIRCHILD MILLER
SPACE SYSTEMS DIVISION

FAILURE EFFECTS ANALYSIS

SYSTEM SSU REFERENCE

COMPONENT Power System

Mode	Failure		Case No.	Symptoms & Consequences		Compensating Provisions	Failure Category
	COMPONENT	MODE		Immediate	System		
(2)		No undervoltage "TURN-OFF" signal	43	Same as case 6 and nonessential loads remain on.	Same as case 5	(a)Command "OFF" nonessential loads as required. (b)Main array may be commanded "ON" to support housekeeping array	II
		No battery "ON-LINE" signal	44	Same as case 6 and battery remains in "OFF-LINE" mode	Same as case 6	Command battery to "enable"(K7)	II
		No Agena "D" battery enable signal	45	Same as case 39	Same as case 39	Command battery to "enable (K7) after array is deployed.	II
(7) No solar energy (GSE) Connected)	Power Control Unit	No GSE battery "OFF-LINE"	46	Conditioned power line to command system remains on	Unable to turn-off battery utilizing GSE.	Repair or replace power control unit	II
		No GSE input power	47	Same as case 2	Same as case 2	Use battery for nonessential loads by commanding (K1) OFF	II
(8) Battery charger "ON" housekeeping array <27.5V		No battery charger "OFF" command	48	Battery charger remains energized	Unable to reduce power loss to solar array	Under-voltage "TURN-OFF" circuit will command charger OFF when array voltage is 24V.	II
(3)		No battery charger "ON" command	49	No charge current to battery or hold-off voltage to SMR	Unable to charge battery when exhausted which results in loss of stand-by power	Redundant Supply	III
(2)		No battery "enable" command	50	Same as case 6	Same as case 6	Same as case 6	II

FORM SSD-

FAIRCHILD HILLER
SPACE SYSTEMS DIVISION

FAILURE EFFECTS ANALYSIS

SYSTEM SSU REFERENCE

COMPONENT Power System

Mode	Failure		Case No.	Symptoms & Consequences		Compensating Provisions	Failure Category
	COMPONENT	MODE		Immediate	System		
(8)	Power Control Unit	No charge "OFF-LINE" command	51	No charge current to battery	Same as case 18	A limited charge may be applied to the battery by commanding charger to "charge" mode (K2) and reducing the load to the standby SMR	III
		No battery charge	52	Same as case 51	Unable to charge battery once it is exhausted.	Same as case 18	II
		No battery "Hold-off" command	53	Charge current remains to battery and "hold-off" supply to SMR is limited.	Unable to disconnect battery from charger fully, and unable to supply full charger current to SMR	Command battery charger and battery "OFF" K7 &K9 to conserve battery life.	II
(5)		No data handling system "OFF" command	54	Data handling system remains energized	Unable to command "OFF" data handling system	Undervoltage "Turn-off" circuit will command data handling system "OFF" when array voltage is 24V	II
		No data handling system "ON" command	55	No supply to data handling system	Loss of data handling system	Redundant circuits	III
(8)		No standby SMR "OFF" command	56	No battery backup supply to main SMR	Unable to support non-essential loads thru main SMR with the battery	(a)Command battery charger "OFF" (K9) (b)command main array "ON" to support the housekeeping array	II
(4)		No standby SMR "ON" command	57	Battery and charger will supply current to main SMR instead of standby SMR	Lose stand-by supply to command system and draw current from battery and charger	Command battery and charger "OFF" (K7&K9) to conserve life.	II

FAIRCHILD HILLER
SPACE SYSTEMS DIVISION

FAILURE EFFECTS ANALYSIS

SYSTEM SSU REFERENCE

COMPONENT Power System

Mode	Failure		Case No.	Symptoms & Consequences		Compensating Provisions	Failure Category
	COMPONENT	MODE		Immediate	System		
(3)	Power Control Unit	No main SMR "OFF" command	58	No standby back-up to non-essential loads	No effect except when main SMR fails which may cause complete loss of non-essential loads.	None	III
		No main SMR "ON" command	59	No main SMR output	Battery supplies power to non-essential loads and solar array is held-off.	Command battery "OFF-LINE"(K7) and charger "OFF" (K9)so that solar array can supply the loads	II
(9) Conditioned power line nominal (26.5V) and standby inverter OFF		No main inverter "OFF" command	60	Unable to remove main inverter from conditioned power line.	No effect except when main inverter fails which may cause increase power loss to system	Redundant inverters	III
		No main inverter "ON" command	61	No output of main inverter or dc supply to constant current source and phase demodulator	No effect except when standby inverter fails which may cause loss of CMG function	Redundant inverters, command CMG's and stand-by inverter "ON"	III
(10) Conditioned power line nominal (26.5V) and inverter OFF		No standby inverter "ON" command	62	No output of standby inverter or dc supply to constant current source and phase demodulator.	No effect except when main inverter fails which may cause loss of CMG function	Redundant inverters, Command CMG's and main inverter "ON"	III
		No standby inverter "OFF" command	63	Unable to remove standby inverter from conditioned power line	No effect except when standby inverter fails which may cause increased power loss to system	Redundant inverters	III
(9)		No CMG to main inverter command	64	CMG remains inoperative	Lose selection of particular pair of CMG's on main inverter	Same as case 23	III
		No CMG-"To Standby inverter" command	65	CMG remains energized	Unable to Turn-off particular CMG function	Same as case 23	III

FORM SSD-[illegible]

FAIRCHILD HILLER
SPACE SYSTEMS DIVISION

FAILURE EFFECTS ANALYSIS

SYSTEM SERT SSU REFERENCE

COMPONENT Communication Sub-System

Mode	Failure		Case No.	Symptoms & Consequences		Compensating Provisions	Failure Category
	COMPONENT	MODE		Immediate	System		
	Subcommutator	Loss of analog input	1	Lose 1 channel of analog input	Loss of 1 channel of data will not have critical effect on system	Critical data inputs distributed among subcoms so that all status monitoring data inputs are not lost.	II
		Loss of SYNC input	2	Lose all 60 channel subcom data	Loss of data on affected subcom	Same as case 1	II
		Loss of Subcom analog output	3	Same as case 2	Same as case 2	Same as case 1	II
		Loss of clock input	4	Same as case 2	Same as case 2	Same as case 2	II
	Signal Conditioner	Loss of 1 solar cell amplifier output	5	Loss of solar cell monitoring of affected amplifier	Loss of same solar cell housekeeping data	3 solar cell amplifiers provided. All 3 would have to fail to lose solar cell monitoring.	III
		Loss of temperature Sensor Circuit(s) output	6	Loss of affected monitoring sensor	Loss of same temperature monitoring data	None Housekeeping data not critical to mission success	III
		Loss of voltage monitor circuit(s) output	7	Same as case 6	Loss of indication of operational status monitored component.	Same as case 6	II
	Time Code Generator	Reset input at -31V	8	All TCG counters reset to zero. No further time accumulated.	Loss of time code. No command verify 17.5 PPS clocking signal	Command subsystem can function without verify clocking signal.	II
		Reset input at ground	9	Counters cannot be reset by ground command.	Counters cannot be reset by ground command.	None	II
		Upcount input at -31V	10	No up count possible. No down count possible.	Same as case 8		II

FORM SSD-

FAIRCHILD HILLER
SPACE SYSTEMS DIVISION

FAILURE EFFECTS ANALYSIS

SYSTEM SERT II SSU REFERENCE

COMPONENT Telemetry Sub-system

Mode	Failure		Case No.	Symptoms & Consequences		Compensating Provisions	Failure Category
	COMPONENT	MODE		Immediate	System		
	Time Code Generator	Upcount input at +31V	11	No up count possible by ground command	Can not advance clock by ground command	None	II
		Down count input at +31V	12	No down count possible. No up count		None	II
		+28V power line input increased above specified input (31V)	13	Unit may not be in spec. +40V, probable regulator damage for extended period of operation at levels above +40V.	Loss of time code and probable loss of command verify clocking signal (17.5PPS	Same as case 8	II
		Voltage input decreases below specified level	14	Unit may not be in spec.	Same as case 13		II
		Loss of any decade decimal counter stage	15	Loss of time code	Loss of time code. Command verify clocking signal still available	None	II
	Calibrator	Loss of +5 volt ref. open mode	16	5V reference does not appear in NRZ output	Only +2.46V reference available for data analysis	None	II
		Loss of +5 volt ref.	17	5V reference and 2.46V reference do not appear in NRZ	Data analysis more difficult in some cases impossible	None	II
		Loss of +2.46V ref open mode	18	2.46V reference does not appear in NRZ	Only +5V reference available for data analysis	None	II
		Loss of +2.46V ref. shorted mode	19	Same as case 17	Same as case 17	None	II
	PCM Multicoder	Loss of analog input	20	Loss of analog data associated with faulted channel	Some data lost until switch to standby multicoder	Standby redundant PCM multicoder	II
		Loss of code generator inputs	21	Time code lines (2) lost	Same as case 20	Standby redundant PCM multicoder	II
		Loss of NRZ filtered output	22	Loss of real time data	Same as case 20	Standby redundant PCM multicoder	II
		Loss of NRZ unfiltered output	23	Loss of stored data	Same as case 20	Standby redundant PCM multicoder	II

FORM SSD-0017 [illegible]

FAIRCHILD HILLER
SPACE SYSTEMS DIVISION

FAILURE EFFECTS ANALYSIS

SYSTEM SERT II SSU REFERENCE

COMPONENT Telemetry Sub-system

Mode	Failure		Case No.	Symptoms & Consequences		Compensating Provisions	Failure Category
	COMPONENT	MODE		Immediate	System		
	PCM Multicoder	Loss of digital input	24	Lose of digital data	Same as case 20	Standby redundant PCM multicoder	II
		Clock output	25	Loss of 2 subcoms	Same as case 20	Standby redundant PCM multicoder	II
	Low Pass Filter & Passive Isolator	Loss of input from Tape Recorder No. 1	26	Loss of IRIG channel 10	No effect. Data available for readout from Tape Recorder No. 2	Standby redundant Tape recorder	II
		Loss of input from Tape Recorder No. 2	27	Same as case 26	No effect. Data available for readout from Tape Recorder No. 1	Same as case 26	II
		Loss of output	28	Same as case 26	Same as case 26	Standby redundant IRIG channel 10 VCO	II
		Loss of output	29	Same as case 26	Same as case 27	Standby redundant IRIG channel 10 VCO	II
	Tape Recorder	Lack of record command	30	Loss of record input circuit in system control logic	Recorder will not record data. Recorder will not move in the record direction. Recorder will reach an inoperative mode at reproduce E.O.T.* excessive current drain at record input terminal.	Redundant recorder	II
		Constant Record command	31	Same as case 30	Recorder will record and reproduce data for one system cycle, then recorder will reach an inoperative mode at reproduce E.O.T.	Redundant recorder	II
		Lack of reproduce command	32	Loss of reproduce input command circuit in system control logic	Recorder will not move in the reproduce direction nor reproduce data. Recorder will reach an inoperative mode at record E.O.T. Excessive current drain at record input terminal.	Redundant recorder	II
		Constant Reproduce	33	Same as case 32	Record will reproduce and record data for one system cycle than it will reach an inoperative mode at record E.O.T.	Redundant recorder	II

FORM 550-0002

* End Of Travel

FAIRCHILD HILLER
SPACE SYSTEMS DIVISION

FAILURE EFFECTS ANALYSIS

SYSTEM SERT II SSU REFERENCE

COMPONENT Telemetry Subsystem

Mode	Failure		Case No.	Symptoms & Consequences		Compensating Provisions	Failure Category
	COMPONENT	MODE		Immediate	System		
	Tape Recorder (Cont)	Lack of stop command	34	Recorder cannot be stopped by ground command	Recorder cannot be stopped by ground command. Stop indicator will be inoperative. Constant current drain at stop input command terminal.	Redundant recorder	II
		Constant Stop Command	35	Recorder will be inoperative.	Recorder will be inoperative. Stop indicator will always be operating.	Redundant Recorder	II
		Lack of reproduce E.O.T. Indication.	36	No indication	Reproduce indicator will always be inoperative.	Redundant recorder	II
		Constant Reproduce E.O.T. Indication	37	Recorder will be inoperative.	Recorder will be inoperative	Redundant recorder	II
		No regulated power -28.5 VDC In.	38	Same as case 37			II
		Lack of Power Return	39	Same as case37			II
		Lack of record E.O.T. Indication	40	Same as case 37			II
		Lack of stop indication	41	No stop indication	No stop indication	Redundant recorder	II
		Constant Stop Indication	42	Recorder will be inoperative	Recorder will be inoperative	Redundant Recorder	II
		Lack of chassis ground	43	None	None	None	III
		Lack of channel 1 input	44	No output data from channel 1	No output data from channel 1	Redundant recorder	II
		Lack of channel 1 signal return	45	Same as case 44			II
		Lack of channel 1 output	46	Same as case 44			II
		Lack of channel 2 output	47	No reproduce data from channel 2	No reproduce data from channel 2	Redundant recorder	II
		Lack of channel 2 signal return	48	Same as case 47			II

FORM SSD-0007 1/65

FAIRCHILD HILLER
SPACE SYSTEMS DIVISION

FAILURE EFFECTS ANALYSIS

SYSTEM SERT II SSU REFERENCE

COMPONENT Telemetry Subsystem

Mode	Failure		Case No.	Symptoms & Consequences		Compensating Provisions	Failure Category
	COMPONENT	MODE		Immediate	System		
	Tape Recorder (Cont)	Lack of channel 2 monitor	49	Same as case 47			II
		Lack of channel 1 monitor	50	Same as case 44			II
	VCO & MIXER Amplifier	Loss of VCO input	51	Lose one IRIG channel	Loss of real time and or stored data until switched to standby VCO	Standby redundant VCO	II
		Loss of VCO output	52	Same as case 51			II
		Loss of mixer input	53	Lose input to transmitter	Loss of real time and or stored data until switch to standby mixer	Standby redundant mixer amplf.	II
		Loss of mixer output	54	Same as case 53			II

FORM SSD-00-7 (-)

FAIRCHILD MILLER
SPACE SYSTEMS DIVISION

FAILURE EFFECTS ANALYSIS

SYSTEM SERT II SSU REFERENCE

COMPONENT Communication Sub-System

Mode	Failure		Case No.	Symptoms & Consequences		Compensating Provisions	Failure Category
	COMPONENT	MODE		Immediate	System		
	Telemetry Transmitter	No power output	1	Loss of telemetry data. Loss of beacom CW signal to network stations	No immediate effect	Redundant transmitter	II
		Power degradation	2	Same as case 1	Same as case 1	System has large power margin	II
		Degradation of modulation frequency response	3	This failure mode only distorts leading and trailing edged of digital pulses. Analog data are degraded	No effect - data is still present	Transmitter is designed to have extended high frequency response	III
		CW output only	4	Loss of telemetry data.	No immediate effect.	Redundant transmitter	II
		Intermittent output	5	Intermittent loss of telemetry data.	No immediate effect.	Redundant transmitter	II
		Increased noise output	6	Possible degradation of PCM data	No effect.	Redundant transmitter	II
	Command Receiver	Loss of output	7	No input to decoder	No immediate effect	Redundant receiver	II
		Loss of AGC	8	Receiver output amplitude becomes dependent on RF input	No immediate effect	Redundant receiver	II
		Frequency drift	9	Same as case 7			II
		Loss of sensitivity	10	Command may not be received	Same as case 7		II
	Diplexer	Increased VSWR	11	Reduce range of communication	No immediate effect.	Redundant diplexer	II
		Increased insertion loss	12	Same as case 11			II
		Decreased isolation	13	Transmitter output coupled into receiver	No immediate effect.	Redundant receiver	II
	Hybrid Ring Isolator	Increased VSWR	14	Reduced range of communication		System design has large margin	II
		Increased insertion loss	15	Same as case 14			

FAIRCHILD HILLER
SPACE SYSTEMS DIVISION

FAILURE EFFECTS ANALYSIS

SYSTEM SERT II SSU REFERENCE

COMPONENT Communication Sub-system

Mode	Failure		Case No.	Symptoms & Consequences		Compensating Provisions	Failure Category
	COMPONENT	MODE		Immediate	System		
	Command Decoder	Loss of ability to generate a specific command	16	Failure to execute command	No immediate effect	Critical functions have redundant command outputs	II
		B+ turn off circuitry mal-function	17	Continuous power drain when no commands are being issued.	No immediate effect	Decoder cleared from ground control	II
		Output shorted	18	Possible loss of six commands	Some loss of command capability redundant transistor in series limits outputs lost	Critical functions have redundant command outputs	II
		Loss of command verify TM encoder	19	Unable to confirm command	Loss of command verification	Command verifi- may be read out through telemetry link to ground	II
		Issue false command in addition to proper command	20	Undesired function performed in spacecraft.	False command can be executed	Command verifi-cation may be read out through telemetry link to ground	II
		Loss of ability to detect erroneous format	21	Decoder becomes susceptible to noise and/or stray signals:which may result in erroneous tones being stored in decoder.	No effect	Command verify feature should detect this condi-tion stored com-mand need not be executed.	III
	Command Relay Junction Box	Failure to issue command	22	Loss of command(s) to SSU/spacecraft interface: SSU/Agena interface: and within the SSU	No effect	Redundant com-mand lines within CRJB	II
		Loss of com-mand verify capability	23	Loss of command verification signal to ground.	No effect	a)Not essential for mission success. b)Spacecraft is read out to ground from telemetry link.	III

FORM SSD 0607 1/7

FAIRCHILD HILLER
SPACE SYSTEMS DIVISION

FAILURE EFFECTS ANALYSIS

SYSTEM SERT II SSU REFERENCE

COMPONENT Communication Sub-system

Mode	Failure		Case No.	Symptoms & Consequences		Compensating Provisions	Failure Category
	COMPONENT	MODE		Immediate	System		
	Monopole Antennae	Failure to Deploy	24	Some degradation of antenna system radiation coverage	No effect.	Remaining 3 monopoles give a pattern in excess of minimun requirements.	II

FORM 350-